

2

NAVAL POSTGRADUATE SCHOOL

Monterey, California

AD-A155 608



DTIC
ELECTE
JUL 1 1985
S B D

THESIS

"HEAD-ON" SCATTERING OF A TUBULAR CYLINDER
OF FINITE LENGTH
FOR RADAR TARGET IDENTIFICATION PURPOSES

by

David Geller

March 1985

Thesis Advisor:

Hung-Mou-Lee

Approved for public release; distribution is unlimited

85 06 17 063

DTIC FILE COPY

REPORT DOCUMENTATION PAGE		READ INSTRUCTIONS BEFORE COMPLETING FORM
1. REPORT NUMBER	2. GOVT ACCESSION NO.	3. RECIPIENT'S CATALOG NUMBER
4. TITLE (and Subtitle) "Head-On" Scattering of a Tubular Cylinder of Finite Length for Radar Target Identification Purposes		5. TYPE OF REPORT & PERIOD COVERED Master's Thesis; March 1985
		6. PERFORMING ORG. REPORT NUMBER
7. AUTHOR(s) David Geller		8. CONTRACT OR GRANT NUMBER(s)
9. PERFORMING ORGANIZATION NAME AND ADDRESS Naval Postgraduate School Monterey, California 93943		10. PROGRAM ELEMENT, PROJECT, TASK AREA & WORK UNIT NUMBERS
11. CONTROLLING OFFICE NAME AND ADDRESS Naval Postgraduate School Monterey, California 93943		12. REPORT DATE March 1985
		13. NUMBER OF PAGES 156
14. MONITORING AGENCY NAME & ADDRESS (if different from Controlling Office)		15. SECURITY CLASS. (of this report) UNCLASSIFIED
		15a. DECLASSIFICATION/DOWNGRADING SCHEDULE
16. DISTRIBUTION STATEMENT (of this Report) Approved for public release; distribution is unlimited		
17. DISTRIBUTION STATEMENT (of the abstract entered in Block 20, if different from Report)		
18. SUPPLEMENTARY NOTES		
19. KEY WORDS (Continue on reverse side if necessary and identify by block number) Electromagnetic Scattering; Target Identification; Back- Scattering Cross-Section; Finite Tubular Cylinder; <i>Radial Cross Section</i>		
20. ABSTRACT (Continue on reverse side if necessary and identify by block number) This thesis studies the "Head-on" back scattering of a finite tubular cylinder with a circular cross-section and a very thin conducting wall. At this aspect angle, the back scattered fields depend only on the first Fourier component of the circumferential variations of the ϕ -current. Measurements of several scaled tubular cylinders were taken and the experimental results were compared to theoretical data available. This thesis is part of an ongoing project of target identification through the investigation of the cross section of a target over a broad frequency band.		

Approved for public release; distribution is unlimited.

"Head-on" Scattering of a Tubular Cylinder
of Finite Length
for Radar Target Identification Purposes.

by

David Geller
Lieutenant, Israeli Navy
B.S., Technion-Israeli High Institute of Technology, 1977

Submitted in partial fulfillment of the
requirements for the degree of

MASTER OF SCIENCE IN ELECTRICAL ENGINEERING

from the

NAVAL POSTGRADUATE SCHOOL
March 1985

Author:

David - Geller
David Geller

Approved by:

Hung-Mou Lee
Hung-Mou Lee, Thesis Advisor

Jin-Fu Chang
Jin-Fu Chang, Second Reader

Harriet B. Rigas
Harriet B. Rigas, Chairman,
Department of Electrical and Computer Engineering

John N. Dyer
John N. Dyer,
Dean of Science and Engineering

ABSTRACT

This thesis studies the "Head-on" back scattering of a finite tubular cylinder with a circular cross-section and a very thin conducting wall.

At this aspect angle, the back scattered fields depend only on the first Fourier component of the circumferential variations of the ϕ -current.

Measurements of several scaled tubular cylinders were taken and the experimental results were compared to theoretical data available.

This thesis is part of an ongoing project of target identification through the investigation of the cross-section of a target over a broad frequency band.



Accession For	
NTIS GRA&I	<input checked="" type="checkbox"/>
DTIC Tab	<input type="checkbox"/>
Unannounced	<input type="checkbox"/>
Justification	
By	
Distribution/	
Availability Codes	
Dist	Avail and/or Special
A-1	

TABLE OF CONTENTS

I.	INTRODUCTION	9
II.	ELECTROMAGNETIC SCATTERING THEORY	12
	A. ANALYTICAL BACKGROUND	14
	1. Definition of Radar Cross-section	14
	2. Polarization Scattering Matrix	15
	3. Methods of Obtaining the Scattering Matrix	18
	B. SCATTERING BY A FINITE TUBULAR CYLINDER	20
III.	MEASUREMENTS AND RESULTS	34
	A. LABORATORY DESCRIPTION	34
	1. System Configuration	34
	2. Instrumentation	38
	3. Targets	39
	B. MEASUREMENT PROCEDURE	43
	1. Calibration of the System	43
	2. Measurements of the Targets	44
	3. Sources of Measurement Errors	46
IV.	SUMMARY AND CONCLUSIONS	105
	A. ANALYSIS OF MEASURED DATA	105
	B. CONCLUSIONS AND RECOMENDATIONS	122
	APPENDIX A: COMPUTER PROGRAMS	130
	APPENDIX B: CHRACTERISTIC OF THE ABSORBER OF THE ANECHOIC CHAMBER	151
	LIST OF REFERENCES	153
	BIBLIOGRAPHY	155
	INITIAL DISTRIBUTION LIST	156

LIST OF TABLES

I	ANTENNAS SPECIFICATION	38
II	LIST OF EXPERIMENTAL DEVICES	39
III	TARGET-CHARACTERISTICS	41
IV	CYLINDER 1 : MEASUREMENT DATA	86
V	CYLINDER 2 : MEASUREMENT DATA	87
VI	CYLINDER 3 : MEASUREMENT DATA	88
VII	CYLINDER 4 : MEASUREMENT DATA	89
VIII	CYLINDER 5 : MEASUREMENT DATA	90
IX	CYLINDER 6 : MEASUREMENT DATA	91
X	CYLINDER 7 : MEASUREMENT DATA	92
XI	CYLINDER 8 : MEASUREMENT DATA	93
XII	CYLINDER 9 : MEASUREMENT DATA	94
XIII	CYLINDER 10 : MEASUREMENT DATA	95
XIV	CYLINDER 11 : MEASUREMENT DATA	96
XV	CYLINDER 12 : MEASUREMENT DATA	97
XVI	CYLINDER 13 : MEASUREMENT DATA	98
XVII	CYLINDER 14 : MEASUREMENT DATA	99
XVIII	CYLINDER 15 : MEASUREMENT DATA	100
XIX	CYLINDER 16 : MEASUREMENT DATA	101
XX	CYLINDER 17 : MEASUREMENT DATA	102
XXI	CYLINDER 18 : MEASUREMENT DATA	103
XXII	CYLINDER 19 : MEASUREMENT DATA	104
XXIII	CYL16.4:1 RATIO	118
XXIV	CYL.2,4:1 RATIO	119
XXV	CYL.18,4:1 RATIO	120
XXVI	CYL.15,4:1 RATIO	121
XXVII	CYL.4,6:1 RATIO	122
XXVIII	CYL.14,6:1 RATIO	123

XXIX	CYL.19,6:1 RATIO	124
XXX	CYL.17,6:1 RATIO	125

LIST OF FIGURES

2.1	The Scattering Problem	13
2.2	The Antenna Polarization Angle	16
2.3	The Tubular Cylinder	23
2.4	The Cylinder and the Incident Field	31
3.1	Block Diagram of the System	36
3.2	Configuration of the Anechoic Chamber	37
3.3	Tubular Cylinder with Fins	42
3.4	The Geometry Range	45
3.5	Cylinder 1: Cross-section	48
3.6	Cylinder 2 : Cross-section	49
3.7	Cylinder 3 : Cross-section	50
3.8	Cylinder 4 : Cross-section	51
3.9	Cylinder 5 : Cross-section	52
3.10	Cylinder 6 : Cross-section	53
3.11	Cylinder 7 : Cross-section	54
3.12	Cylinder 8 : Cross-section	55
3.13	Cylinder 9 : Cross-section	56
3.14	Cylinder 10 : Cross-section	57
3.15	Cylinder 11 : Cross-section	58
3.16	Cylinder 12 : Cross-section	59
3.17	Cylinder 13 : Cross-section	60
3.18	Cylinder 14 : Cross-section	61
3.19	Cylinder 15 : Cross-section	62
3.20	Cylinder 16 : Cross-section	63
3.21	Cylinder 17 : Cross-section	64
3.22	Cylinder 18 : Cross-section	65
3.23	Cylinder 19 : Cross-section	66
3.24	Cylinder 1 : Phase	67

3.25	Cylinder 2 : Phase	68
3.26	Cylinder 3 : Phase	69
3.27	Cylinder 4 : Phase	70
3.28	Cylinder 5 : Phase	71
3.29	Cylinder 6 : Phase	72
3.30	Cylinder 7 : Phase	73
3.31	Cylinder 8 : Phase	74
3.32	Cylinder 9 : Phase	75
3.33	Cylinder 10 : Phase	76
3.34	Cylinder 11 : Phase	77
3.35	Cylinder 12 : Phase	78
3.36	Cylinder 13 : Phase	79
3.37	Cylinder 14 : Phase	80
3.38	Cylinder 15 : Phase	81
3.39	Cylinder 16 : Phase	82
3.40	Cylinder 17 : Phase	83
3.41	Cylinder 18 : Phase	84
3.42	Cylinder 19 : Phase	85
4.1	Theory Cross section Curve, $(h/a)=4$	108
4.2	Experimental Cross section Curve, $(h/a)=4$	109
4.3	Theory Phase Curve, $(h/a)=4$	110
4.4	Experimental Phase Curve, $(h/a)=4$	111
4.5	Theory Cross section Curve, $(h/a)=6$	112
4.6	Experimental Cross section Curve, $(h/a)=6$	113
4.7	Theory Phase Curve, $(h/a)=6$	114
4.8	Experimental Phase Curve, $(h/a)=6$	115
4.9	Summary Cross section Curve, $(h/a)=4$	116
4.10	Summary Cross section Curve, $(h/a)=6$	117
4.11	Cylinder 15 with Fins, 90 Deg	128
4.12	Cylinder 15 with Fins, 45 Deg	129

I. INTRODUCTION

Identifying a target by its back scattering signal is desirable if different actions are to be taken towards different targets. At a time when warfare is no longer conducted face to face, but missiles have the ability to destroy their targets long before they come within visual range, it has become necessary to identify targets by some means other than vision. The identification is needed because of the fact that current operational policy requires a positive identification of a target before destroying it. This in a sense completely negates the prime capability of sophisticated weapon-systems. For example, the HARPOON missile whose range is far beyond the horizon prevents a visual identification of the target from the firing platform. A fact that limits the use of it to only specific situations under severe restrictions.

At present, most identifications are done with radars with which the presence of a target can be detected. In addition to the fact that the presence of a target can be discovered, information about its position, speed and acceleration may be obtained. An experienced radar operator can sometimes distinguish a big target from a small target by its spot-size on the radar screen, but this is not enough to identify the target.

To enhance our capability of identifying a target, it is advantageous to look at resonances excited by electromagnetic fields of different frequencies incident on the target. The reasons for looking at this particular range of frequencies are the following: First, at resonance the scattered fields are stronger compared to non-resonance situations. The

back-scattering cross-sections are larger and the target can be detected more easily. Second, the resonance frequencies and the amplitudes and phase shifts of the scattered fields at these frequencies are determined by the geometry of the target. Since the number of targets of our interest are finite, the identity of a target is revealed by examining a small data base.

This thesis is part of an ongoing project of target-identification through the investigation of the wide-band cross-section of a target. A finite tubular cylinder which has a circular cross section and a very thin conducting wall serves as the canonical target. The finite tubular cylinder is chosen because of its resemblance to a missile body and because theoretical formulations are available for its surface current distribution and scattered fields.

The tubular cylinder was placed in an anechoic chamber and was irradiated with an incident electromagnetic wave. While irradiated by the incident electromagnetic wave, surface currents were excited and generated scattered-field. The surface current had an axial and a circumferential component. The circumferential current circled around the cylinder while the axial current traveled along the cylinder and was reflected at the ends. At the same time, the incident wave kept impinging on the cylinder and excited new surface currents which added to the existing ones. At a certain frequency, the newly excited axial current might add constructively to the current reflected from one end, resulted in a large axial current, which gave a strong scattered field. Or the newly excited circumferential current might add constructively to the current which had made a complete circle around the cylinder, and a strong scattered field could be observed.

This thesis studied the "head-on" back scattering of the cylinder. At this aspect angle, the back scattered fields depended only on the first Fourier component of the circumferential variation of the ϕ -current. Measurements of several scaled tubular cylinders were taken and the experimental results were compared to theoretical data available.

For the next step of this project, more complicated models evolving from a tubular cylinder to a missile will be constructed and studied. Fins will be added, one end of the cylinder will be closed and rounded to perturb the model further and finally wings will be added to make a true missile model. By comparing the scattering data of the models to those of the tubular cylinders, the effects of the successive perturbations to the physical structure on the back-scattering cross-section and phase shift will be investigated.

Chapter II deals in its first part with electromagnetic back scattering theory in general, the definition of radar cross section, the polarization matrix and methods to obtain it. Its second part contains the solution to the electromagnetic back-scattering of a tubular cylinder with finite length. Chapter III describes some CW step frequency cross section measurements which are carried out, including the experimental setup, the measurement procedures and the measured results. Chapter IV deals with data analysis, compares the experimental results to theoretical data and presents some conclusions and recommendations for the future.

II. ELECTROMAGNETIC SCATTERING THEORY

A typical problem in electromagnetic scattering consists of these main elements.

1. Transmitting system: RF source and antennas.
2. An object of arbitrary shape and size as a target.
3. Receiving system: Antenna and receiving equipment to determine the amplitude, phase and polarization of fields at any point in space.

The transmitting system causes incident fields \vec{E}^i, \vec{H}^i to imping upon the target. The current in the source induces time-varying distributions of oscillating charges and currents in the scatterer. These currents cause scattered, or reradiated fields \vec{E}^s, \vec{H}^s . The total fields \vec{E}^T, \vec{H}^T are the vector sum of the incident and scattered fields.

In order to simplify the theoretical problem, it is usually assumed that the source is not coupled to the target. This fact enables one to obtain the scattered field by subtracting the incident fields from the total fields.

A configuration of the scattering problem is shown in Figure 2.1

This chapter deals with the analytical background, the definition of radar cross-section, the polarization scattering matrix, and finally the specific problem of the scattering by a finite tubular cylinder.

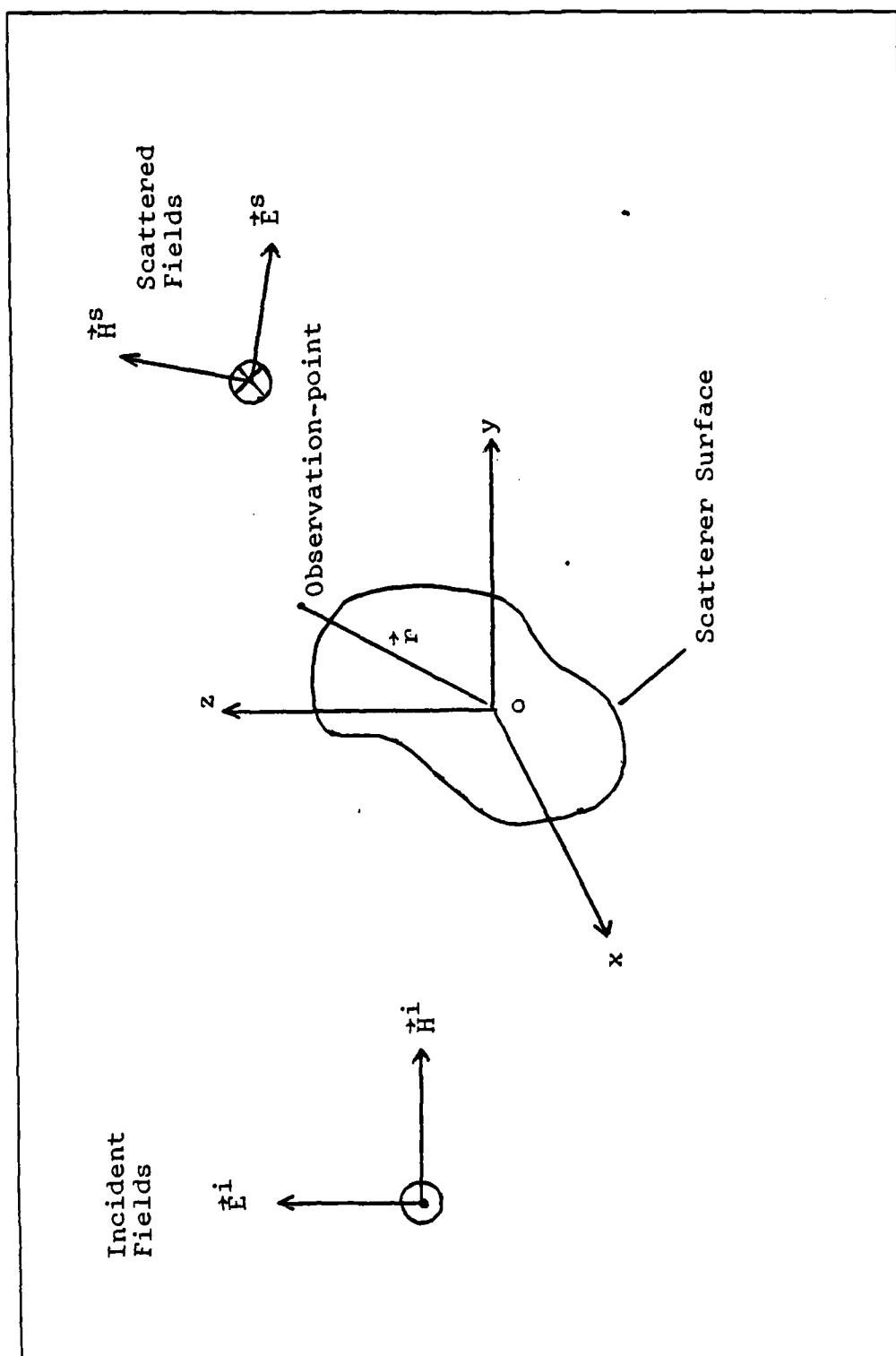


Figure 2.1 The Scattering Problem

A. ANALYTICAL BACKGROUND

1. Definition of Radar Cross-section

The radar cross-section of a target is a quantitative measure of the ratio of power density in the vector signal scattered in the direction of the receiver to the power density of the radar wave incident upon the target. The vectorial nature of the electromagnetic interaction requires specifications of the polarization of the incident wave with reference to target orientation in three dimensions. Radar operating frequency is an additional parameter which must be specified.

Thus, a single number specification for the radar cross section holds for a particular target, a specific polarization and the frequency of the incident wave, the aspect angle of the target relative to the incident wave, and the polarization of the receiving antenna.

The radar cross-section is defined to be independent of range to the target. This definition holds under far field assumption. Which means that the target is sufficiently far from the transmitting antenna to justify the assumption that the incident wave is planar at the target and the scattered wave is also planar in the neighborhood of the receiving antenna.

The theoretical definition of the radar cross-section relates incident to scattered electromagnetic fields, as given in equation 2.1

$$\sigma = 4\pi R^2 \lim_{R \rightarrow \infty} \left| \frac{E_s}{E_o} \right|^2 \quad (\text{eqn 2.1})$$

where:

E_o = magnitude of electric field component of incident electromagnetic field at the target.

E_s = magnitude of electric field component of scattered electromagnetic field as measured by a hypothetical observer.

R = distance from target to the hypothetical observer.

The radar cross-section σ has the dimensions of area m^2 .

The limiting process is introduced in equation 2.1 to assure that the distance at which the hypothetical observation is made, is far enough from the target. Under the free-space conditions assumed, the quantity $|E_s/E_o|^2$ is proportional to the power flux density of the scattered waves.

2. Polarization Scattering Matrix

The radar cross-section of a target depends upon the target shape and material, the angle (or angles, in a case of bistatic system) at which the target is viewed, radar frequency, and the polarization of the radar-transmitting and receiving antennas.

In particular, if a target is viewed at a specific aspect angle with a single frequency, the radar cross section depends upon polarization [Ref. 1].

The polarization scattering matrix is introduced in order to express target reradiation independent of radar polarization [Ref. 2].

Scattering is expressed as an explicit function of radar polarization, when matrices describing the polarization properties of antennas and target are defined.

The transmitting and receiving antennas can be represented by the matrices:

$$\hat{q} = \begin{bmatrix} \cos \phi_t & - \\ \sin \phi_t e^{j\delta t} & - \end{bmatrix} \quad (\text{eqn 2.2})$$

$$\hat{p} = [\cos\phi_r \quad \sin\phi_r e^{j\delta_r}] \quad (\text{eqn 2.3})$$

where:

\hat{q} = column matrix defining the polarization of the transmitting antenna.

\hat{p} = row matrix defining the polarization of the receiving antenna.

ϕ = an angle which when $\delta=0$, denotes the orientation of the linear polarization of the antenna when used for transmitting, referred to the horizontal plane.

δ = phase angle.

t = denotes transmitting antenna.

r = denotes receiving antenna.

The configuration of the cylinder for the measurement in this thesis and the antenna polarization angle are shown in Figure 2.2

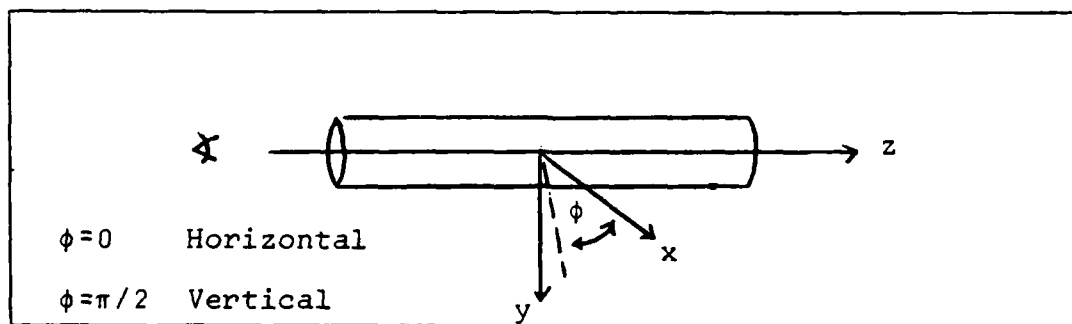


Figure 2.2 The Antenna Polarization Angle

The radar cross-section of a target observed by a transmitting antenna with polarization q and a receiving antenna with polarization p is given by equation 2.4

$$\sigma = |\hat{p} S \hat{q}|^2 \quad (\text{eqn 2.4})$$

where S denotes the complex scattering matrix used to represent the polarization properties of the target. Assuming a uniform plane incident wave, the scattering matrix is a linear relation between the incident field and the scattered far field from the target.

With p and q defined by equations 2.2 and 2.3 the scattering matrix S is a 2*2 matrix as shown below in equation 2.5

$$S = \begin{bmatrix} \sqrt{\sigma_{HH}} e^{j\rho_{HH}} & \sqrt{\sigma_{HV}} e^{j\rho_{HV}} \\ \sqrt{\sigma_{VH}} e^{j\rho_{VH}} & \sqrt{\sigma_{VV}} e^{j\rho_{VV}} \end{bmatrix} \quad (\text{eqn 2.5})$$

where:

- $\sqrt{\sigma}$ = magnitude of the scattering matrix element.
- ρ = phase of the scattering matrix element.
- H = denotes horizontal polarization.
- V = denotes vertical polarization.

The scattering matrix is symmetrical ($\sqrt{\sigma_{HV}} = \sqrt{\sigma_{VH}}, \rho_{HV} = \rho_{VH}$) in at list two cases .

1. Bistatic scattering when the body is a perfect conductor.

2. Back-scattering from an arbitrary body.

The transmitting and receiving antennas used in our case are linearly horizontally polarized.

The expressions for the transmitting and receiving antennas under this condition are:

$$\hat{q} = \begin{bmatrix} 1 \\ 0 \end{bmatrix} \quad (\text{eqn 2.6})$$

$$\hat{p} = [1 \quad 0] \quad (\text{eqn 2.7})$$

since $\phi = 0$.

The radar cross-section is:

$$\sigma = \sigma_{HH} \quad (\text{eqn 2.8})$$

3. Methods of Obtaining the Scattering Matrix

Ideally one would compute the radar cross-section of a target through the formal solution of Maxwells equations. Those equations should be solved for the boundary conditions appropriate to the target.

The major mathematical method for obtaining an exact solution is the separation of variables.

Formal solutions via separation of variables are possible only for a few special cases. In those cases the wave equation is separable in a coordinate system, having a

coordinate surface that coincides with the surface of the body [Ref. 3]. This situation explains why exact solutions are rare, and for many practical problems, the use of approximations is the only practical approach.

The integral equation formulation shows that electromagnetic scattering of an incident plane wave by an arbitrary body can be described in terms of an integral of various vector products. Those vector products involve the surface electric and magnetic fields. One form which is convenient for this purpose is the Chu-Stratton integral. [Ref. 4]. This integral is an exact representation of the scattered electromagnetic field. It is given in terms of an integration over a complete surface enclosing the body in question. In particular, if there were available knowledge of the total distribution of electric and magnetic fields about the body, insertion of these values in the Chu-Stratton integral would permit the immediate solution of the scattering problem.

Numerical schemes have been designed to solve the integral equations approximately. High speed digital computers are needed to establish surface currents flowing on the target. For example surface current distribution can be computed by a finite difference solution to a network of simultaneous equations [Ref. 5].

Because of limitation of computation time and storage capability, the finite difference solution is applicable only when the dimensions of the target do not exceed a very few wavelengths.

For targets larger than a few wavelengths in dimension, asymptotic methods are frequently used. There are three levels of complexity:

The simplest approach is the geometric optics approach. It treats ray bundles by the laws of reflection and refraction [Ref. 6]. However, geometric-optics fails

to distinguish the effects of polarization and the wave nature of the problem.

The second approach is the physical optics. In this approach the local current density, at each point on the illuminated portion of the body, is assumed to be identical to that which would flow at that point on an infinite tangent plane [Ref. 7]. Physical optics is not valid for applications entailing accurate specification effects [Ref. 8].

The third approach is the geometric diffraction theory. This approach is an extension of geometric optic that accounts for diffraction [Ref. 9]. The technique combines the simplicity inherent in the ray approach with the necessary consideration of wavelengths and phases of the wave. But it never include resonances of the target.

B. SCATTERING BY A FINITE TUBULAR CYLINDER

When a cylinder is irradiated with an incident electromagnetic wave, surface current is excited on the cylinder. This surface current will radiate and generate the scattered field.

Electromagnetic scattering from conducting objects in a homogeneous, isotropic medium can be treated as a boundary value problem. By use of the Stratton-Chu equations, integrodifferential equations can be set up for the current distribution on the surfaces of the objects, with the Greens function in the medium as the kernel.

The current distribution on the surface of a tubular cylindrical conductor with negligible wall thickness, excited by an incident electromagnetic field, can be written as a pair of coupled integrodifferential equations with the sum of the inside and outside surface currents as the unknown and the incident tangential electric field on

the surface of the conductor as the given quantity. Such a coupled integrodifferential equations were given by Lee [Ref. 16].

$$(1 + \frac{1}{l_1^2} \frac{\partial^2}{\partial z^2}) \int_{-1}^1 dz_0 K_{z,n}(z_0) G_n(l_1 | z - z_0 |, l_2) \quad (\text{eqn 2.9})$$

$$+ \frac{i n}{l_1 l_2} \frac{\partial}{\partial z} \int_{-1}^1 dz_0 K_{\phi n}(z_0) G_n(l_1 | z - z_0 |, l_2) = - \frac{2i}{l_1 l_2 \xi_0} E_{zn}^{sc}(z).$$

$$\int_{-1}^1 dz_0 K_{\phi n}(z_0) \left\{ \frac{1}{2} [G_{n-1}(l_1 | z - z_0 |, l_2) \right. \quad (\text{eqn 2.10})$$

$$+ G_{n+1}(l_1 | z - z_0 |, l_2)] - \frac{n^2}{l_2^2} G_n(l_1 | z - z_0 |, l_2)$$

$$+ \frac{i n}{l_1 l_2} \frac{\partial}{\partial z} \int_{-1}^1 dz_0 K_{zn}(z_0) G_n(l_1 | z - z_0 |, l_2) = - \frac{2i}{l_1 l_2 \xi_0} E_{\phi n}^{sc}(z).$$

equations 2.9 and 2.10 can be obtained from the Stratton-Chu equations, together with the edge conditions that:

$$K_z(0, z) = 0 \cdot (1 - z^2)^{1/2} \quad \text{as } |z| \rightarrow 1 \quad (\text{eqn 2.11})$$

In the previous equations:

sc-denotes-scattered.

i -denotes-incident.

$$\xi = (\mu / \epsilon)^{1/2}$$

and

$$G_n(l_1|z-z_0|, l_2) = \quad (\text{eqn 2.12})$$

$$\int_{-\pi}^{\pi} \frac{d\phi}{2\pi} l_1^{-in(\phi-\phi_0)} \cdot G[l_1|z-z_0|, 2l_2|\sin(\phi-\phi_0)/2|]$$

$$G(x_1, x_2) = \{ \exp[i(x_1^2 + x_2^2)^{1/2}] \} (x_1^2 + x_2^2)^{1/2} \quad (\text{eqn 2.13})$$

The following equations, 2.14 and 2.15 are boundary conditions for the tangential electric field components on a perfectly conducting surface.

$$E_{zn}^{sc}(z) + E_{zn}^i(z) = 0 \quad -1 < z < 1 \quad (\text{eqn 2.14})$$

$$E_{\phi n}^{sc}(z) + E_{\phi n}^i(z) = 0 \quad -1 < z < 1 \quad (\text{eqn 2.15})$$

The cylinder is assumed to be in a medium with homogeneous isotropic permittivity ϵ and permeability μ . The half length of the cylinder l_1 and the radius l_2 are measured in $1/k$, with $k = \omega(\epsilon\mu)^{1/2}$ being the wave number, so that $l_1 = kh$ and $l_2 = ka$.

The coordinate system is scaled so that the tubular cylinder occupies the region $-1 < z < 1, \rho = 1$ as shown in Figure 2.3

On the surface, $\rho = 1$, there are scattered electric field $E_{\phi}^{sc}(\phi, Z)$, the incident electric field $E_{\phi}^i(\phi, Z)$ and for $-1 < Z < 1$, the surface current $\vec{K}(\phi, Z)$, which is the sum of the

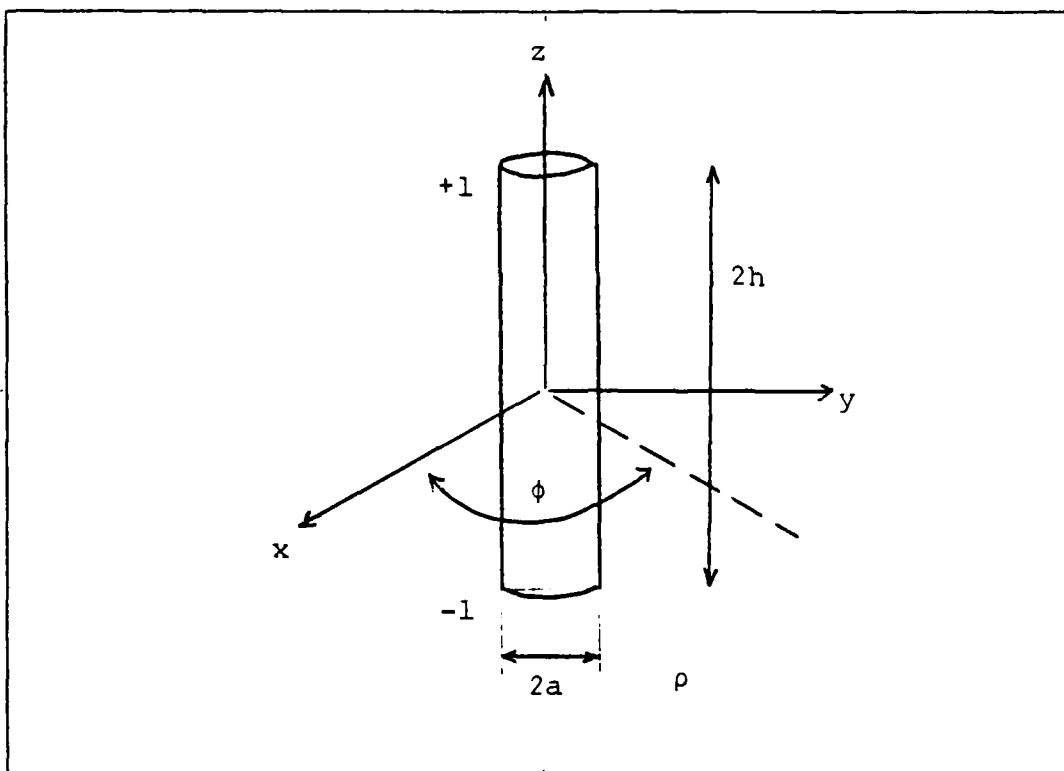


Figure 2.3 The Tubular Cylinder

outer surface current $\vec{K}^+(\phi, Z)$ on $\rho=1^+$ and the inner surface current $\vec{K}^-(\phi, Z)$ on $\rho=1^-$.

The surface currents can be represented as:

(eqn 2.16)

$$K_z(\phi, z) = \sum_{n=-\infty}^{\infty} e^{jn\phi} K_{zn}(z) = \sum_{n=0}^{\infty} [K_{zn}^{(+)}(z) \cos n\phi + iK_{zn}^{(-)}(z) \sin n\phi].$$

where

$$K_{z0}^{(+)}(z) = K_{z0}(z).$$

$$K_{zn}^{(+)}(z) = K_{zn}(z) + K_{z,-n}(z)$$

$$K_{z,0}^{(-)}(z) = 0$$

(eqn 2.17)

$$K_{\phi}(\phi, z) = \sum_{n=-\infty}^{\infty} e^{jn\phi} K_{\phi n}(z) = \sum_{n=0}^{\infty} [K_{\phi,n}^{(+)}(z) \cos n\phi + i K_{\phi,n}^{(-)}(z) \sin n\phi].$$

where

$$K_{\phi,0}^{(+)}(z) = K_{\phi,0}(z).$$

$$K_{\phi,n}^{(+)}(z) = K_{\phi,n}(z) + K_{\phi,-n}(z).$$

$$K_{\phi,0}^{(-)}(z) = 0.$$

$K_z(\phi, z)$ is the axial current density, and $K_{\phi}(\phi, z)$ is the circumferential current density.

In the far field where:

$$K|\vec{r}| = (l_2^2 \rho^2 + l_1^2 z^2)^{1/2} \gg 1 \quad (\text{eqn 2.18})$$

and

$$K|\vec{r}| \gg (l_1^2 + l_2^2)^{1/2} \geq K|\vec{r}_0| \quad (\text{eqn 2.19})$$

$$\begin{aligned}
-\frac{2i}{1_1 1_2 \xi_0} E_z(\rho, \phi, z) &= \sin^2 \theta \int_{-1}^1 dz_0 \int_{-\pi}^{\pi} \frac{d\phi_0}{2\pi} G(\vec{r}-\vec{r}_0) K_z(\phi_0, z_0) - \\
&\sin \theta \cos \theta \int_{-1}^1 dz_0 \int_{-\pi}^{\pi} \frac{d\phi_0}{2\pi} G(\vec{r}-\vec{r}_0) \sin(\phi - \phi_0) \quad (\text{eqn 2.20}) \\
&K_\phi(\phi_0, z_0)
\end{aligned}$$

$$\begin{aligned}
-\frac{-2i}{1_1 1_2 \xi_0} E_\rho(\rho, \phi, z) &= -\sin \theta \cos \theta \int_{-1}^1 dz_0 \int_{-\pi}^{\pi} \frac{d\phi_0}{2\pi} G(\vec{r}-\vec{r}_0) K_z(\phi_0, z_0) + \\
&\cos^2 \theta \int_{-1}^1 dz_0 \int_{-\pi}^{\pi} \frac{d\phi_0}{2\pi} G(\vec{r}-\vec{r}_0) \sin(\phi - \phi_0) K_\phi(\phi_0, z_0). \quad (\text{eqn 2.21})
\end{aligned}$$

$$\begin{aligned}
\frac{-2i}{1_1 1_2 \xi_0} E_\phi(\rho, \phi, z) &= \int_{-1}^1 dz_0 \int_{-\pi}^{\pi} \frac{d\phi_0}{2\pi} G(\vec{r}-\vec{r}_0) \cos(\phi - \phi_0) K_\phi(\phi_0, z_0) \\
&\quad (\text{eqn 2.22})
\end{aligned}$$

In spherical coordinates, the expressions are simpler.
Because:

$$E_r(r, \theta, \phi) = E_\rho(\rho, \phi, z) \sin \theta + E_z(\rho, \phi, z) \cos \theta \quad (\text{eqn 2.23})$$

$$E_{\theta}(r, \theta, \phi) = E_{\rho}(\rho, \phi, z) \cos \theta - E_z(\rho, \phi, z) \sin \theta$$

(eqn 2.24)

equations 2.20, 2.21 and 2.22 can be written in the following form:

$$-\frac{2i}{l_1 l_2 \xi_0} E_{\theta}(r, \theta, \phi) = 0 \quad (\text{eqn 2.25})$$

$$-\frac{2i}{l_1 l_2 \xi_0} E_{\theta}(r, \theta, \phi) = -\sin \theta \int_{-1}^1 dz_0 \int_{-\pi}^{\pi} \frac{d\phi_0}{2\pi} G(\vec{r} - \vec{r}_0) K_z(\phi_0, z_0) + \quad (\text{eqn 2.26})$$

$$\cos \theta \int_{-1}^1 dz_0 \int_{-\pi}^{\pi} \frac{d\phi_0}{2\pi} G(\vec{r} - \vec{r}_0) \sin(\phi - \phi_0) K_{\phi}(\phi_0, z_0)$$

$$-\frac{2i}{l_1 l_2 \xi_0} E_{\phi}(r, \theta, \phi) = \int_{-1}^1 dz_0 \int_{-\pi}^{\pi} \frac{d\phi_0}{2\pi} G(\vec{r} - \vec{r}_0) \cos(\phi - \phi_0) K_{\phi}(\phi_0, z_0)$$

(eqn 2.27)

where

(eqn 2.28)

$$G(\vec{r}-\vec{r}_0) = G(\vec{r}) \exp^{-il_2 \sin \theta \cos(\phi-\phi_0)} \exp^{-il_1 \cos \theta z_0}$$

since:

(eqn 2.29)

$$\int_{-\pi}^{\pi} \frac{d\phi}{2\pi} \cos n\phi \exp^{-il_2 \sin \theta \cos(\phi-\phi_0)} = i^{-n} J_n(l_2 \sin \theta)$$

(eqn 2.30)

$$\begin{aligned} \int_{-1}^1 \frac{dz_0}{\pi \sqrt{1-z_0^2}} \cos p v \exp^{-il_1 \cos v z_0} &= \int_0^{\pi} \frac{dv}{\pi} \cos p v \exp^{-il_1 \cos \theta \cos v} \\ &= i^{-p} J_p(l_1 \cos \theta) \end{aligned}$$

and with $z = \cos v$ and the facts that $k_{\phi} \rightarrow (1-z^2)^{1/2}$, $k_z \rightarrow (1-z^2)^{1/2}$ on the edges of the cylinder

$$K_{zn}(z) = \frac{1}{\pi} \sum_{p=0}^{\infty} K_{z,n}^p \sin(p+1)v \quad (\text{eqn 2.31})$$

$$K_{\phi n}(z) = \frac{1}{\pi \sin v} \sum_{p=0}^{\infty} K_{\phi,n}^p \cos p v \quad (\text{eqn 2.32})$$

where $K_{z,n}^{(+)}$ and $K_{\phi,n}^{(+)}$ the sum of the inside and outside currents from equation 2.16

$$K_{z,n}^{(+)} = K_{z,n} + K_{z,-n} \quad (\text{eqn 2.33})$$

$$K_{\phi,n}^{(+)} = K_{\phi,n} + K_{\phi,-n} \quad (\text{eqn 2.34})$$

The final equations for the general case are:

$$E_r(r, \theta, \phi) = 0 \quad (\text{eqn 2.35})$$

$$-\frac{2i}{l_1 l_2 \epsilon_0 G(\vec{r})} E_\theta(r, \theta, \phi) = - \sum_{n=0}^{\infty} \sum_{p=0}^{\infty} i^{-(n+p)} \frac{(p+1) \sin \theta}{l_1 \cos \theta} \quad (\text{eqn 2.36})$$

$$\begin{aligned} & J_{p+1}(l_1 \cos \theta) J_n(l_2 \sin \theta) [K_{zn}^{(+)} P_{\cos n \phi} + i K_{zn}^{(-)} P_{\sin n \phi}] \\ & + \sum_{n=1}^{\infty} \sum_{p=0}^{\infty} i^{-(n+p)} \frac{n \cos \theta}{l_2 \sin \theta} J_p(l_1 \cos \theta) J_n(l_2 \sin \theta) [K_{\phi n}^{(-)} P_{\cos n \phi} \\ & \quad + i K_{\phi n}^{(+)} P_{\sin n \phi}]. \end{aligned}$$

$$- \frac{2i}{l_1 l_2 \xi G(\vec{r})} E_\phi(r, \theta, \phi) =$$

(eqn 2.37)

$$\sum_{n=0}^{\infty} \sum_{p=0}^{\infty} i^{-(n+p)} J_p(l_1 \cos \theta) J_n^1(l_2 \sin \theta) [-K_{\phi n}^{(-)p} \sin n\phi + i K_{\phi n}^{(+)p} \cos n\phi].$$

Since $E_r(r, \theta, \phi) = 0$ in the far field

(eqn 2.38)

$$E_x(r, \theta, \phi) = E_\theta(r, \theta, \phi) \cos \theta \cos \phi - E_\phi(r, \theta, \phi) \sin \phi$$

(eqn 2.39)

$$E_y(r, \theta, \phi) = E_\theta(r, \theta, \phi) \cos \theta \sin \phi + E_\phi(r, \theta, \phi) \cos \phi$$

(eqn 2.40)

$$E_z(r, \theta, \phi) = -E_\theta(r, \theta, \phi) \sin \theta$$

In the special case, with the cylinder positioned head-on to the antennas, the incident and scattered fields can be described as follows:

$\theta = \pi$ (along the Z axis)

The scattered fields are:

(eqn 2.41)

$$\frac{-2i}{l_1 l_2 \xi_0 G(\vec{r})} E_\theta(r, \pi, \phi) = \frac{1}{2} \sum_{p=0}^{\infty} i^{-(p+1)} J_p(l_1) [K_{\phi 1}^{(-)p} \cos \phi + i K_{\phi 1}^{(+)} p \sin \phi]$$

(eqn 2.42)

$$\frac{-2i}{l_1 l_2 \xi_0 G(\vec{r})} E_\phi(r, \pi, \phi) = \frac{1}{2} \sum_{p=0}^{\infty} i^{-(p+1)} J_p(l_1) [-K_{\phi 1}^{(-)p} \sin \phi + i K_{\phi 1}^{(+)} p \cos \phi].$$

or in rectangular coordinates, along the -z axis:

(eqn 2.43)

$$\frac{-2i}{l_1 l_2 \xi_0 G(\vec{r})} E_x(z) = \frac{1}{2} \sum_{p=0}^{\infty} i^{(p-1)} J_p(l_1) K_{\phi 1}^{(-)p}$$

(eqn 2.44)

$$\frac{-2i}{l_1 l_2 \xi_0 G(\vec{r})} E_y(z) = \frac{1}{2} \sum_{p=0}^{\infty} i^{-p} J_p(l_1) K_{\phi 1}^{(+)} p$$

(eqn 2.45)

$$E_z(z) = 0.$$

The configuration of the cylinder and the incident field is shown in Figure 2.4

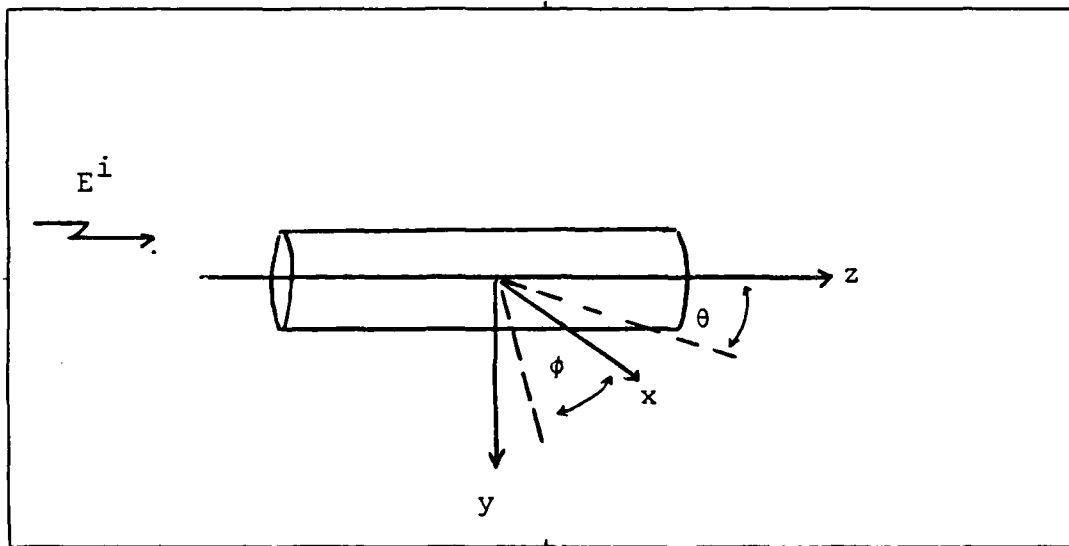


Figure 2.4 The Cylinder and the Incident Field

With the axis of the cylinder chosen along the z-direction and the incident field along the z axis, the incident field is given as:

$$\vec{E}^{inc} = \hat{e}_2 e^{ikz}, \quad \hat{e}_2 = -\hat{x} \quad (\text{eqn 2.46})$$

$$E_{\phi}^{inc} = +\sin\phi e^{ikz} \quad (\text{eqn 2.47})$$

Because E_{ϕ}^{inc} is an odd function in ϕ

$$K_{\phi n}^{(+)}(z) = 0$$

From equations 2.43- 2.45 $E_y(Z)=0$, and $\vec{E}(Z)=\hat{x}E_x(Z)$ along the $-Z$ axis.

Cross-section and phase of a scatterer are defined with a linearly polarized plane incident wave on the scatterer. The incident wave has unit strength and zero phase at the center of the scatterer.

The cross-section is given by:

$$\sigma = \lim_{r \rightarrow \infty} 4\pi r^2 \quad |E^{sc}|^2 \quad (\text{eqn 2.48})$$

and the phase shift is given by:

$$\delta = \arg(1 - ikr E^{sc}) = \arg\left[\sum_{p=0}^{\infty} i^p J_p(l_1) K_{\phi 1}^{(-)p}\right]. \quad (\text{eqn 2.49})$$

since:

$$|E^{SQ}| = \left| \frac{l_1 l_2 \xi_0 G(\vec{r})}{4i} \sum_{p=0}^{\infty} i^{p-1} J_p(l_1) K_{\phi 1}^{(-)p} \right| \quad (\text{eqn 2.50})$$

the cross-section of the finite cylinder is:

$$\sigma = \lim_{r \rightarrow \infty} 4\pi r^2 \left| \frac{l_1 l_2 \xi_0 G(\vec{r})}{4i} \sum_{p=0}^{\infty} i^{p-1} J_p(l_1) K_{\phi 1}^{(-)p} \right|^2 \quad (\text{eqn 2.51})$$

$$= \pi a^2 \left| \frac{kh\xi}{a} \sum_{p=0}^{\infty} i^{p-1} J_p(l_1) K_{\phi 1}^{(-)p} \right|^2$$

III. MEASUREMENTS AND RESULTS

Radar cross-section estimation is as much art as science. The air of mystery that surrounds it will only be removed by an increase in understanding of how a target scatters energy incident upon it.

A complete knowledge of the scattering behavior is available only for few bodies. For these bodies we do not have exact solutions for their radar cross section, the best we can do is to provide approximate values. Such values should be checked against experimental measurements.

This chapter describes some CW step frequency cross-section measurements carried out at the Naval Postgraduate School, including the experimental setup, the measurement procedure and the measurements results.

Computer programs for calibration of the experimental setup and target measurements process are given in Appendix A. An explanation to the programs can be found in previous thesis from the Naval Postgraduate School [Ref. 15].

A. LABORATORY DESCRIPTION

1. System Configuration

The physical setup of the laboratory can be divided into five parts:

- The RF source.
- Transmitting and receiving antennas.
- The anechoic chamber.
- Target mount, targets.
- Control and data processing equipment.

This setup is called a Radar range geometry and is designed for cross section measurements of models. The configuration of the entire system is shown in Figure 3.1 .

A variety of radar range geometries have been developed during the years. Those radar range geometries were characterized by the way they have been designed to eliminate unwanted signals reflected from the foreground and background [Ref. 10]. An important component of the setup at the Naval Postgraduate School is the anechoic chamber [Ref. 11]. The anechoic chamber is used to approximate free space conditions in a closed environment. The anechoic chamber is enclosed with aluminium plates and internally lined with a radio frequency absorbing material. The absorbing material provides the necessary attenuation to the reflections from the walls, floor and ceiling, and the aluminium surface provides protection against external sources of noise such as atmospheric noise, man made noise (radio, television, radar etc) and weather conditions. The characteristics of the absorber material are specified in Appendix B.

The target is supported by a styrofoam stand. The reason for choosing the material, is to minimize coupling between the stand and the target. [Ref. 12].

The radar cross section range utilizes two identical horn antennas to approximate a back scattering system. Both antennas are horizontally polarized. The antennas are mounted on a removable panel located in the front wall of the anechoic chamber. The antennas can be adjusted in all three axis, providing beam steering towards the target. The basic antennas characteristics are given in Table I, and the configuration of the anechoic chamber is shown in Figure 3.2

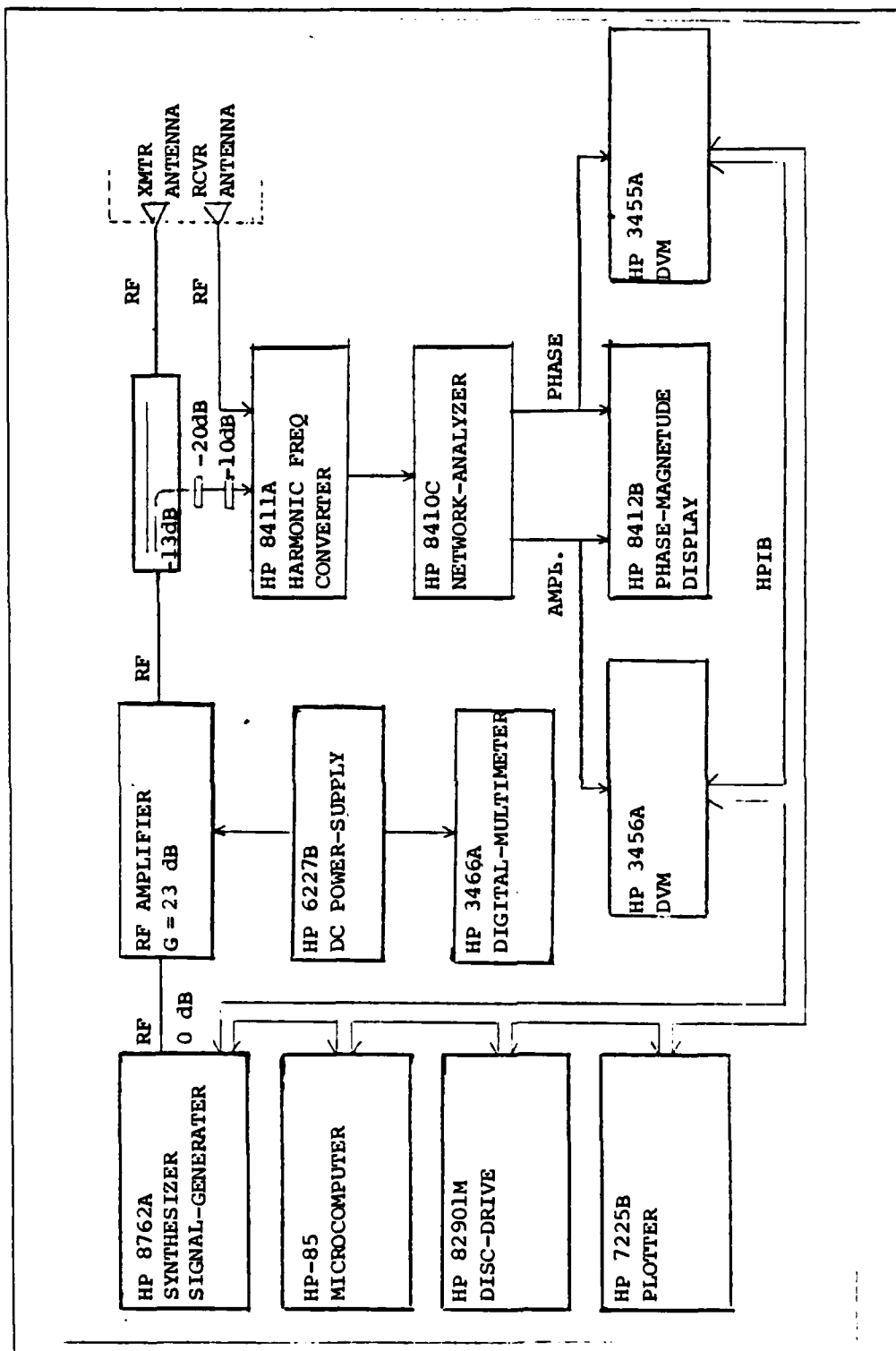


Figure 3.1 Block Diagram of the System

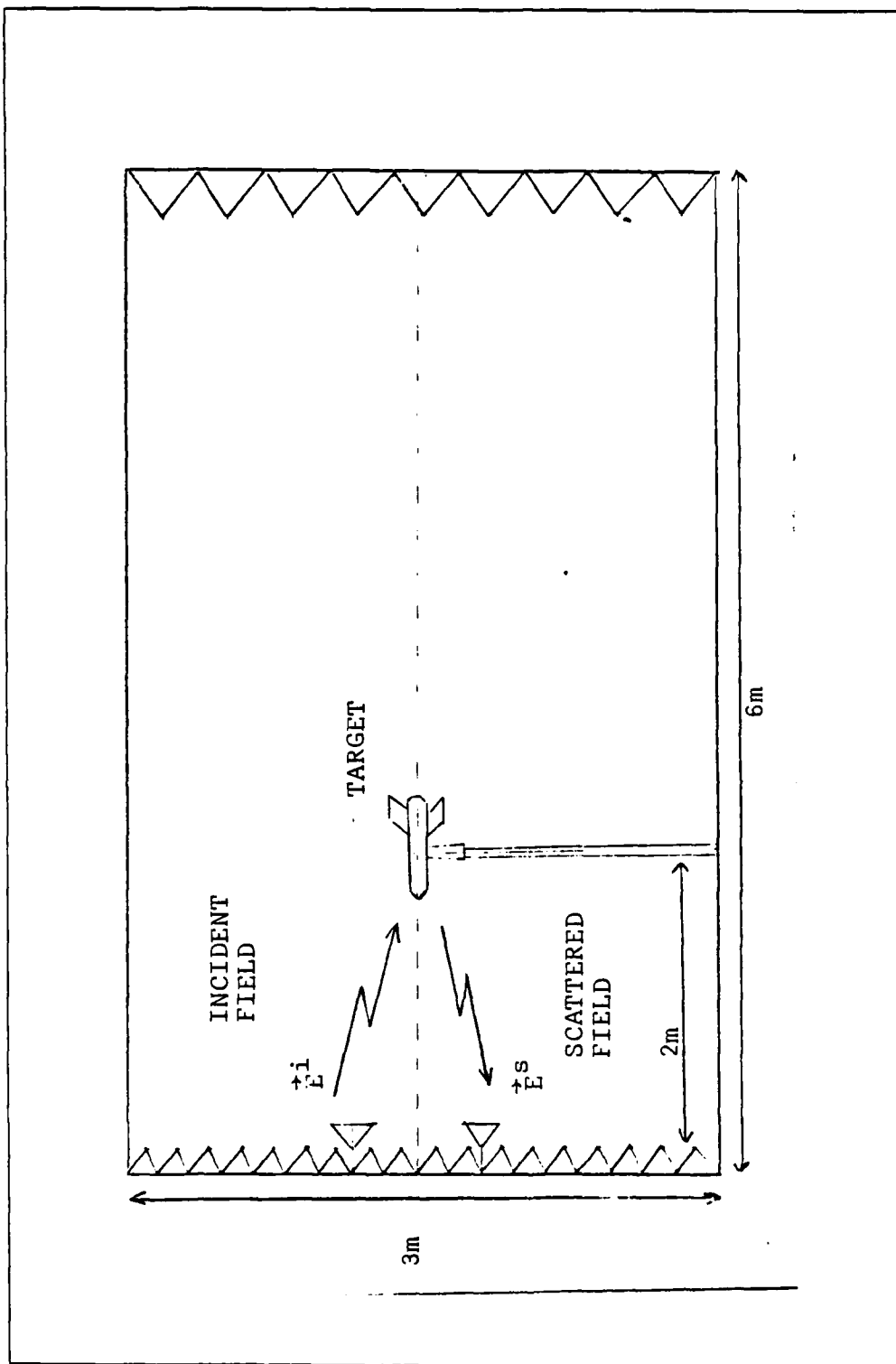


Figure 3.2 Configuration of the Anechoic Chamber

TABLE I
ANTENNAS SPECIFICATION

Frequency range	4-18 GHz
Gain	6-12dB
VSWR (max)	3.2:1
Isolation between cross polarization	<20dB below 5.5 GHz >20dB above 5.5 GHz

2. Instrumentation

The equipment of the experimental setup is listed in Table II .

The RF signal to the system is provided by the signal generator (HP-8672A). The RF output from the signal generator is amplified by an RF amplifier (Avantek-SA-83-2953). (The DC-power supply, HP-6227B, to the amplifier is monitored by a digital multimeter, HP-3466A).

The amplified RF signal passes the directional coupler (Narda-5292) and goes to the transmitting antenna. The directional coupler has a coupling coefficient of -13 dB and provides the reference signal to the harmonic frequency converter (HP-8411A) after the signal is further attenuated by 30 dB. The scattered signal from the target goes through the receiving antenna to the first port of the harmonic frequency converter. The frequency converter and the network analyzer (HP-8410C) convert the test channel signal into two 278 KHz signals containing the magnitude and phase information of the test channel signal relative to the reference channel signal. Both signals enter the phase-magnitude

TABLE II
LIST OF EXPERIMENTAL DEVICES

-Microcomputer	HP-85
-Synthesized Signal Generator	HP-8672A
-Harmonic Frequency converter	HP-8411A
-Network Analyzer	HP-8410C
-Phase-Magnitude Display	HP-8412B
-RF Amplifier	Avantek sa-83-2953
-DC Power supply	HP-6277B
-Digital Multimeter	HP-3466A
-Digital voltmeter	HP-3455A
-Digital voltmeter	HP-3456A
-Flexible Disc Drive	HP-82901M
-Plotter	HP-7225B
-Directional Coupler	Narda 5292

display (HP-8412B) The DC plotter outputs of the display unit are fed to the two DVM's (HP-3455A, HP-3456a).

The complete setup is controlled and the data is processed by the microcomputer (HP-85) and the results are stored on discs.

3. Targets

The most direct means of obtaining knowledges about radar cross sections are by measurement of the radar return from the target itself or from an accurate model of the target [Ref. 13]. One advantage of a radar range is the practicability of testing models that are smaller and cheaper than full scale targets. The radar wavelength is scaled by the same factor as are the dimensions of the model. If D is any given dimension of the target, and D is the equivalent dimension of the model, the following scaling relation is employed:

$$D_M/D_0 = \lambda_M/\lambda_0 \quad (\text{eqn 3.1})$$

where λ_M is the wavelength used for the measurement and λ_0 is the wavelength for which the target radar cross-section is required.

At the same time, the measured cross section is altered in proportion to the change in power captured as a result of dimensional changes. If σ_M is the observed cross section of the model, the target cross section σ_0 is given by:

$$\sigma_0 = \frac{\lambda_0^2}{\lambda_M^2} \sigma_M \quad (\text{eqn 3.2})$$

Exact scaling requires the model conductivity to be equal to the target conductivity multiplied by the ratio (λ_0/λ_M) , and model permittivity and permeability at the test frequency to equal corresponding target electrical properties at the operational frequency. It is necessary to make sure that the surface conductance of the model won't be smaller than the target.

The targets which are tested in the measurements are thin walled tubular cylinders made of brass. There are 20 cylinders of various lengths and diameters. The dimensions of the targets are given in Table III .

For the calibration of the system a 3.187 inch aluminium sphere is used.

Some measurements are taken with a cylinder with fins attached .The description of the cylinder with fins is shown in Figure 3.3 .

TABLE III
TARGET-CHARACTERISTICS

TARGET	LENGTH	DIAMETER	THICKNESS
cylinder 1	2.00"	0.375"	0.012"
cylinder 2	2.00"	0.500"	0.014"
cylinder 3	2.00"	0.750"	0.011"
cylinder 4	2.25"	0.375"	0.012"
cylinder 5	2.25"	0.500"	0.014"
cylinder 6	2.25"	0.750"	0.011"
cylinder 7	2.50"	0.375"	0.012"
cylinder 8	2.50"	0.500"	0.014"
cylinder 9	2.50"	0.750"	0.011"
cylinder 10	2.75"	0.375"	0.012"
cylinder 11	2.75"	0.500"	0.014"
cylinder 12	2.75"	0.750"	0.011"
cylinder 13	3.00"	0.375"	0.012"
cylinder 14	3.00"	0.500"	0.014"
cylinder 15	3.00"	0.750"	0.011"
cylinder 16	1.50"	0.375"	0.012"
cylinder 17	4.50"	0.750"	0.011"
cylinder 18	2.50"	0.625"	0.014"
cylinder 19	3.75"	0.750"	0.011"
cylinder with fins	3.00"	0.750"	0.011"

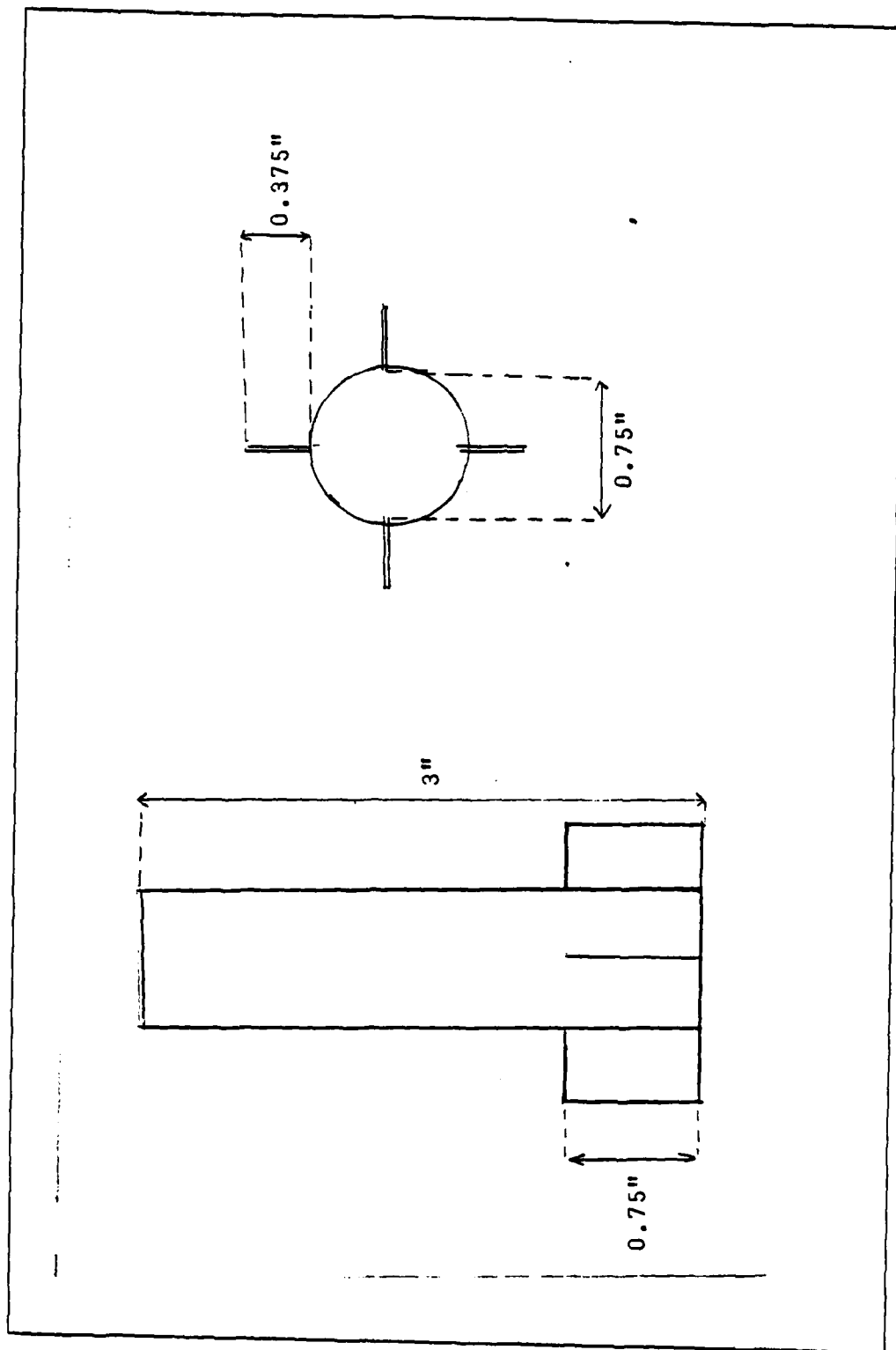


Figure 3.3 Tubular Cylinder with Fins

B. MEASUREMENT PROCEDURE

1. Calibration of the System

As a first step in the measurement, a calibration of the system must be done.

To calibrate the system output, a target of known cross section (usually a metal sphere) is placed at the target support to fix the level of the calibration curve. This measurement assures that the entire system is calibrated in the proper frequency range.

Measurements are taken at many fixed frequencies between 10 to 15 GHz. Since both the transmitting and receiving antennas are horizontally polarized, the measurements are in one dimensional plane.

The calibration of the system is divided into two steps:

1. Take measurements without target in the anechoic chamber. (background data).
2. Insert a 3.187 inch diameter aluminium sphere and repeat the measurements.

With the target in place, the received signal is a vectorial sum of the target echo and the background radiation. By taking background data, direct back scattering from the targets support and the walls of the anechoic chamber can be subtracted from the vector sum.

The quality of the calibration of the system is tested and checked by comparing a new set of measured data on the sphere to their theoretical values whenever a calibration process is done.

After the calibration of the system is accomplished, measurements of target cross sections can be started.

2. Measurements of the Targets

The measurements of the cylinders are taken in the frequency range of 10 to 15 GHz in steps of 0.1 GHz. The decision to limit the frequency range inspite of the ability of the equipment to operate beyond this range is due to the following reason:

Only in this frequency range consistent data can be obtained through averaging the data obtained from several frequency scans.

All the measurements are taken while the cylinders are positioned "Head-on" to the antennas as seen in Figure 3.4 A description of the cylinders tested is given in Table III, and reasons for choosing those particular dimensions for the cylinders are given in Chapter .

As a rule of thumb, far field approximations are good under the following conditions:

$$r > 10\lambda \quad \text{(eqn 3.3)}$$

$$r > 10D \quad \text{(eqn 3.4)}$$

$$r > \frac{2D^2}{\lambda} \quad \text{(eqn 3.5)}$$

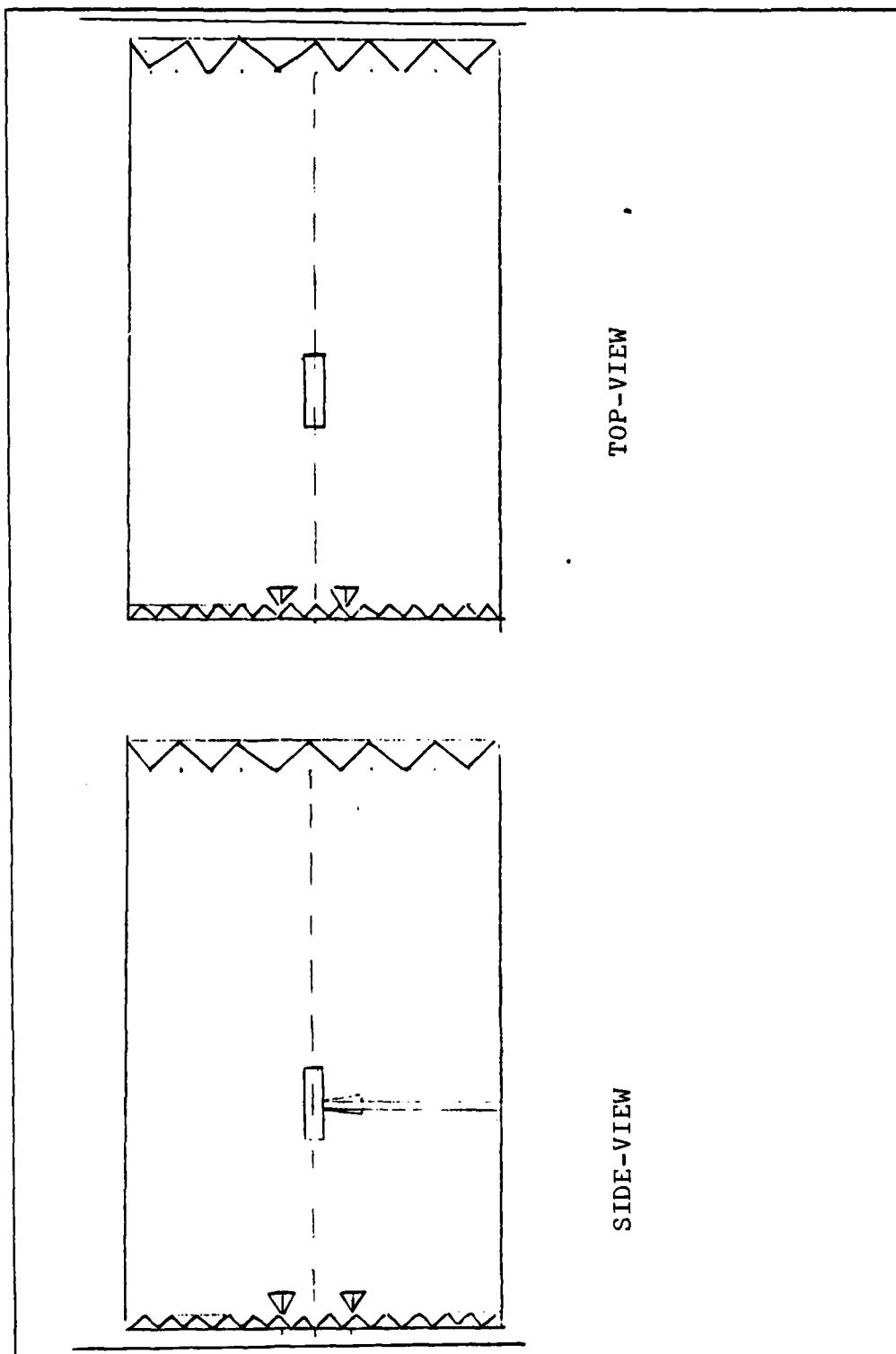


Figure 3.4 The Geometry Range

where r is the distance between the target and the antennas (receiving and transmitting), D is the largest dimension of either the target or the antennas and their separations, and λ is the wavelength. In our case, all conditions are met.

Before each target measurement, calibration of the system is done.

The experimental results for the targets in term of plots of their cross section and phases versus frequency are given at the end of the chapter.

3. Sources of Measurement Errors

Recognition of error sources in the measured data is difficult. Only in few special cases, it is possible to recognize the presence of an error, and to determine its source by observing the deviation of a target cross section versus frequency plot from anticipated behavior.

The errors in the measurement in our case are due to system noise and background noise.

The system noise, is caused mainly by the receiver. The network analyzer (HP-8410C) is a harmonic mixing receiver. It selects a harmonic of its internal VCO for the local oscillator frequency used to down convert the test frequency to the first IF. Harmonic skip errors can occur when the receiver selects a different harmonic (and VCO frequency) for the same frequency between system calibration and target measurement. The local oscillator power varies from one harmonic to another, thus the mixer transfer-characteristic varies. This fact causes random magnitude and phase variations of from 0.1 to 0.4 dB and up to 2 degrees.

As for the background noise, it is caused by coupling between the target and its mechanical support, and by strong coupling between the antennas in low frequencies.

In our case, the coupling between the antennas is reduced by going to higher range of frequencies. The

coupling between the target and its mechanical support is unavoidable and finally the receiver noise is reduced by averaging the measured results.

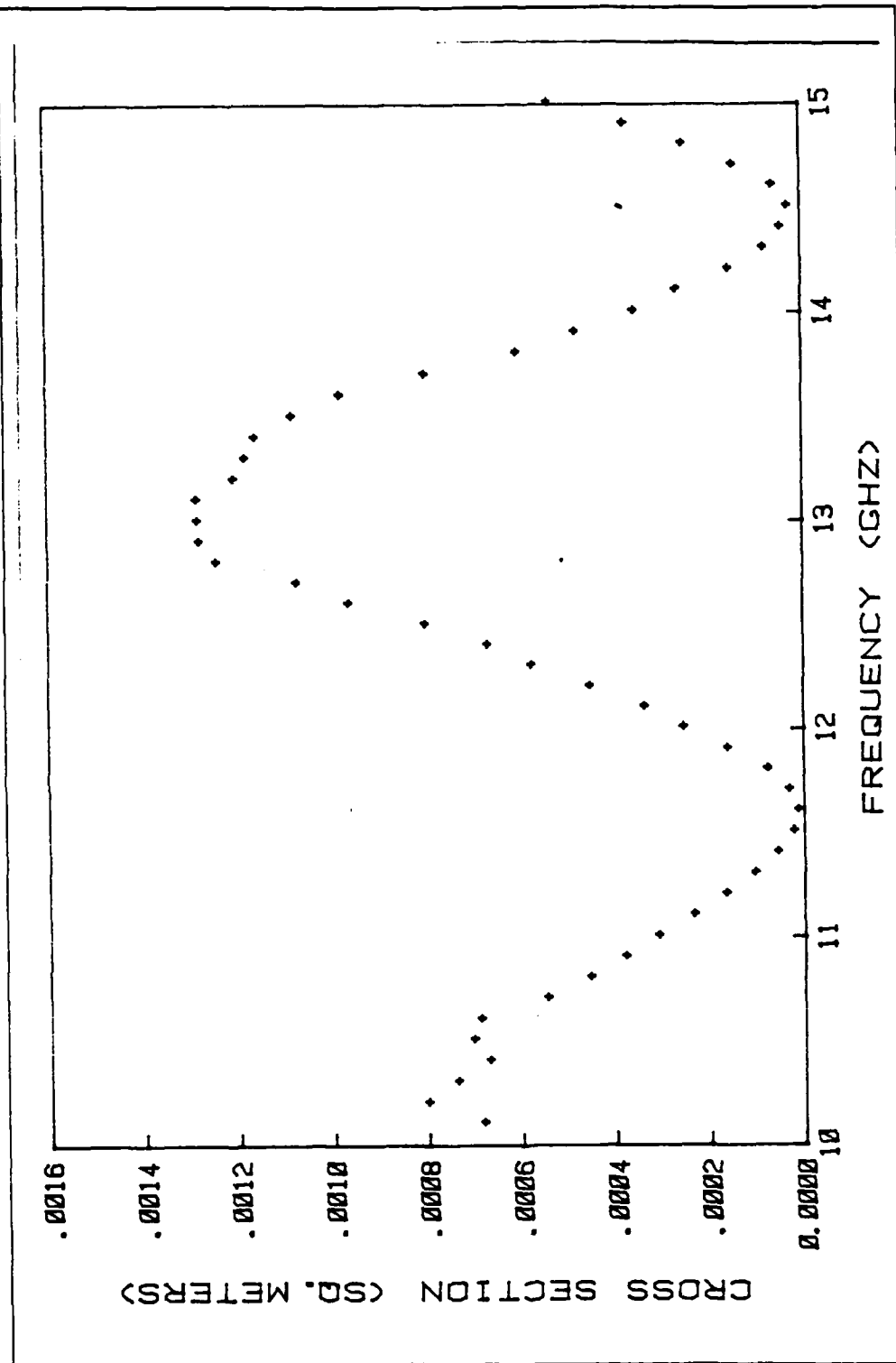


Figure 3.5 Cylinder 1: Cross-section

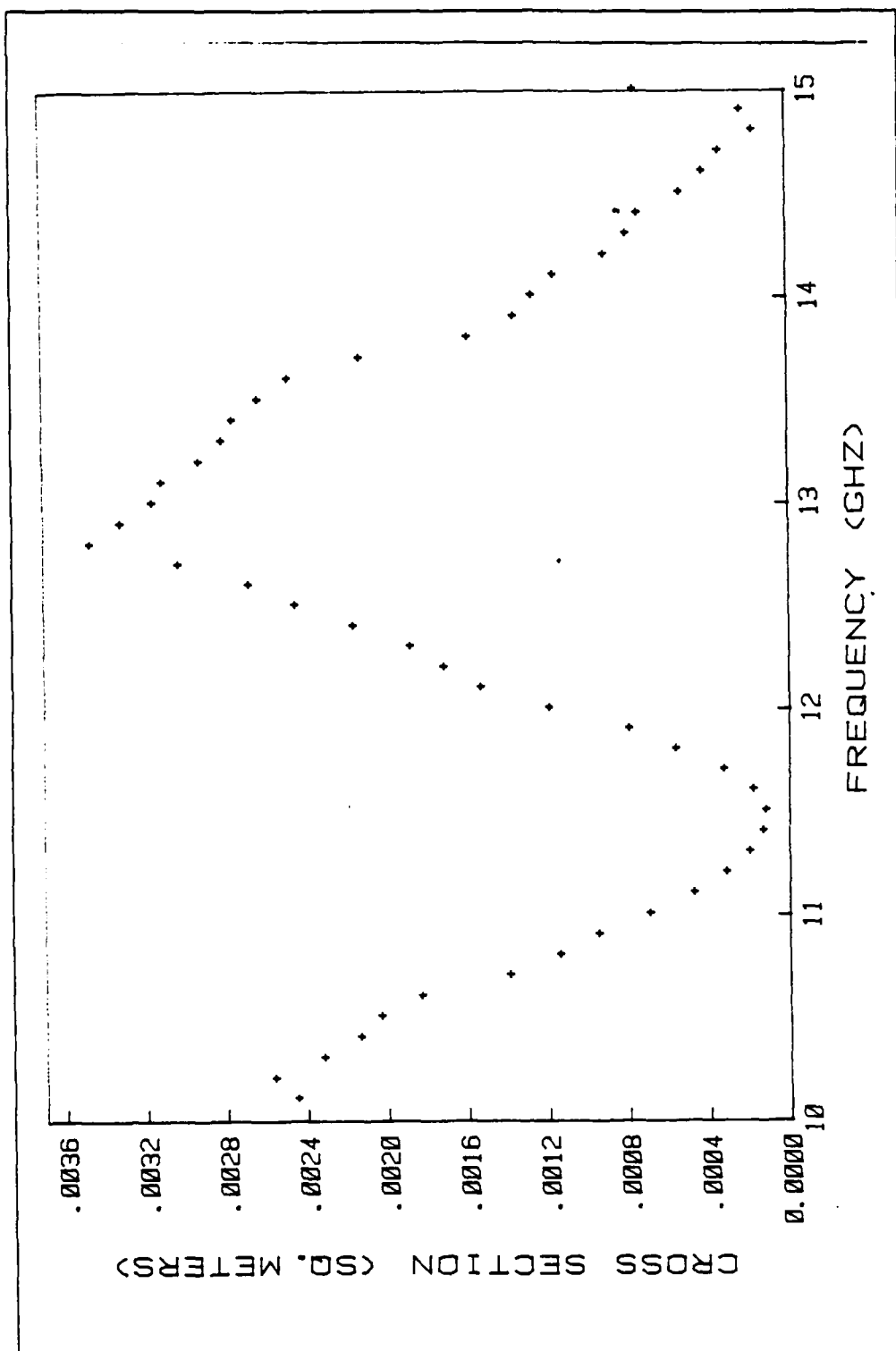


Figure 3.6 Cylinder 2 : Cross-section

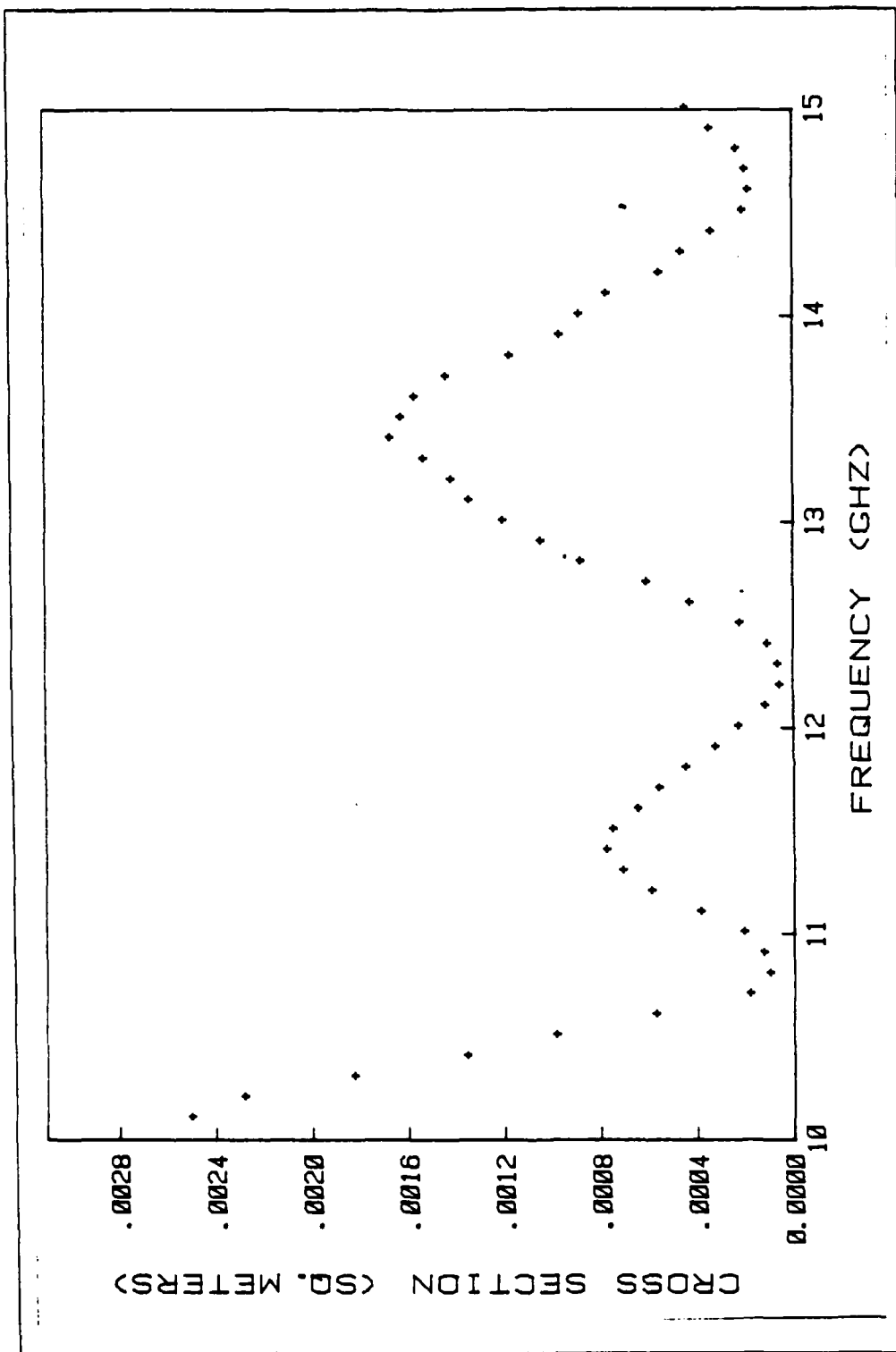


Figure 3.7 Cylinder 3 : Cross-section

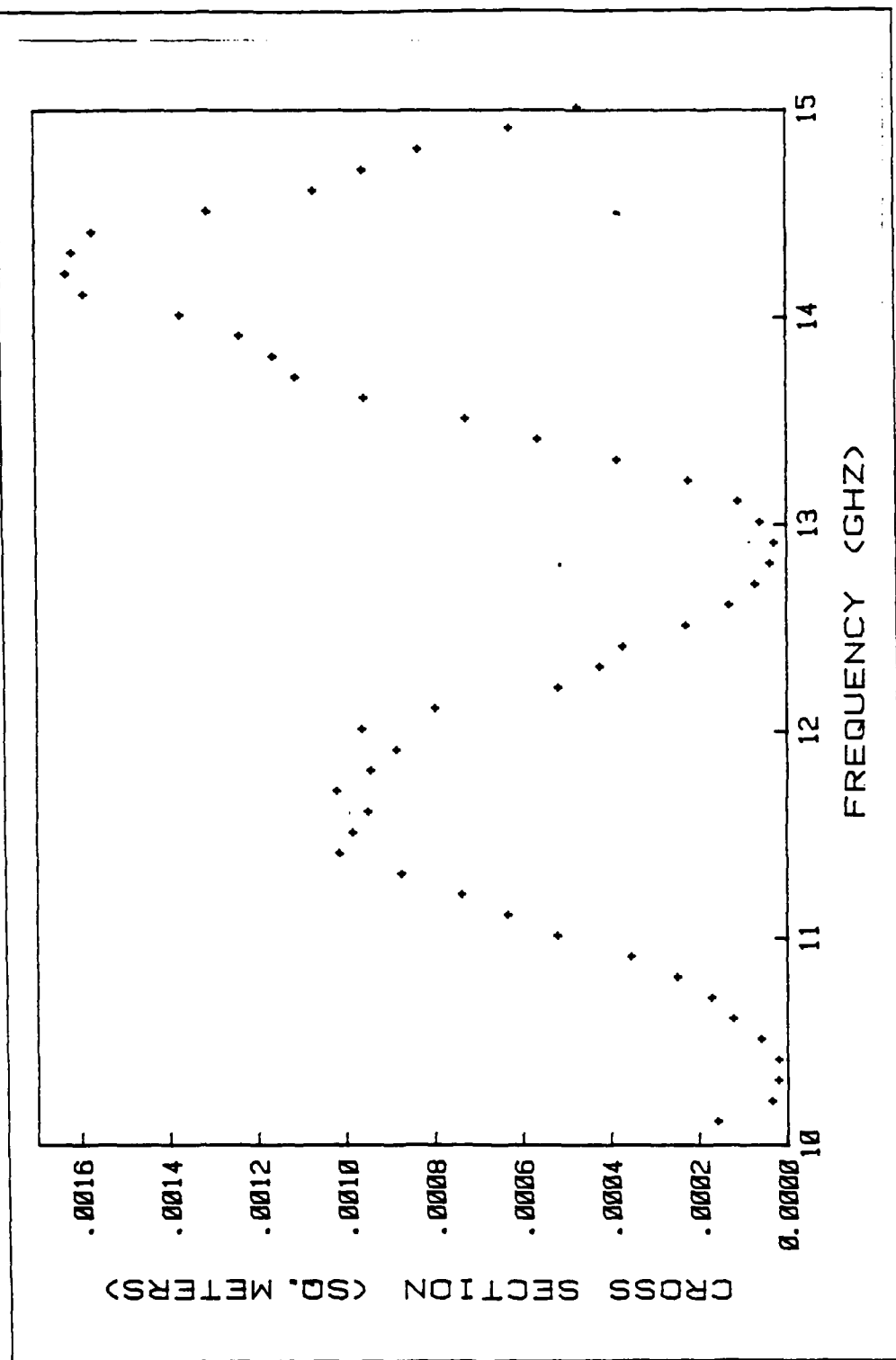


Figure 3.8 Cylinder 4 : Cross-section

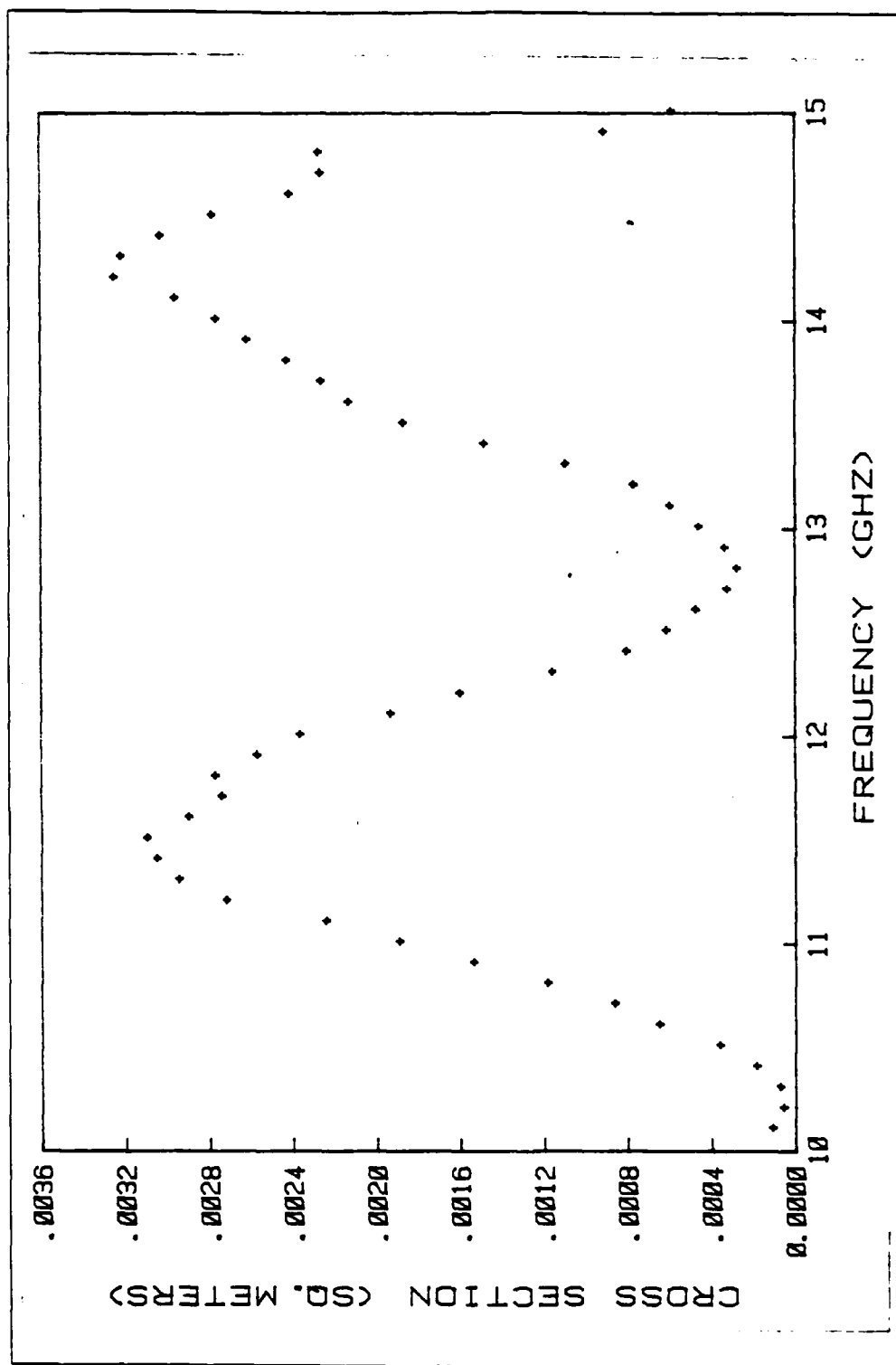


Figure 3.9 Cylinder 5 : Cross-section

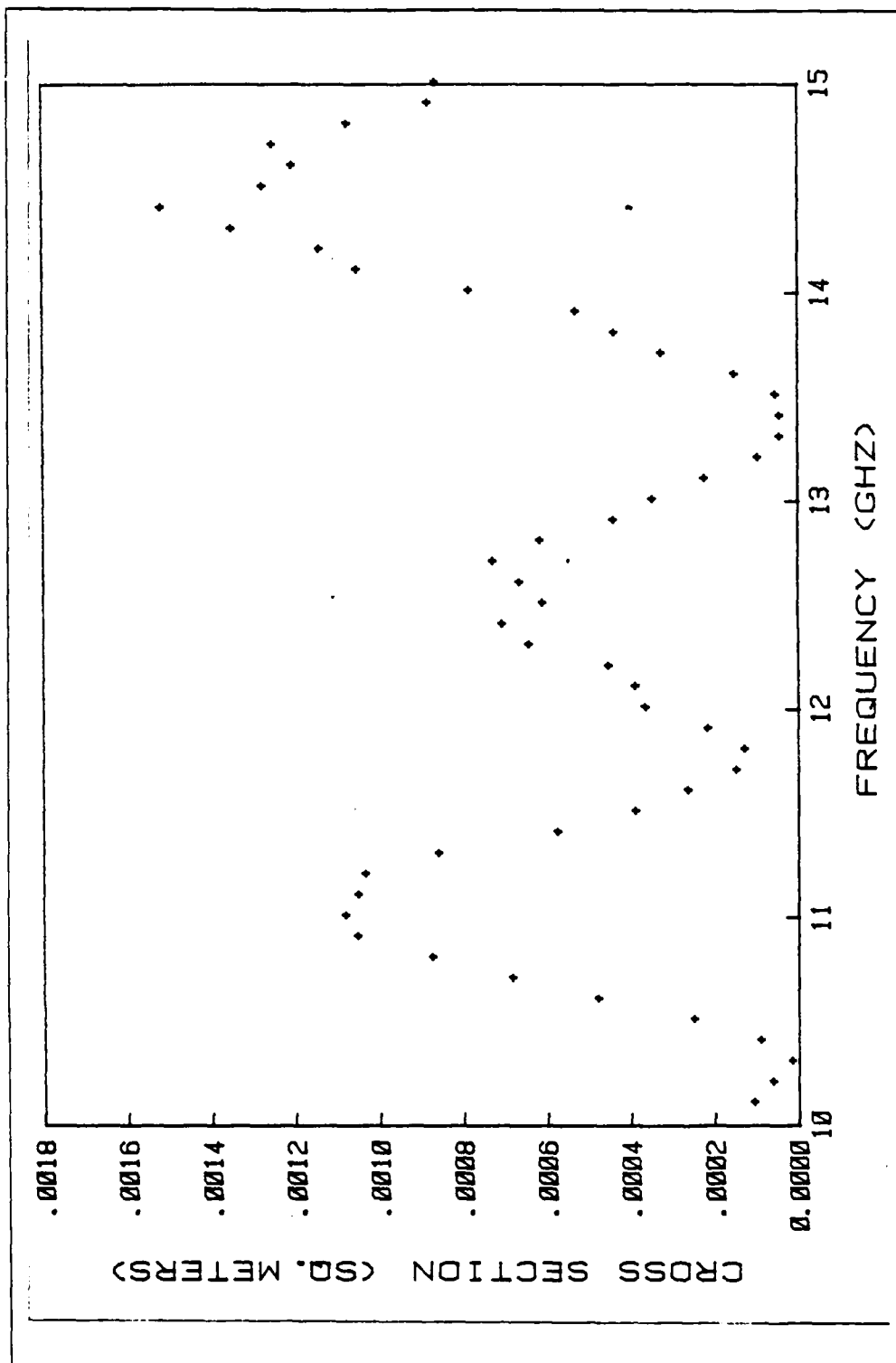


Figure 3.10 Cylinder 6 : Cross-section

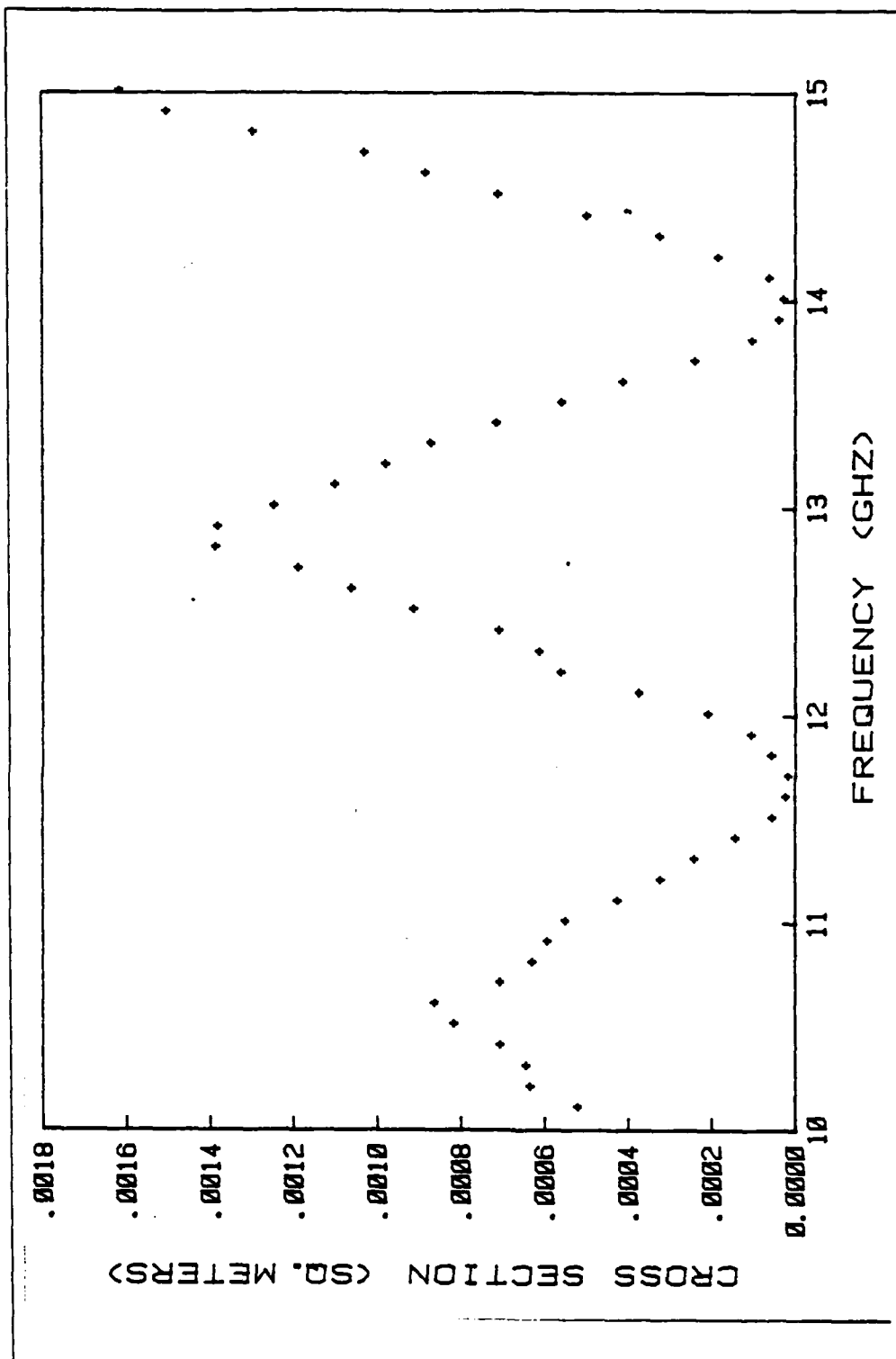


Figure 3.11 Cylinder 7 : Cross-section

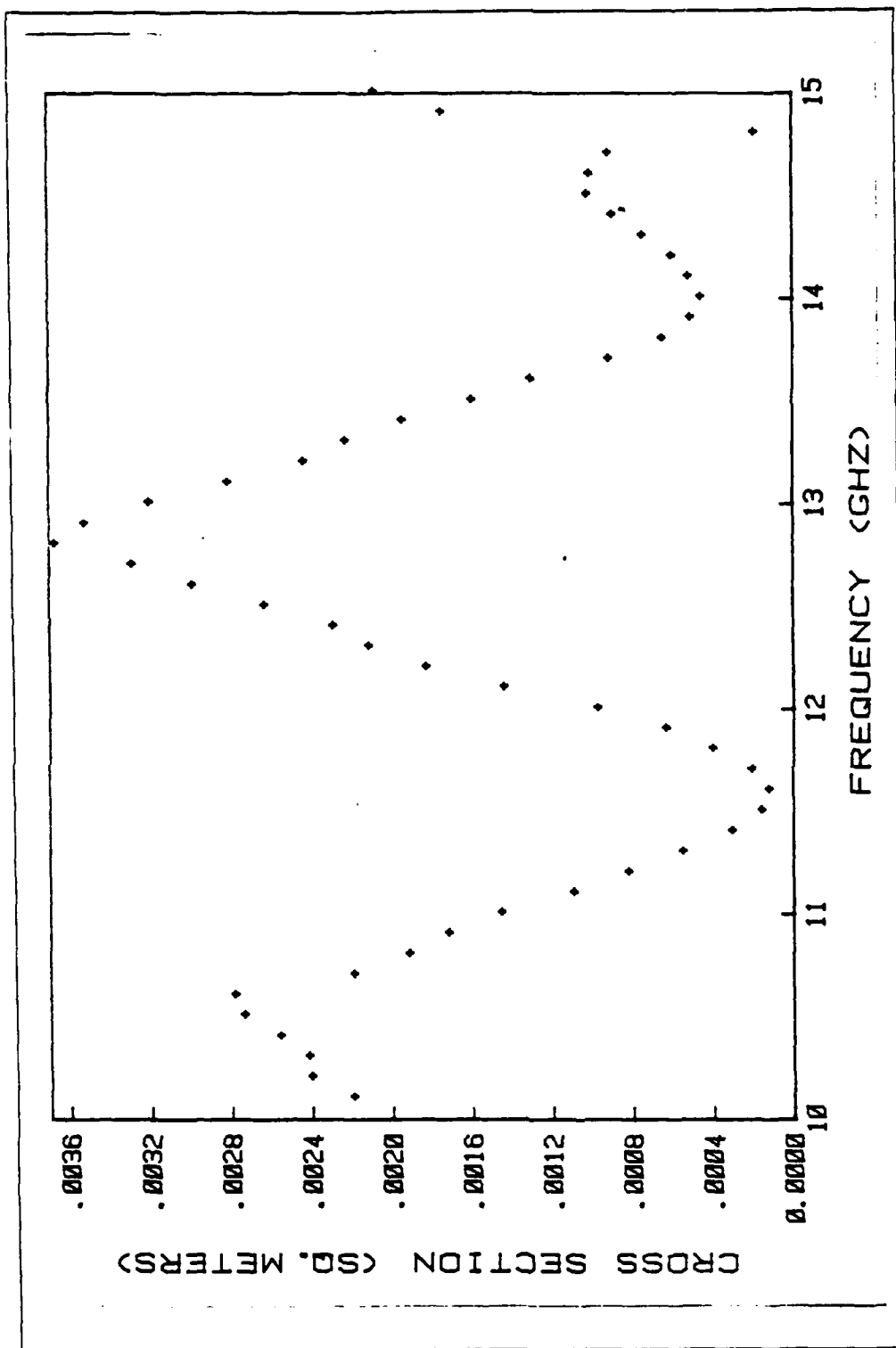


Figure 3.12 Cylinder 8 : Cross-section

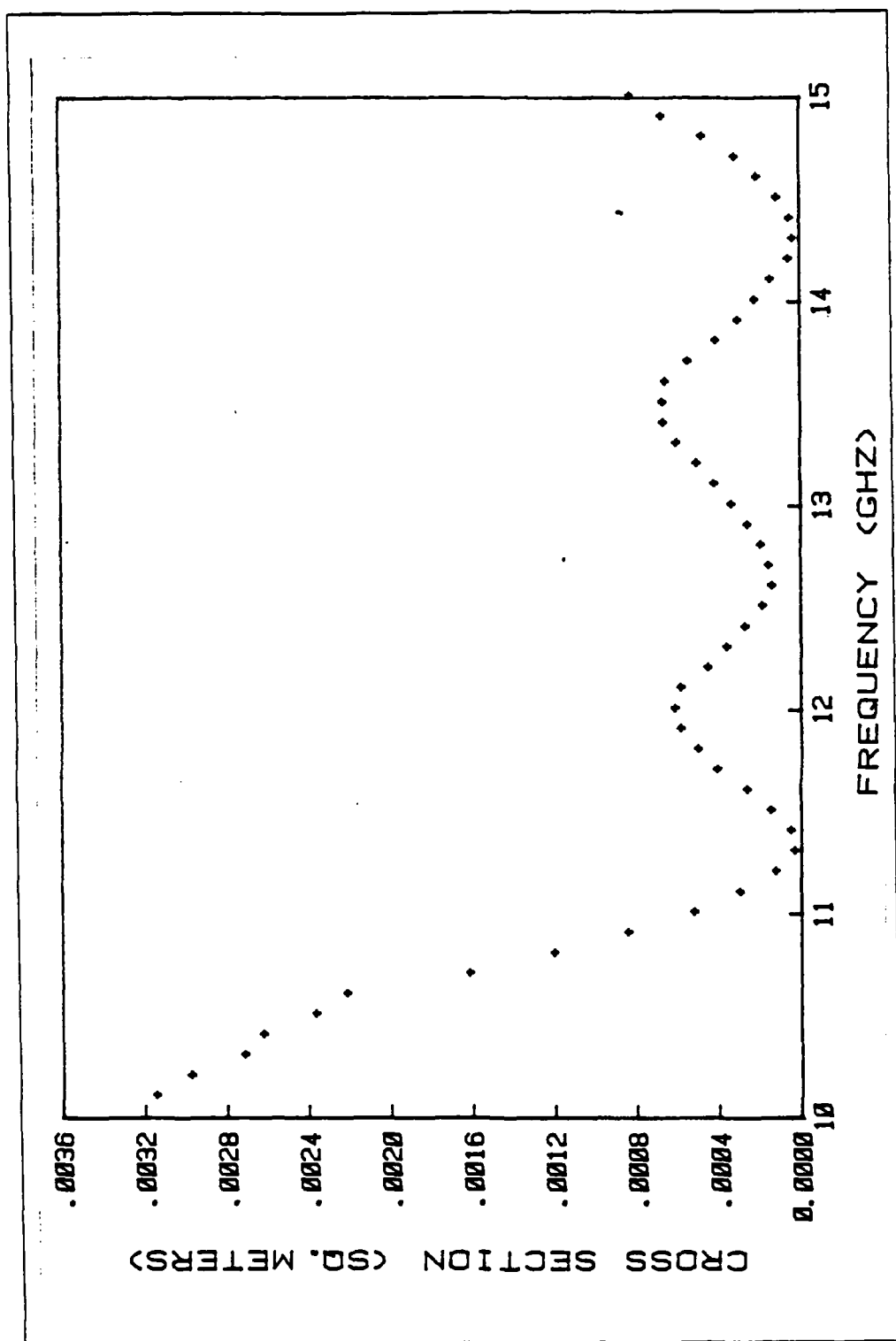


Figure 3.13 Cylinder 9 : Cross-section

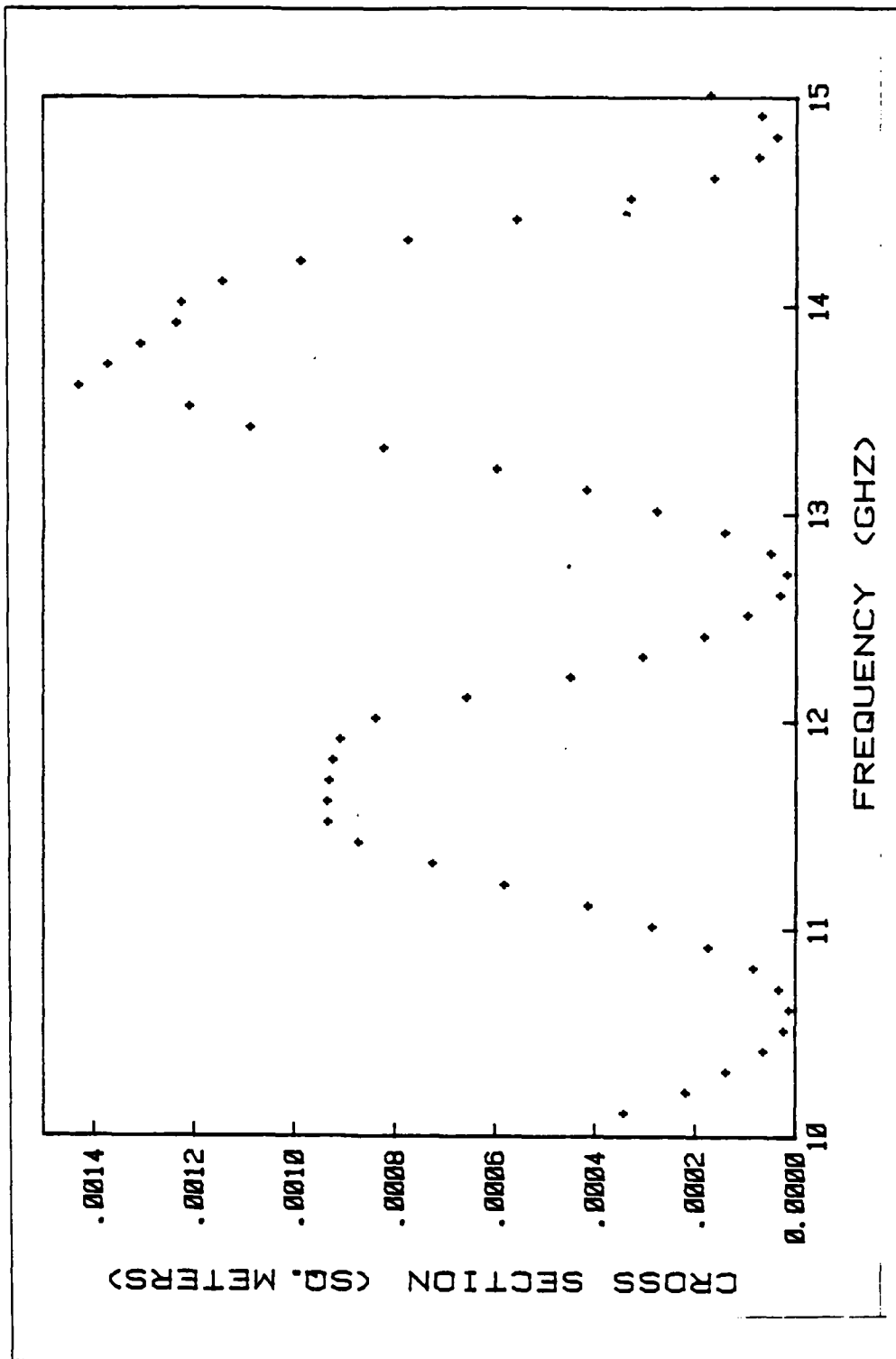


Figure 3.14 Cylinder 10 : Cross-section

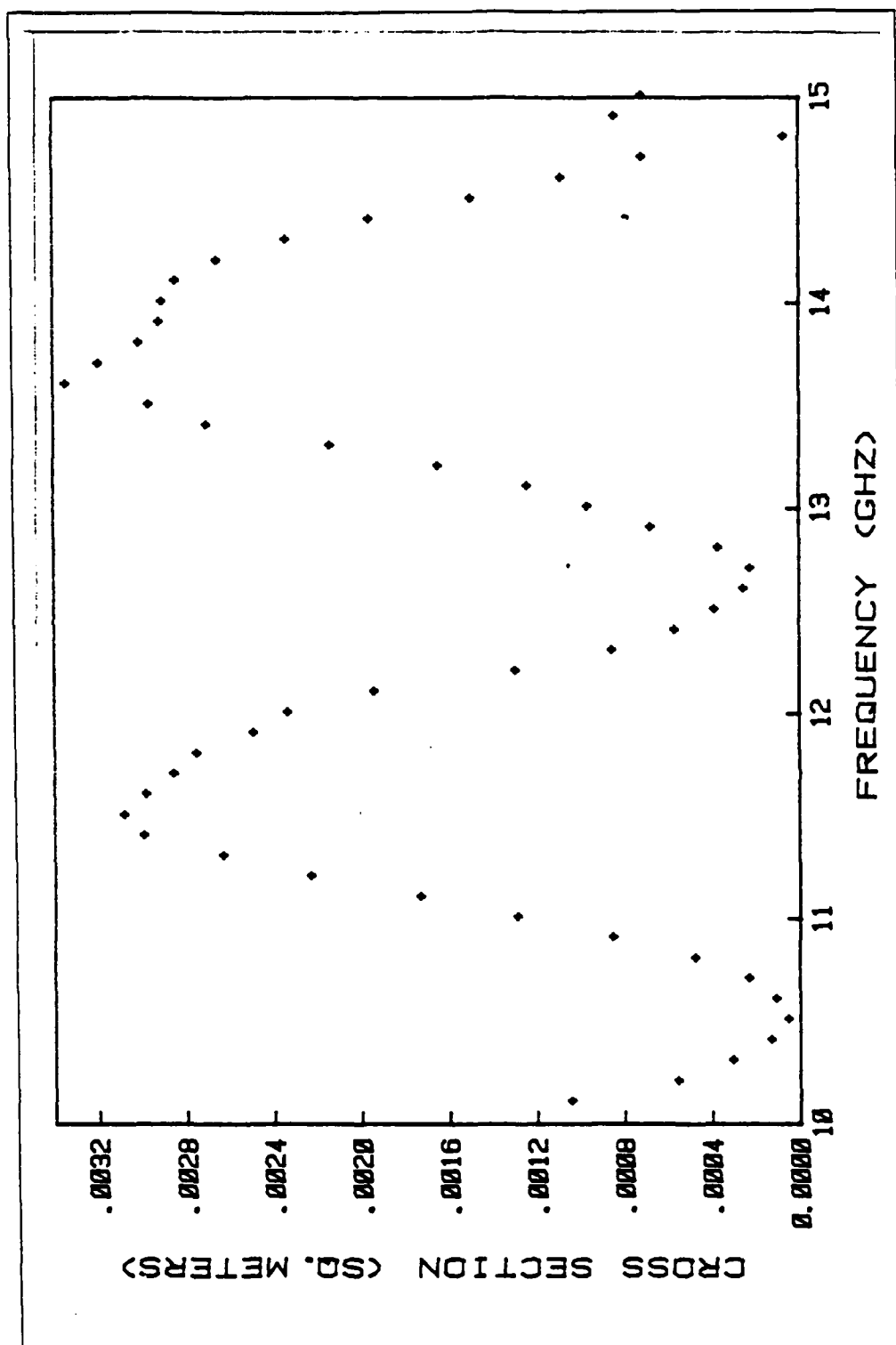


Figure 3.15 Cylinder 11 : Cross-section

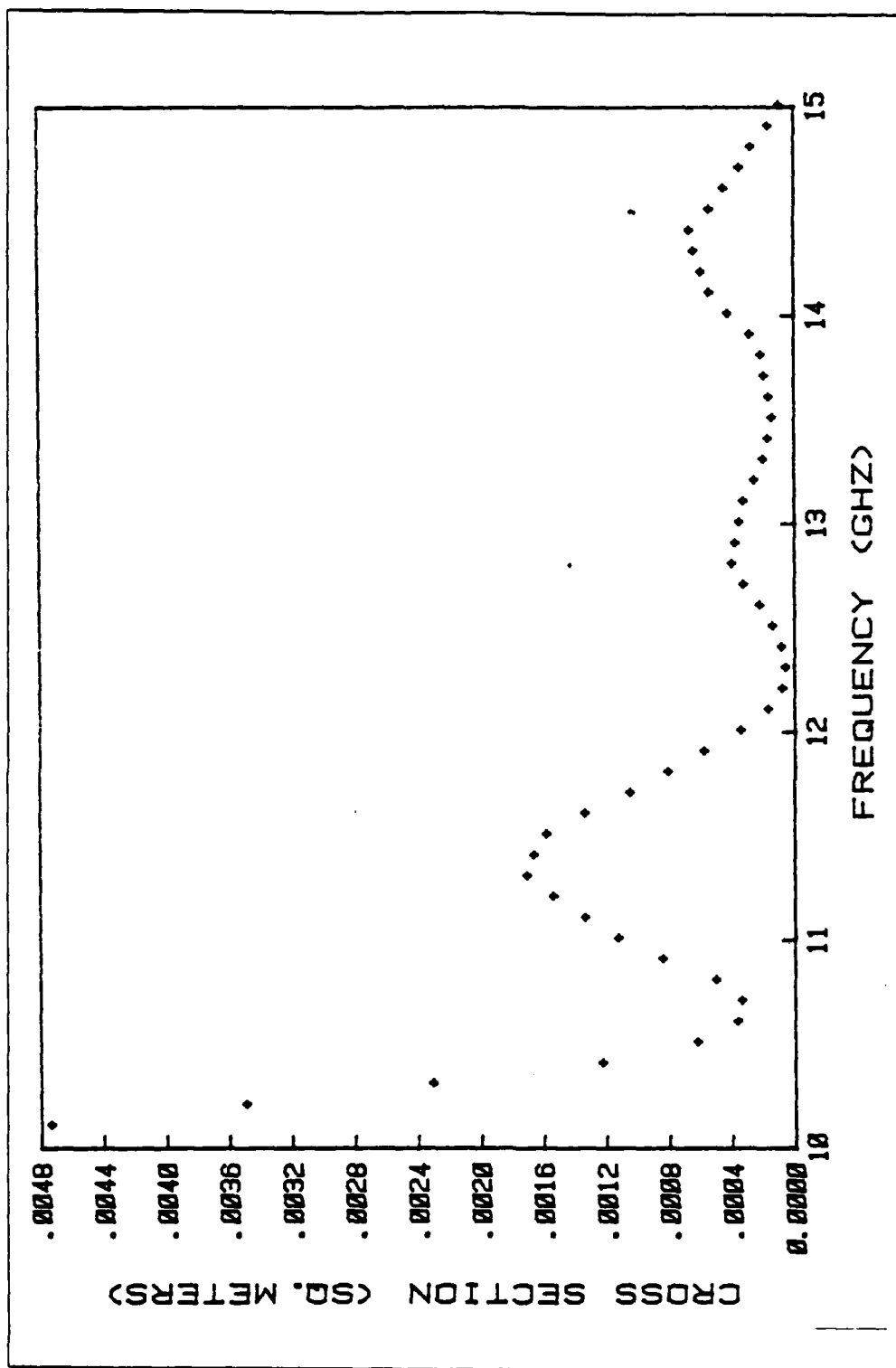


Figure 3.16 Cylinder 12 : Cross-section

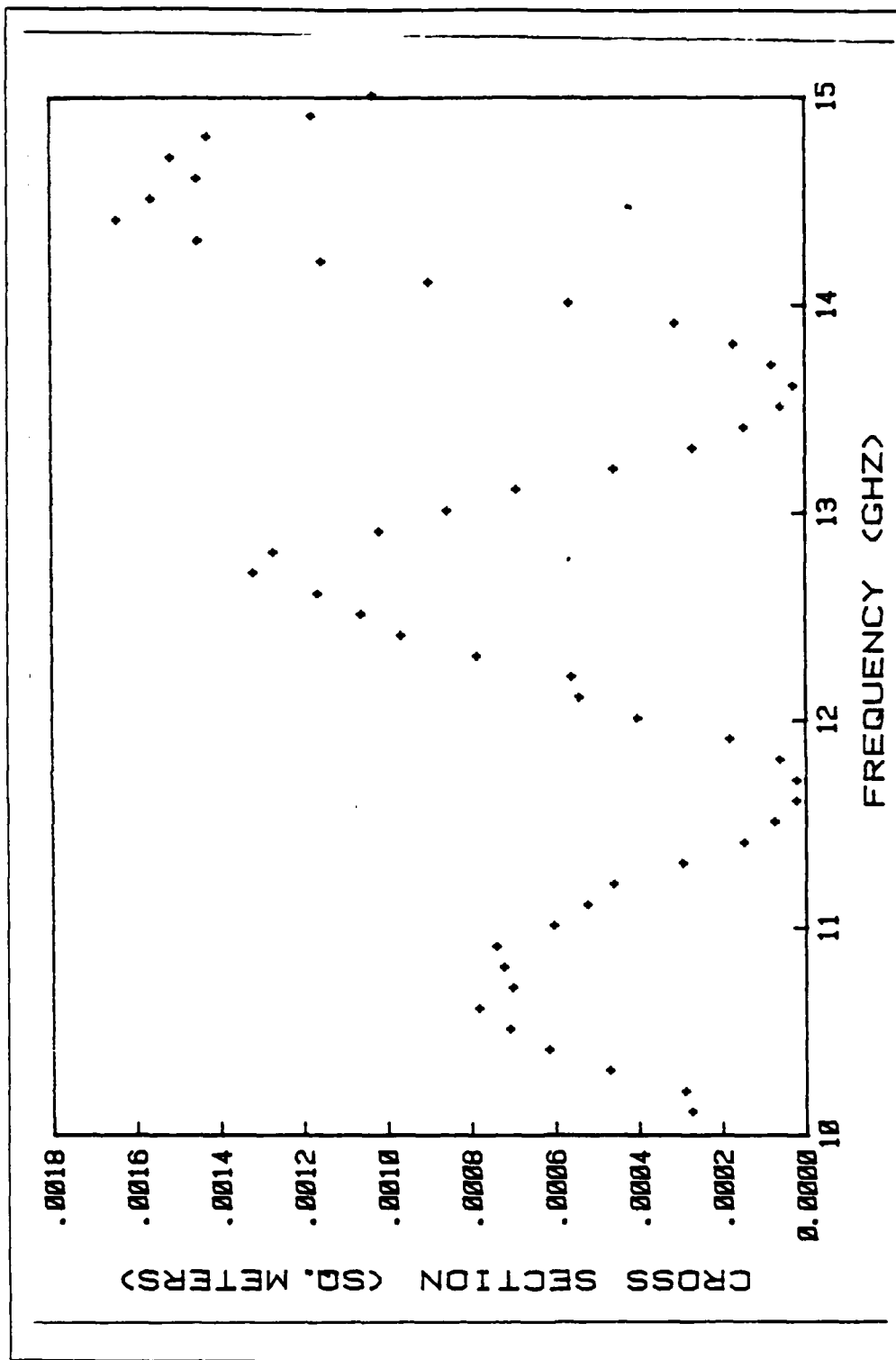


Figure 3.17 Cylinder 13 : Cross-section

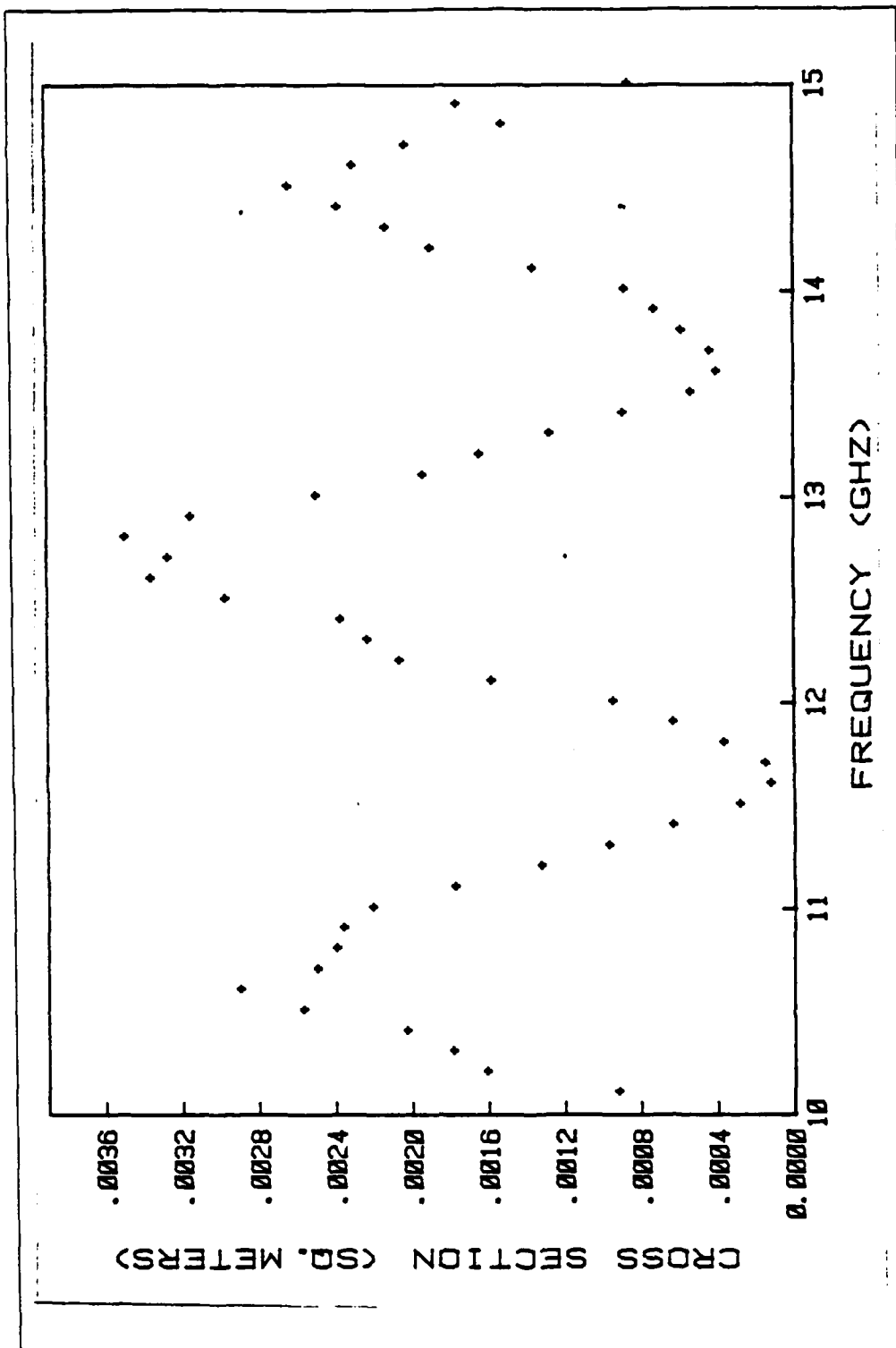


Figure 3.18 Cylinder 14 : Cross-section

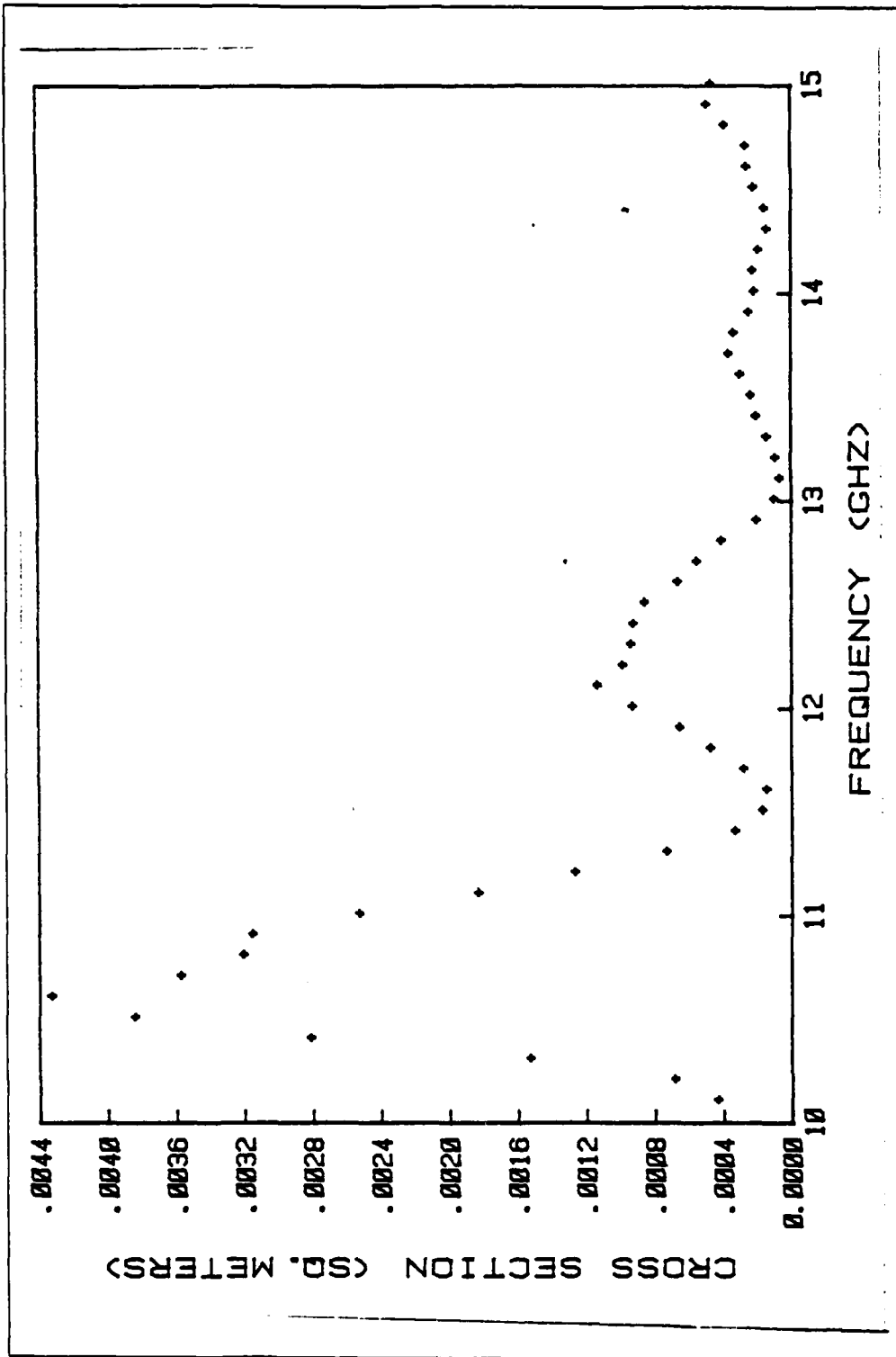


Figure 3.19 Cylinder 15 : Cross-section

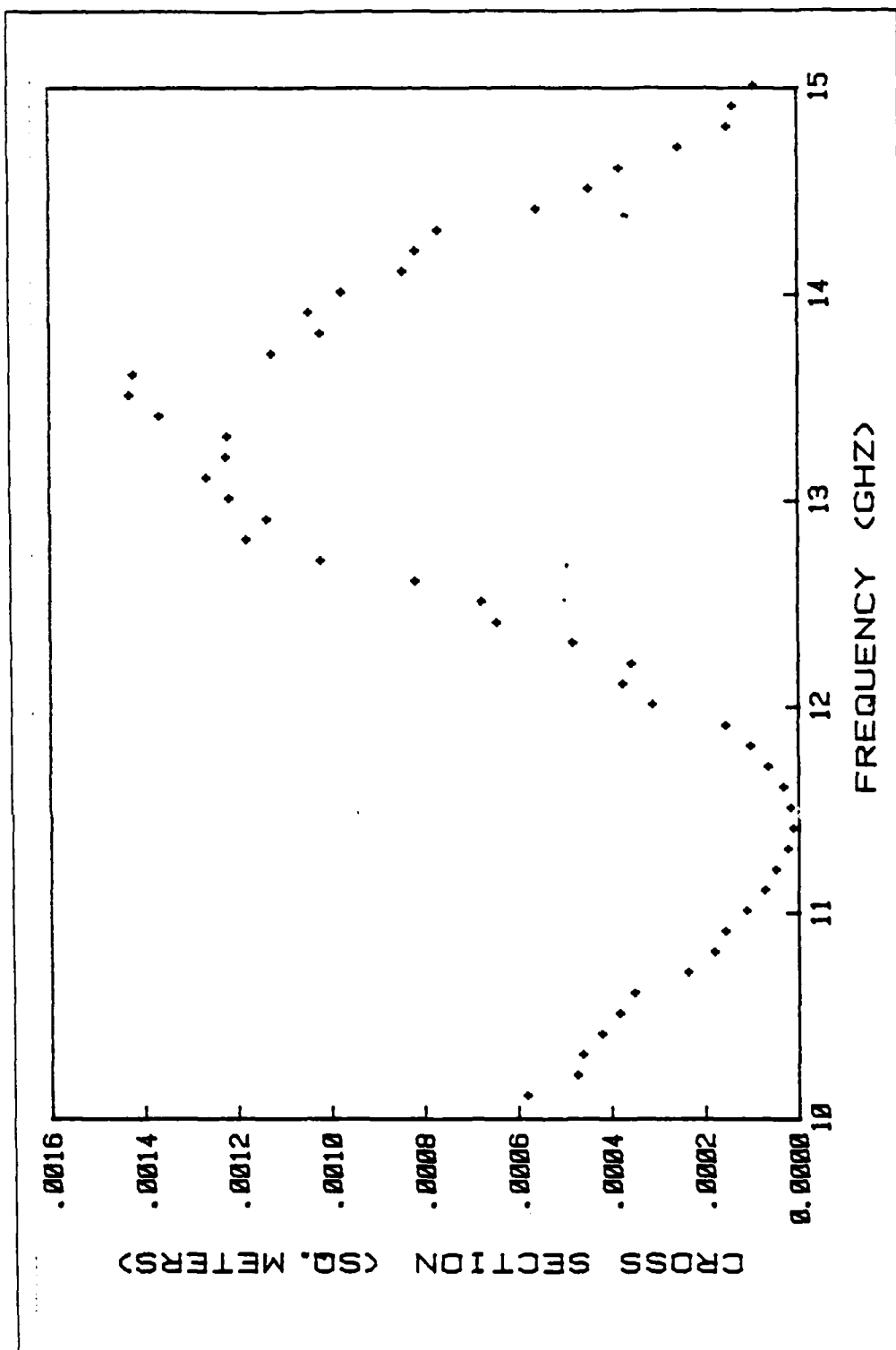


Figure 3.20 Cylinder 16 : Cross-section

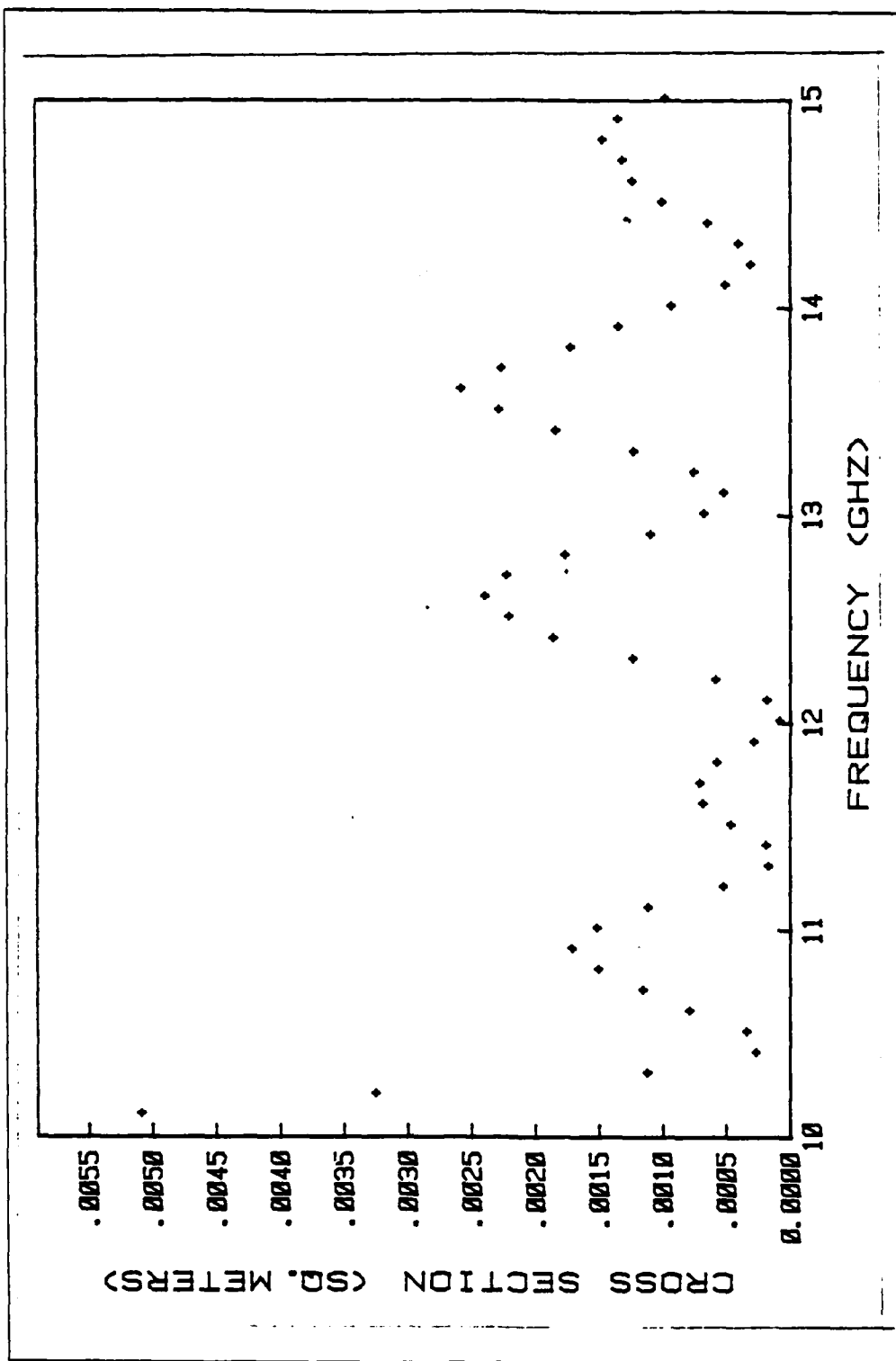


Figure 3.21 Cylinder 17 : Cross-section

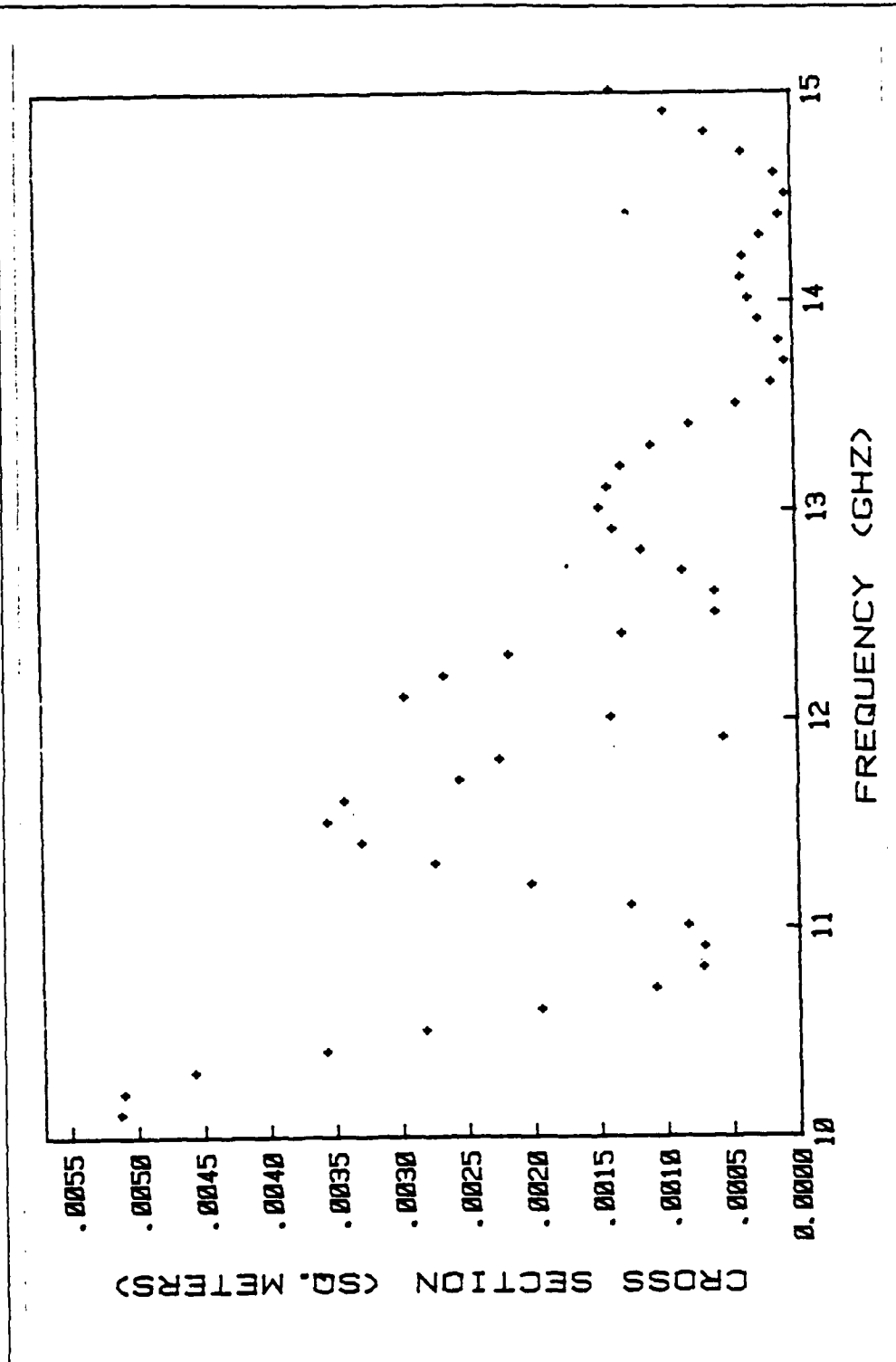


Figure 3.22 Cylinder 18 : Cross-section

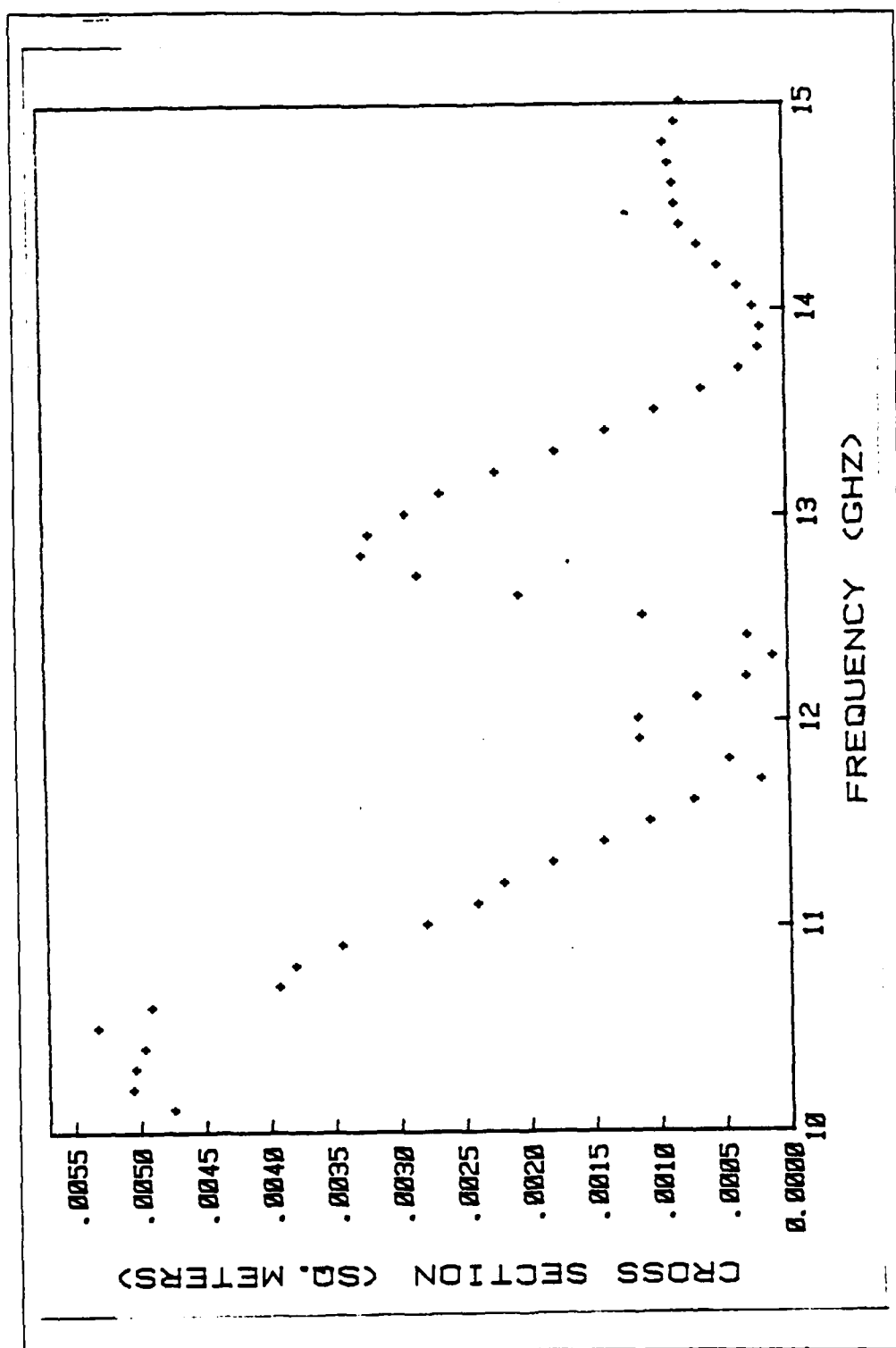


Figure 3.23 Cylinder 19 : Cross-section

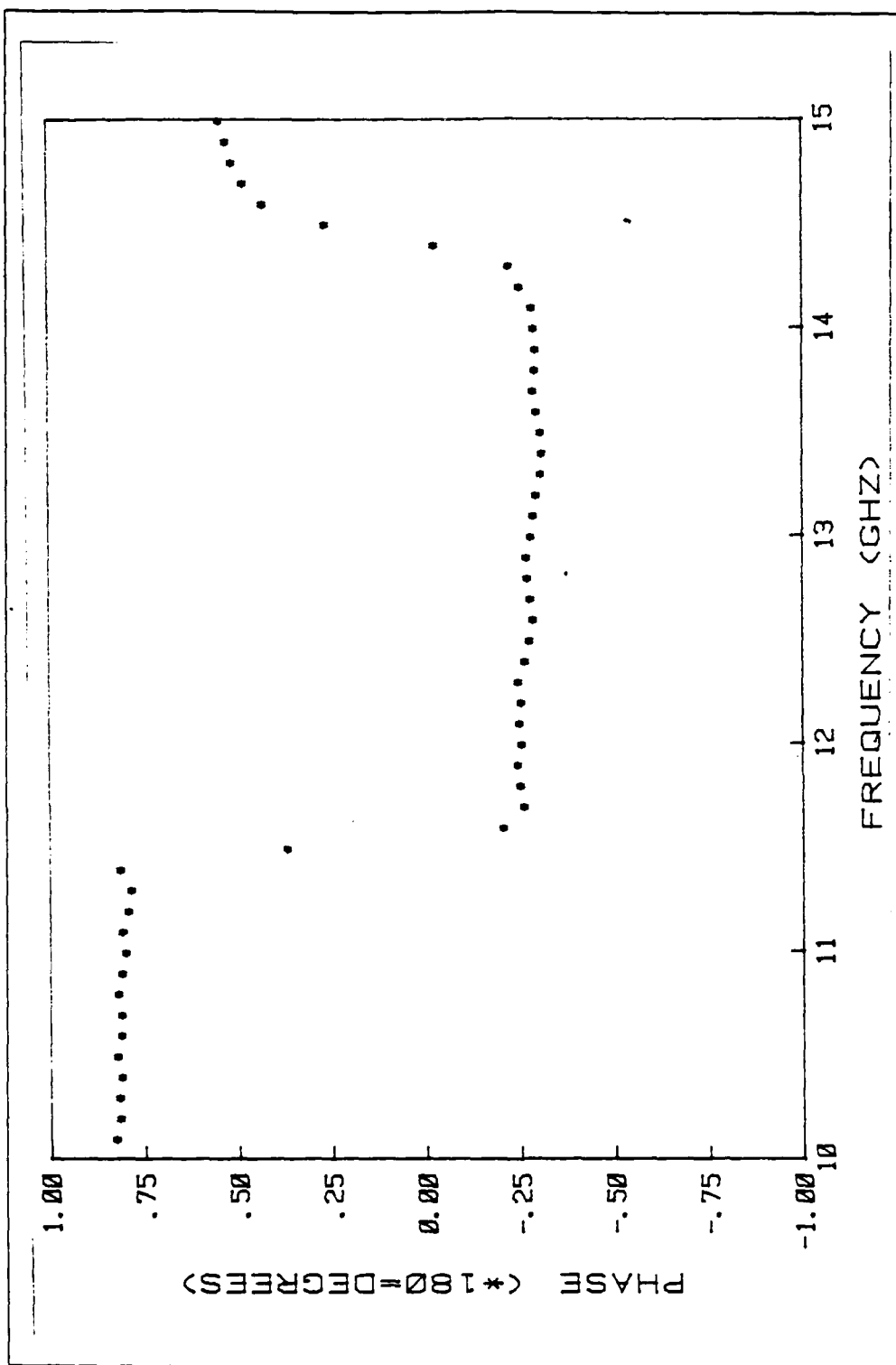


Figure 3.24 Cylinder 1 : Phase

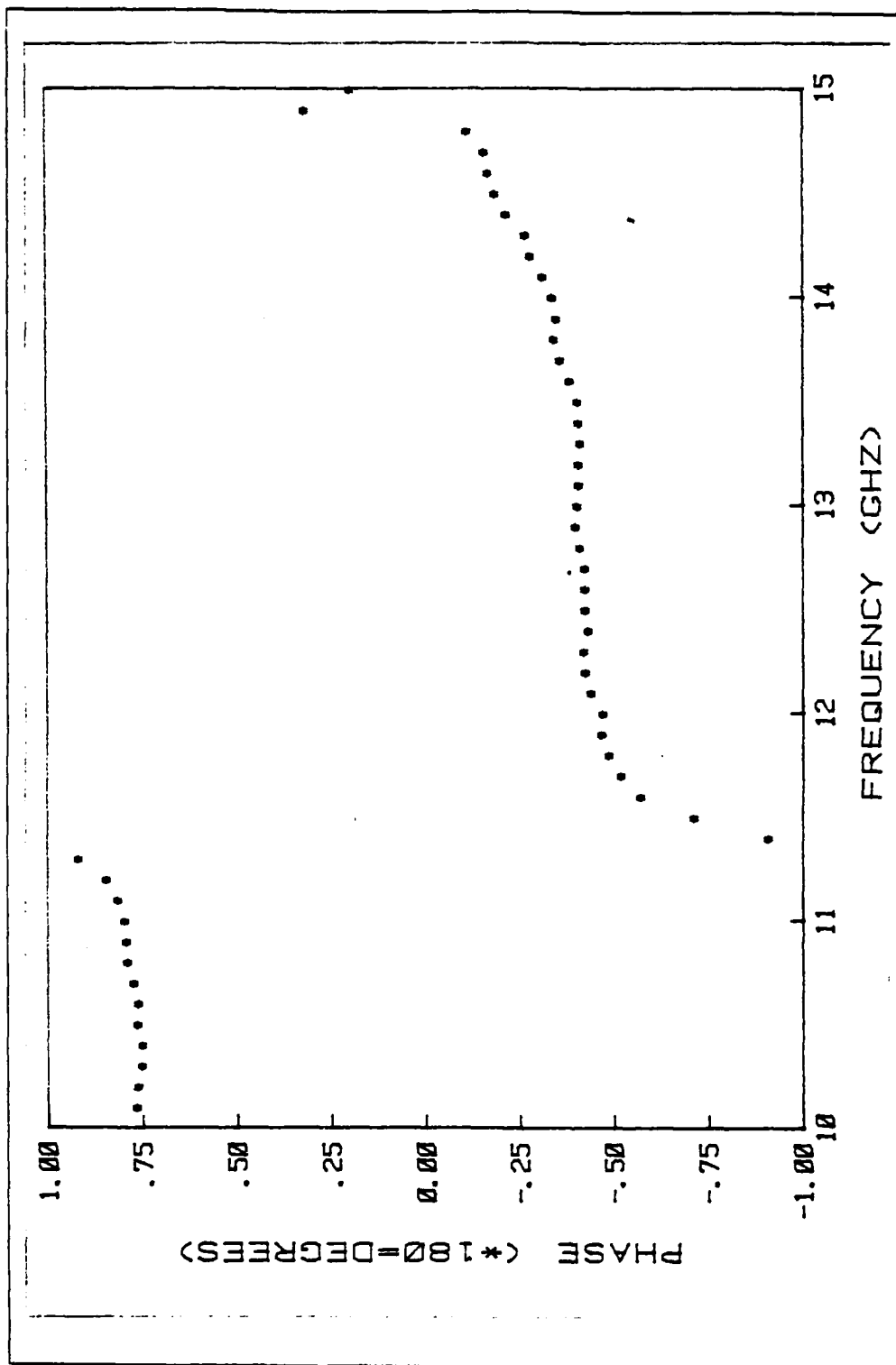


Figure 3.25 Cylinder 2 : Phase

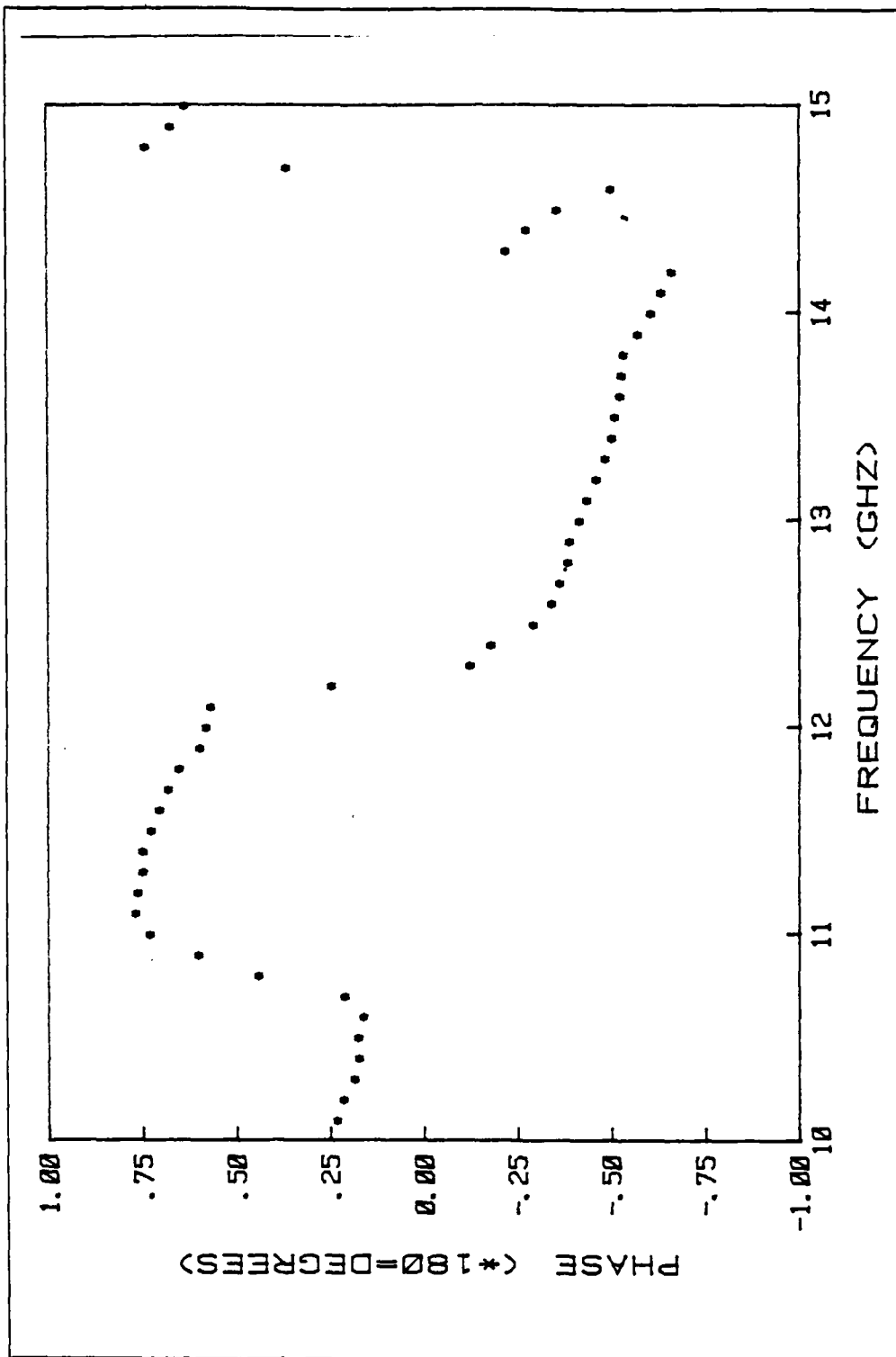


Figure 3.26 Cylinder 3 : Phase

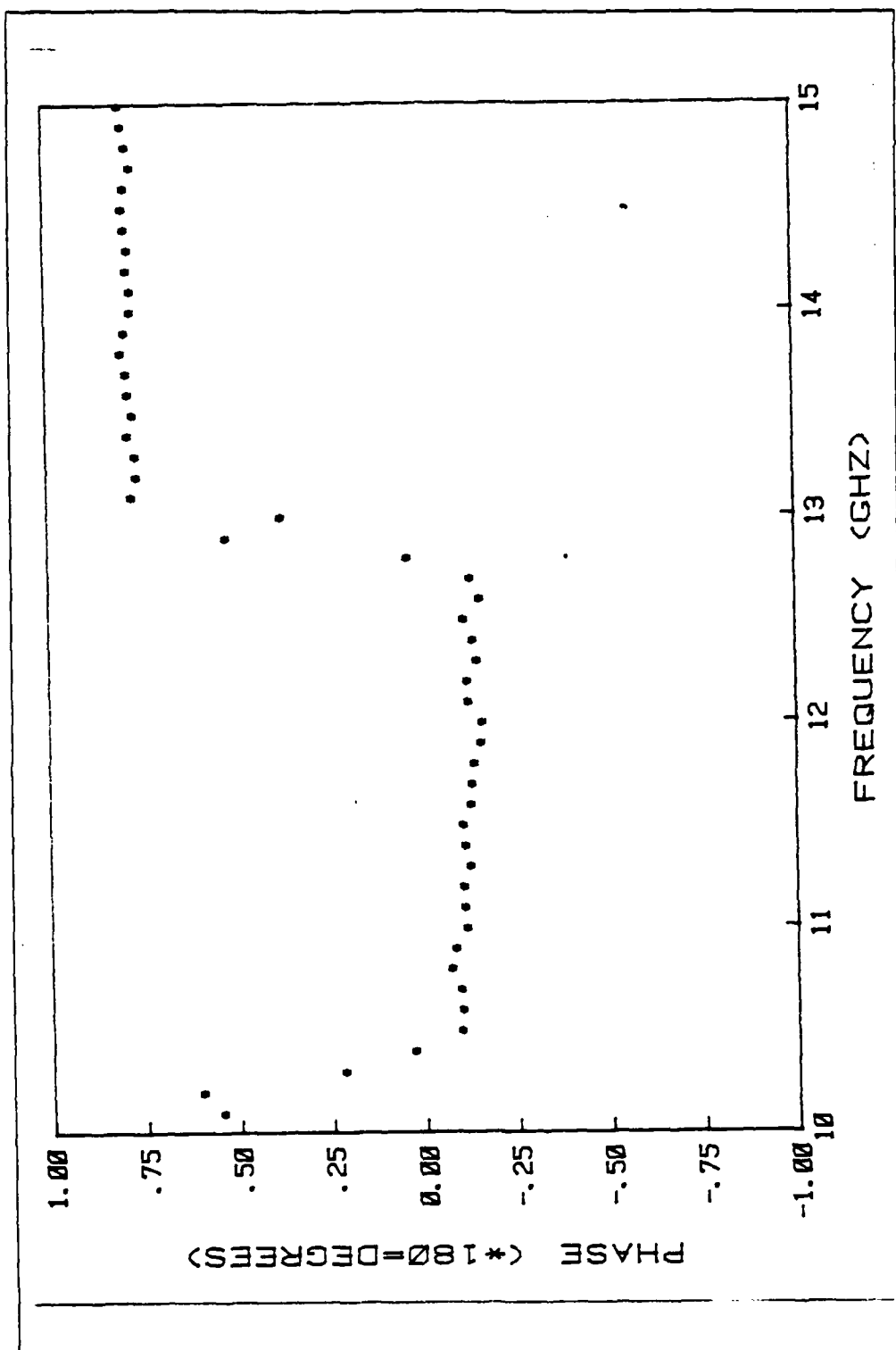


Figure 3.27 Cylinder 4 : Phase

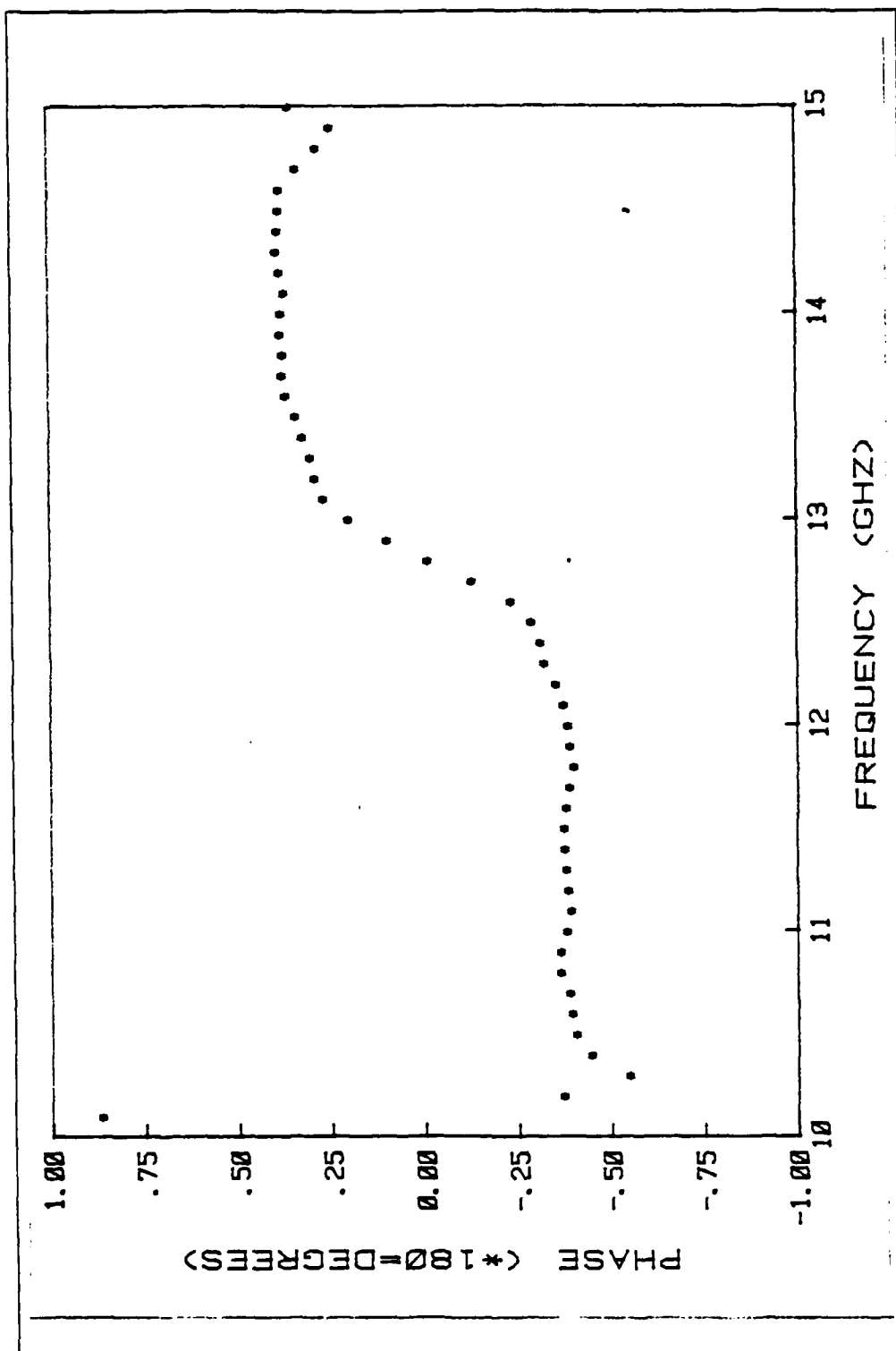


Figure 3.28 Cylinder 5 : Phase

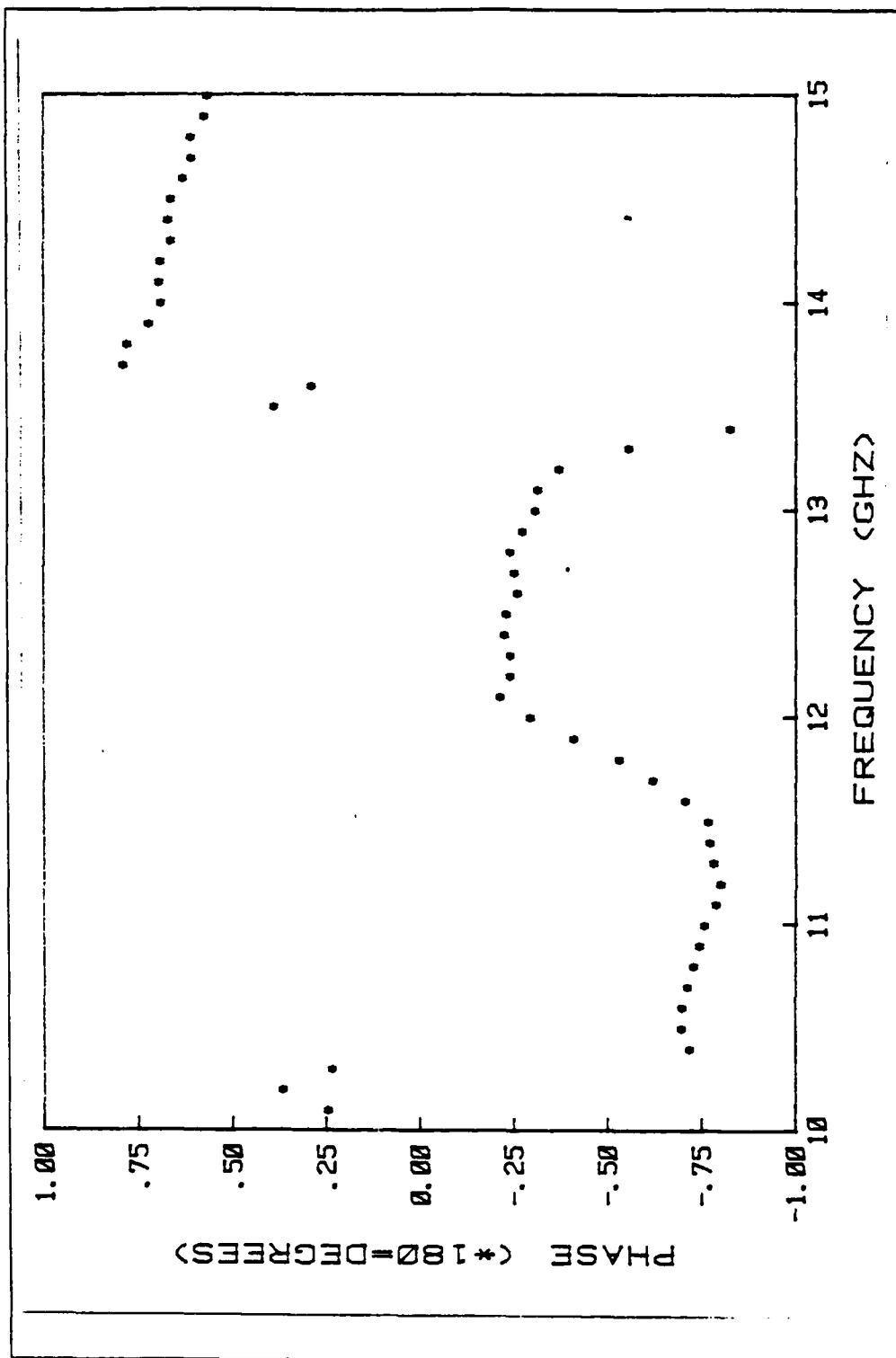


Figure 3.29 Cylinder 6 : Phase

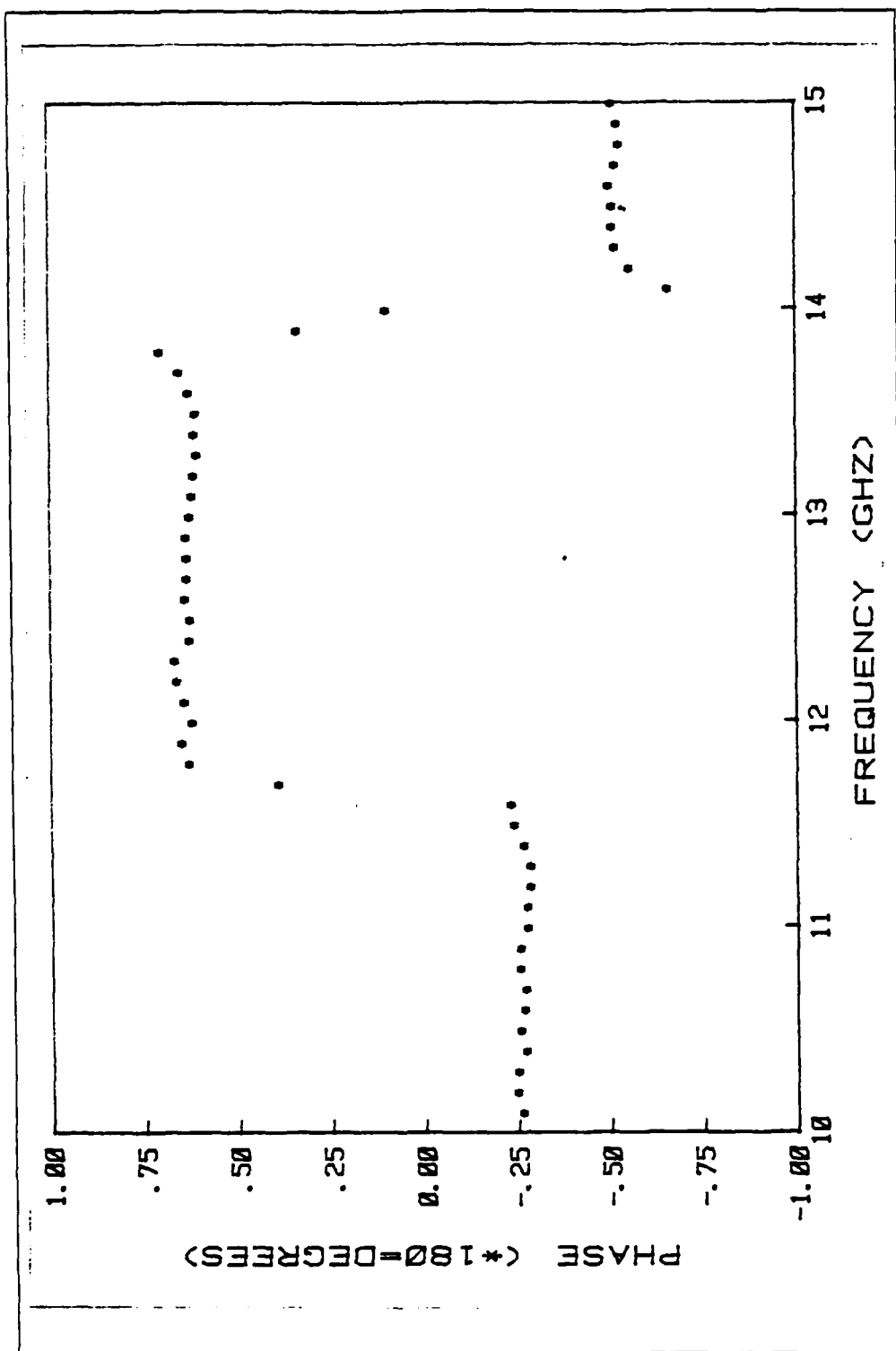


Figure 3.30 Cylinder 7 : Phase

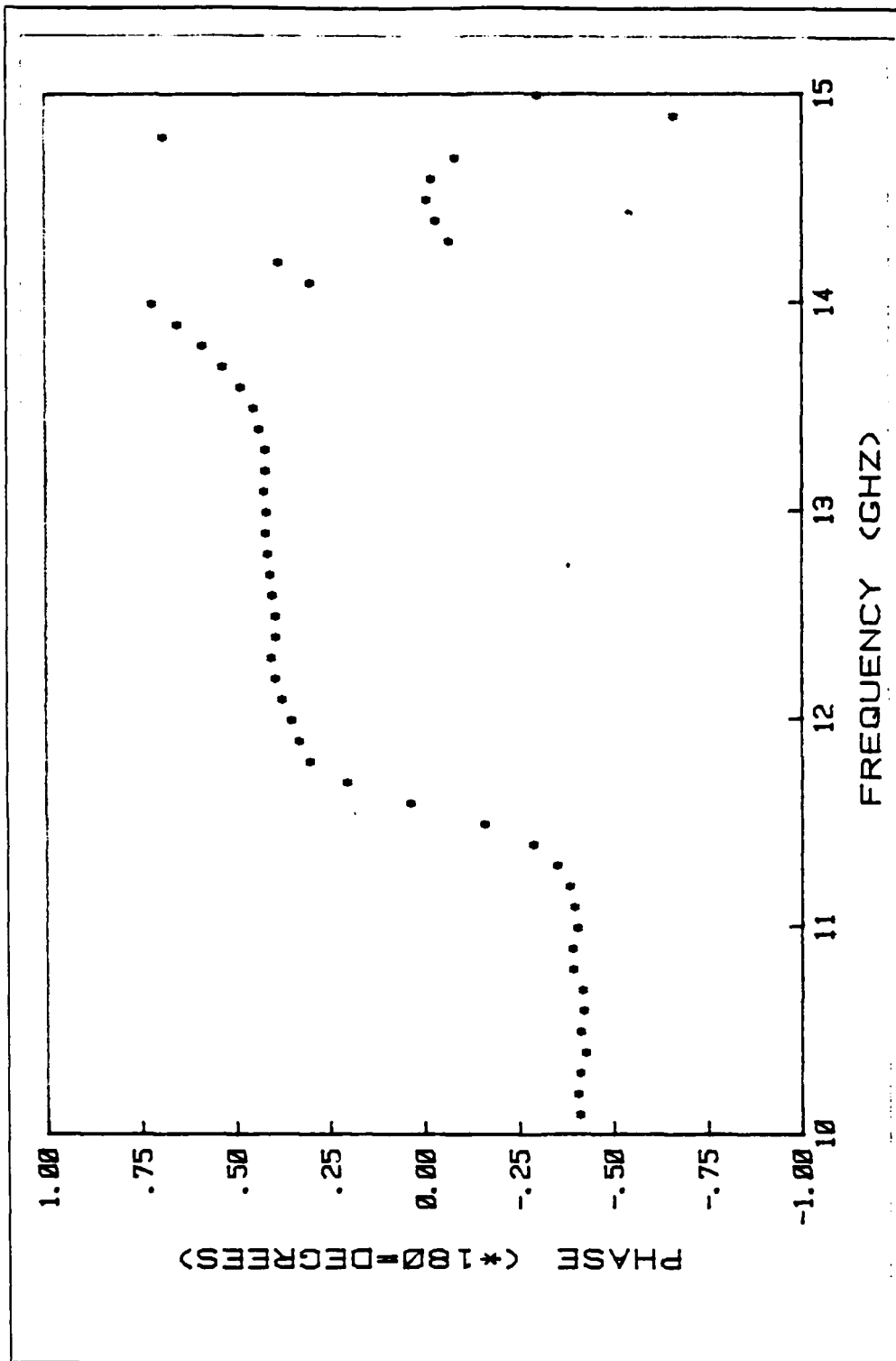


Figure 3.31 Cylinder 8 : Phase

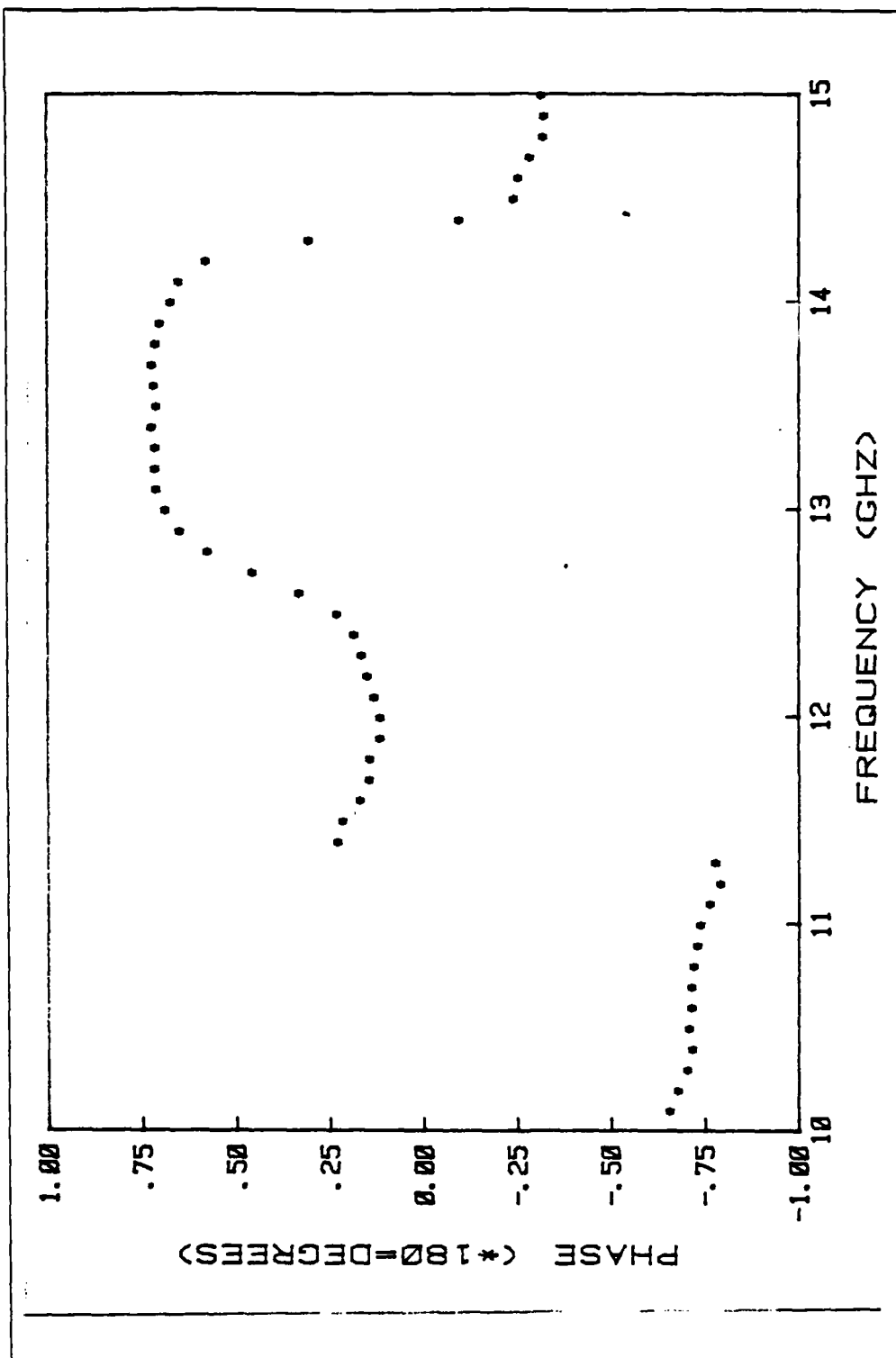


Figure 3.32 Cylinder 9 : Phase

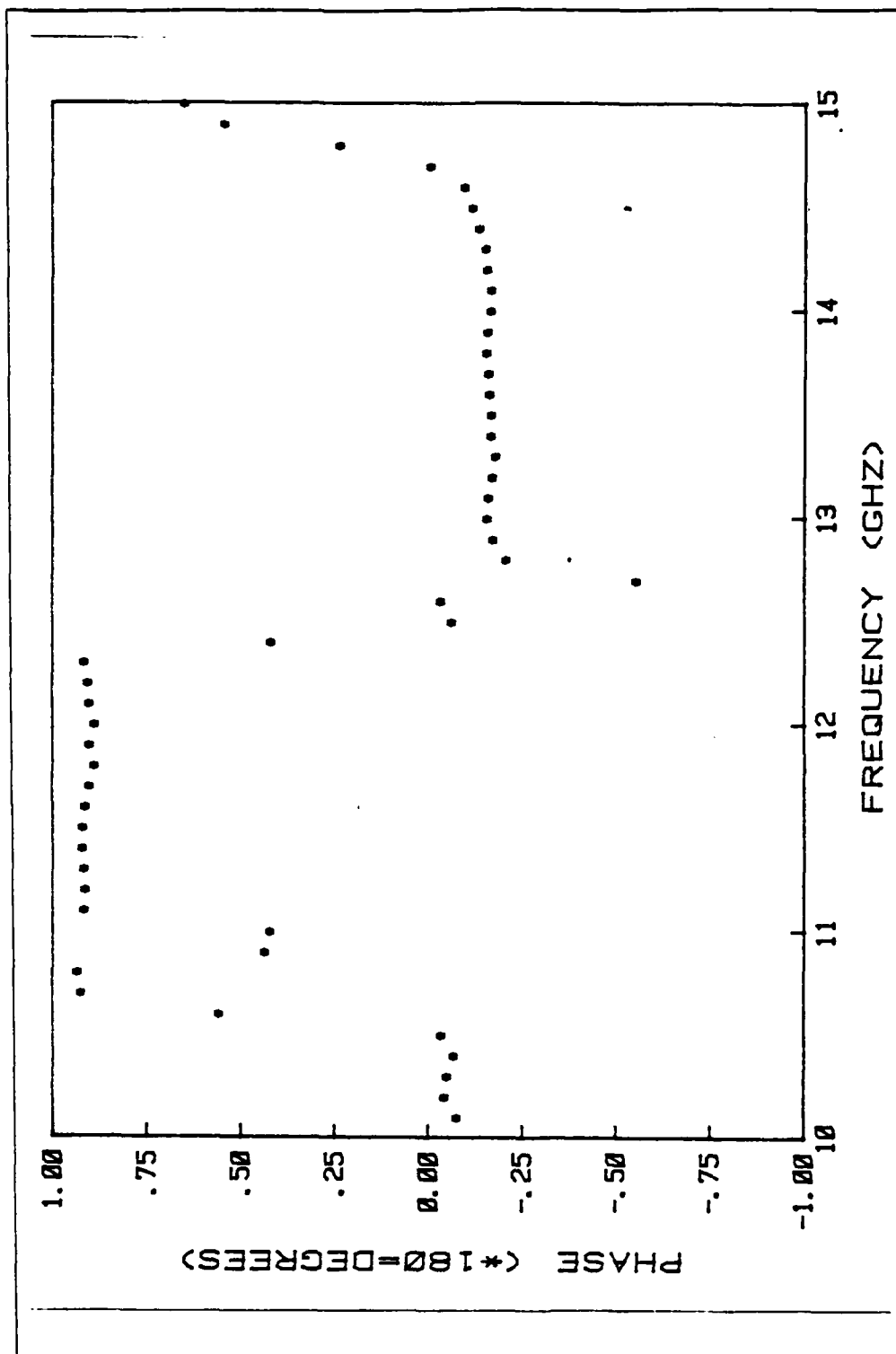


Figure 3.33 Cylinder 10 : Phase

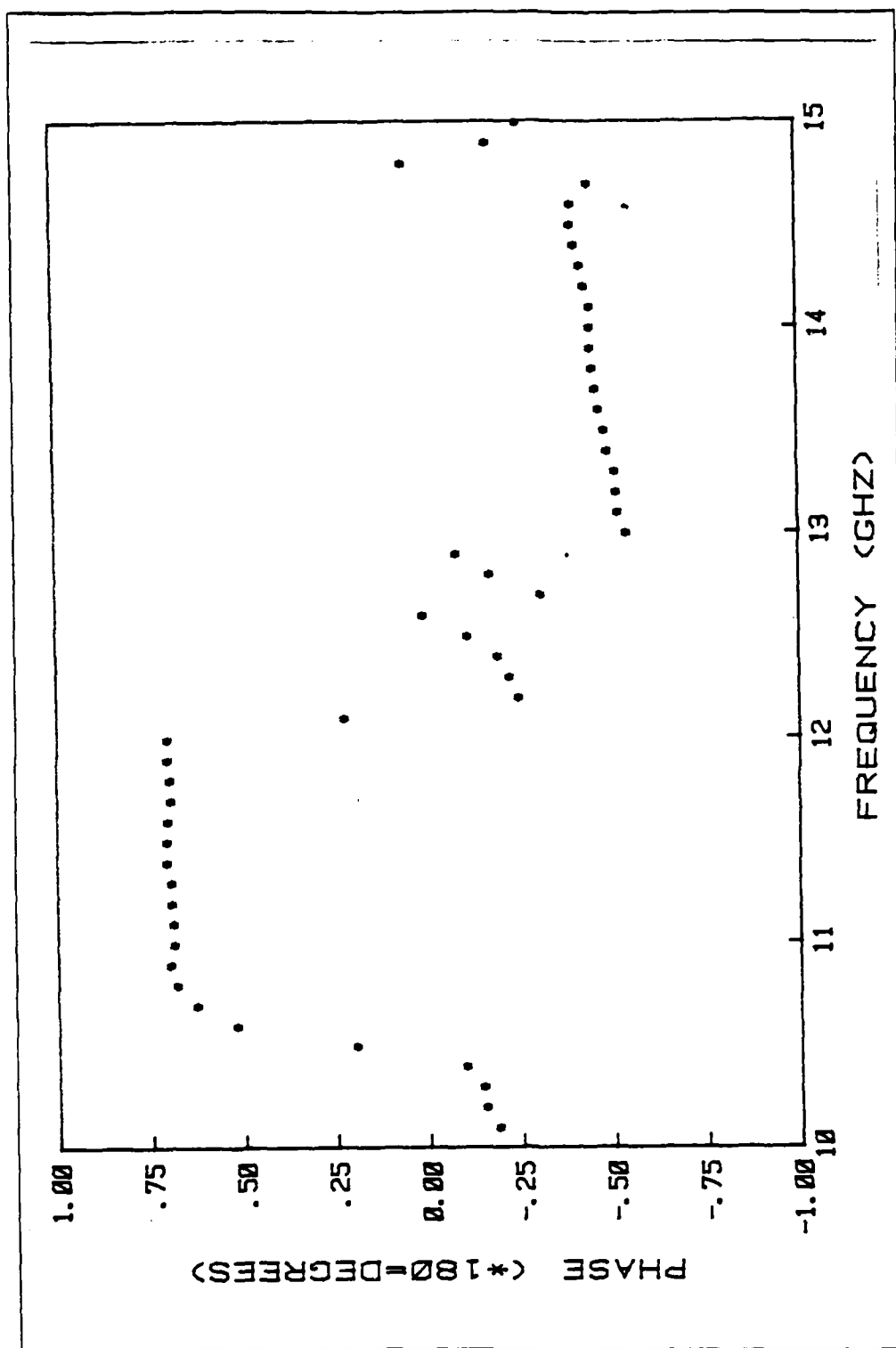


Figure 3.34 Cylinder 11 : Phase

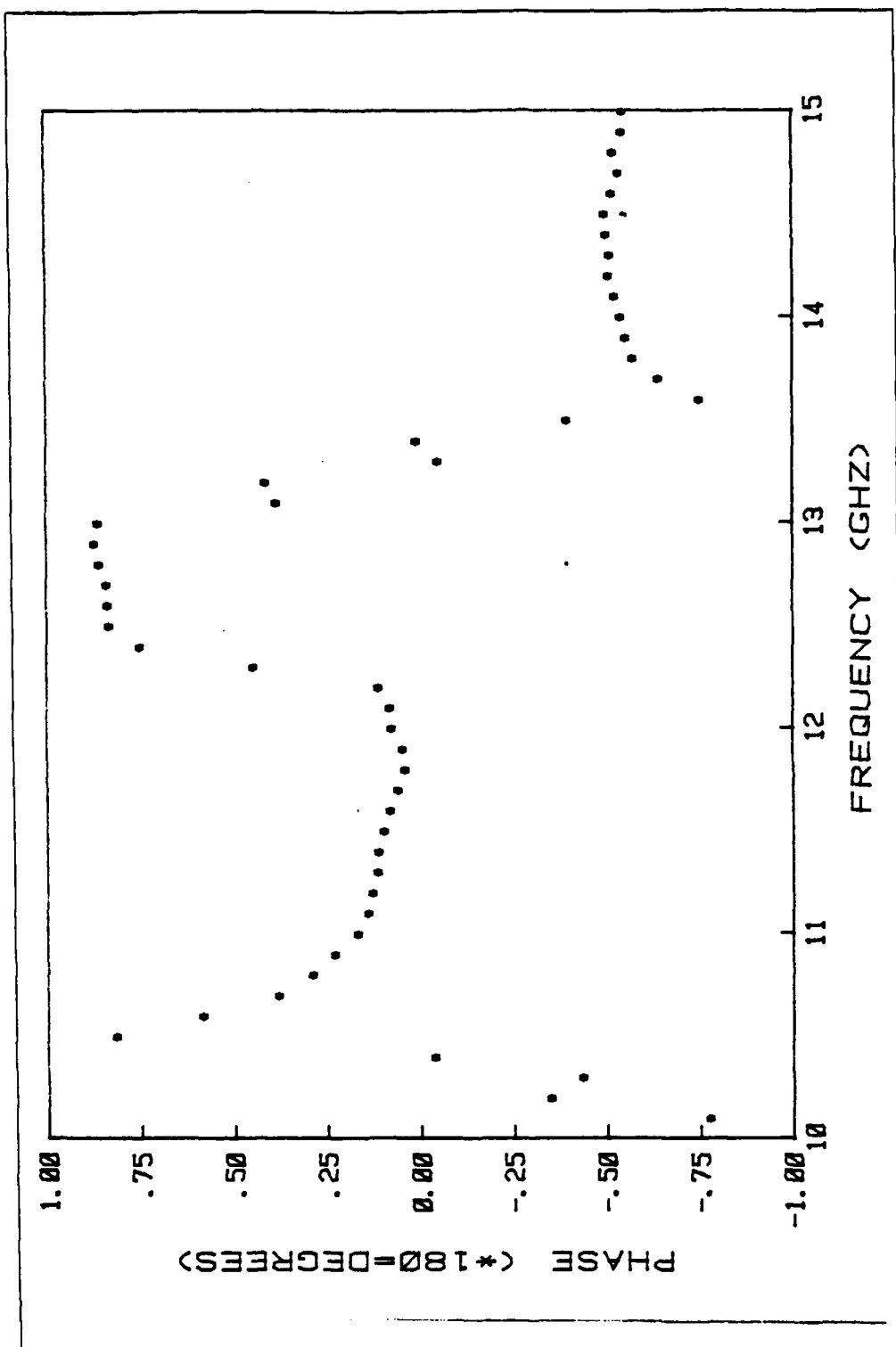


Figure 3.35 Cylinder 12 : Phase

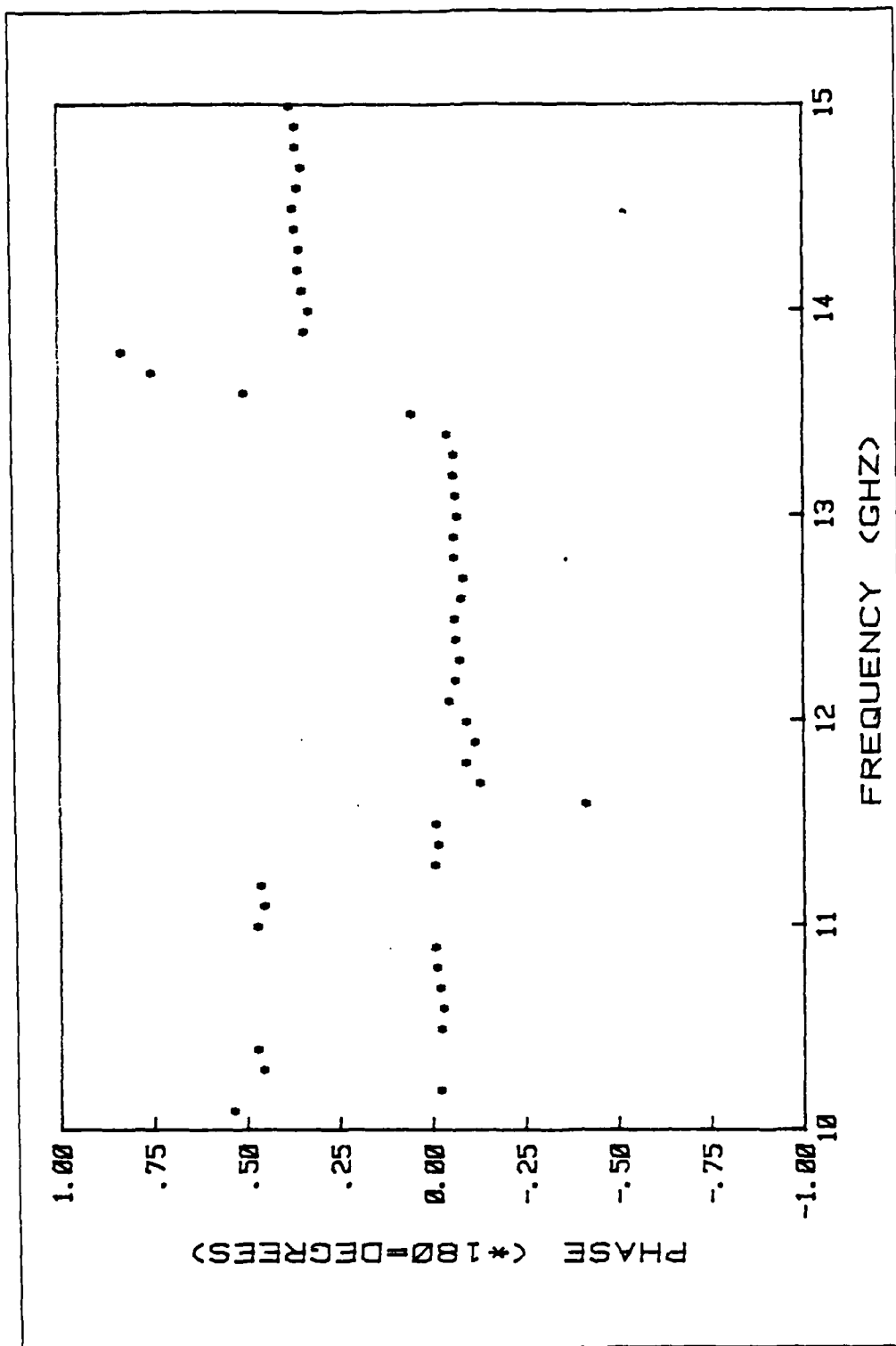


Figure 3.36 Cylinder 13 : Phase

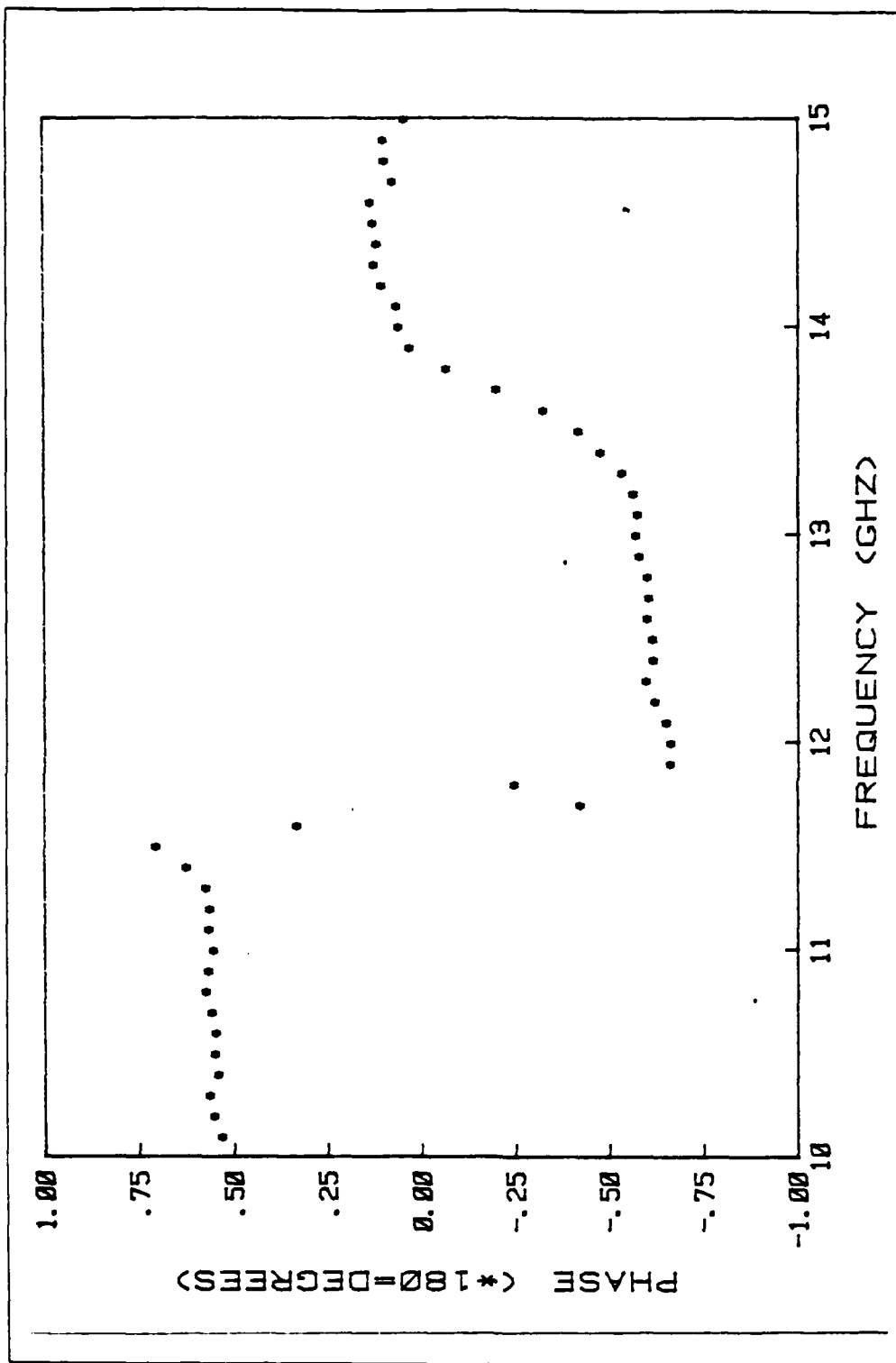


Figure 3.37 Cylinder 14 : Phase

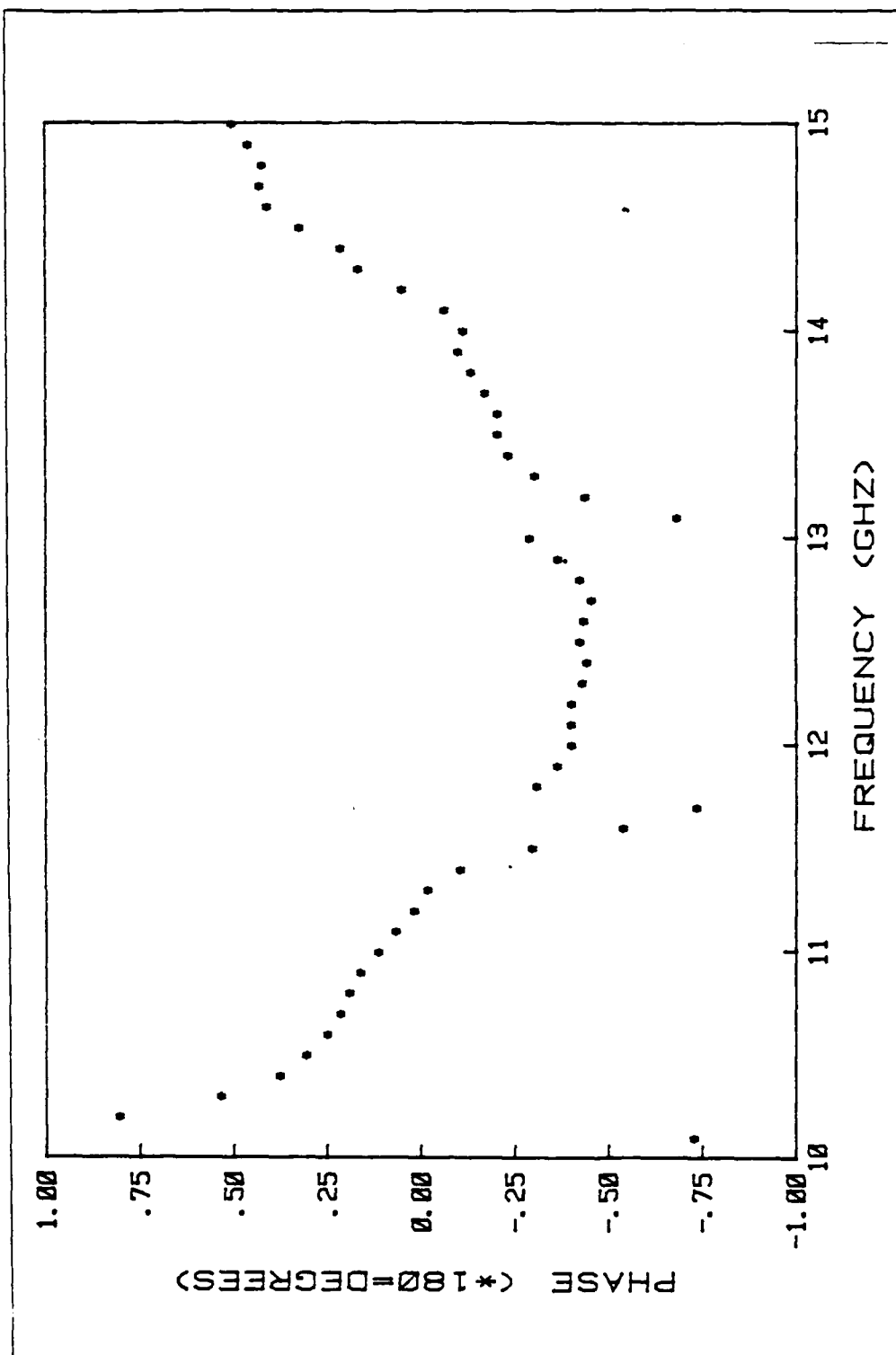


Figure 3.38 Cylinder 15 : Phase

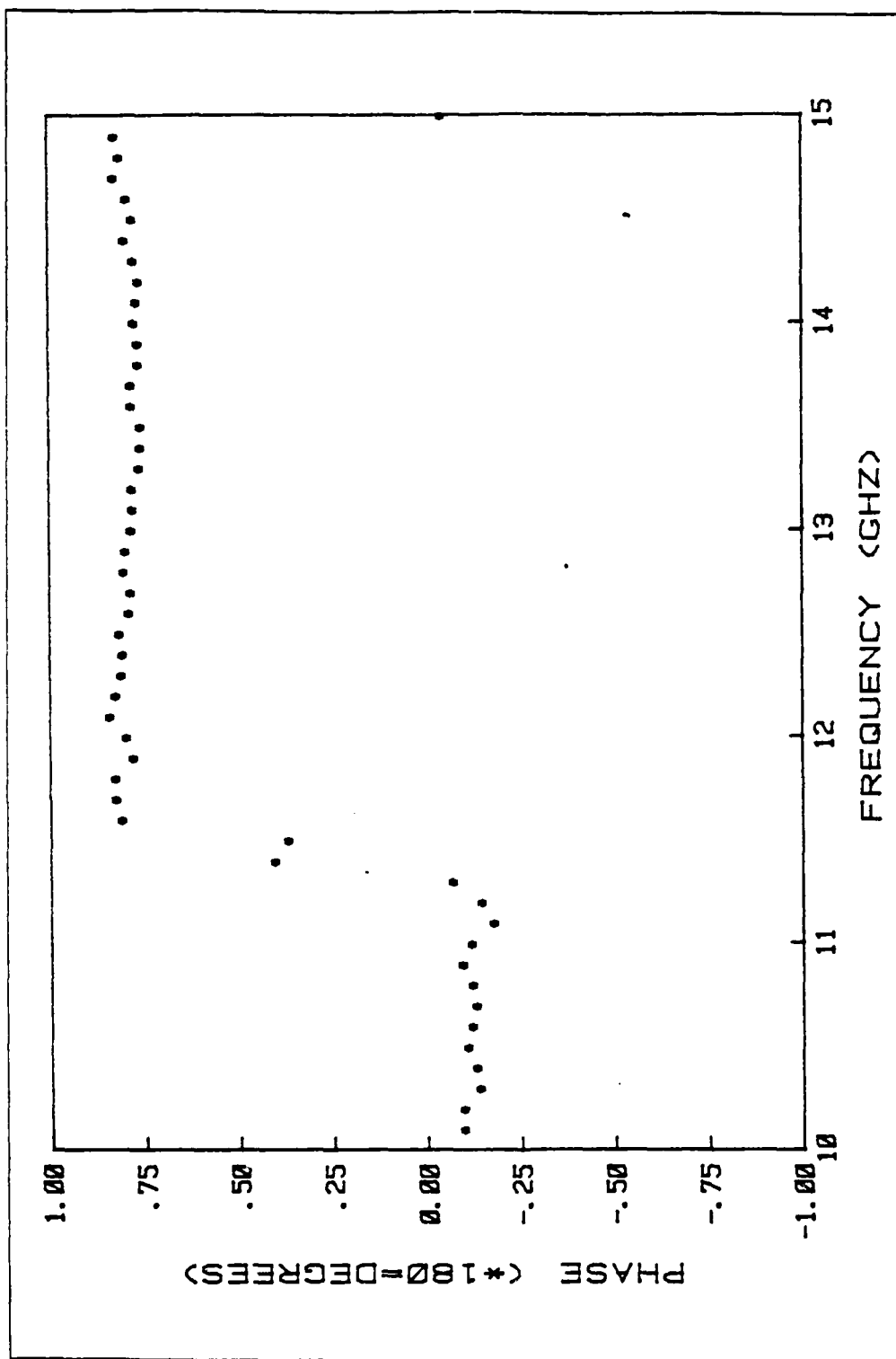


Figure 3.39 Cylinder 16 : Phase

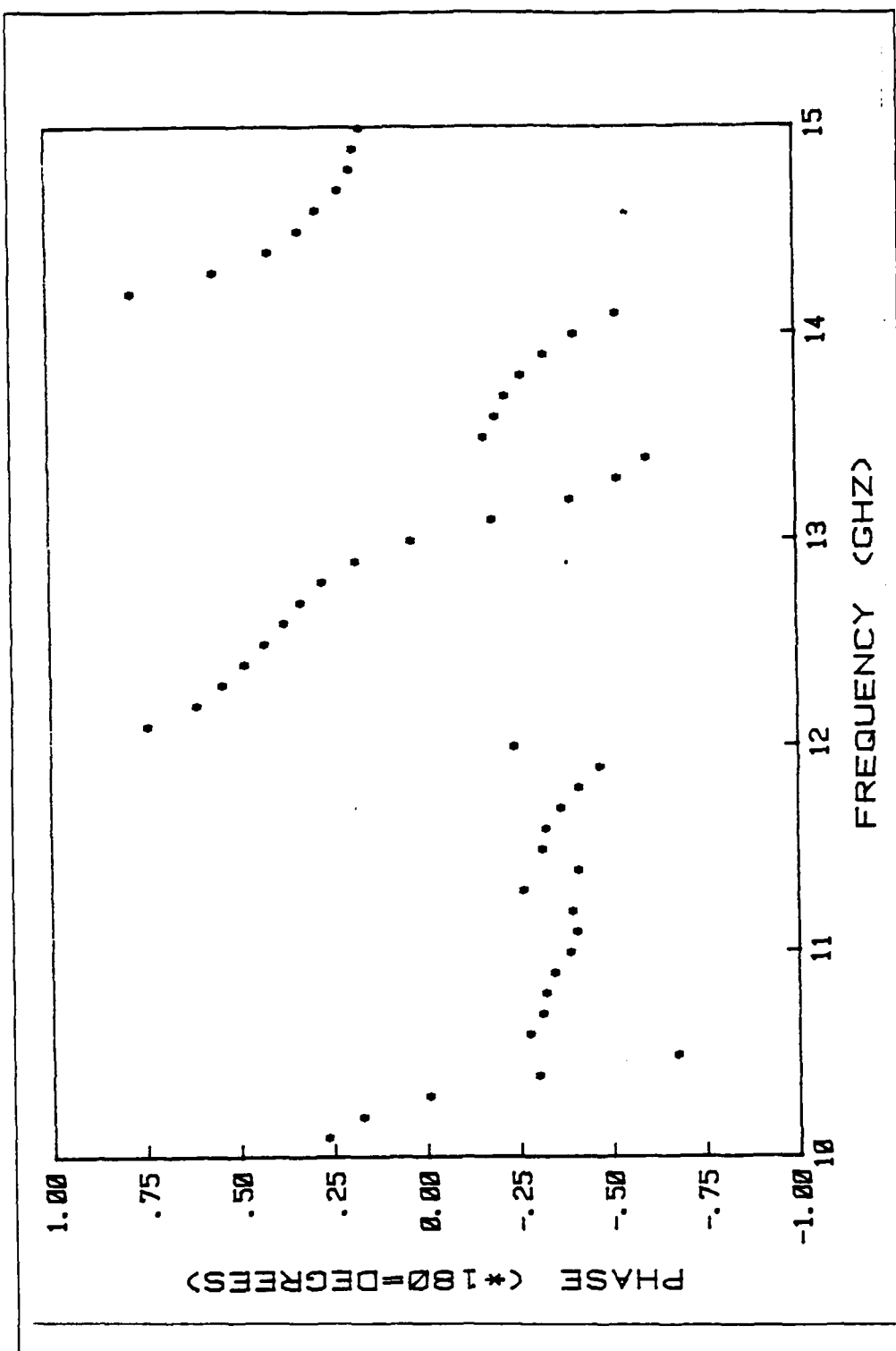


Figure 3.40 Cylinder 17 : Phase

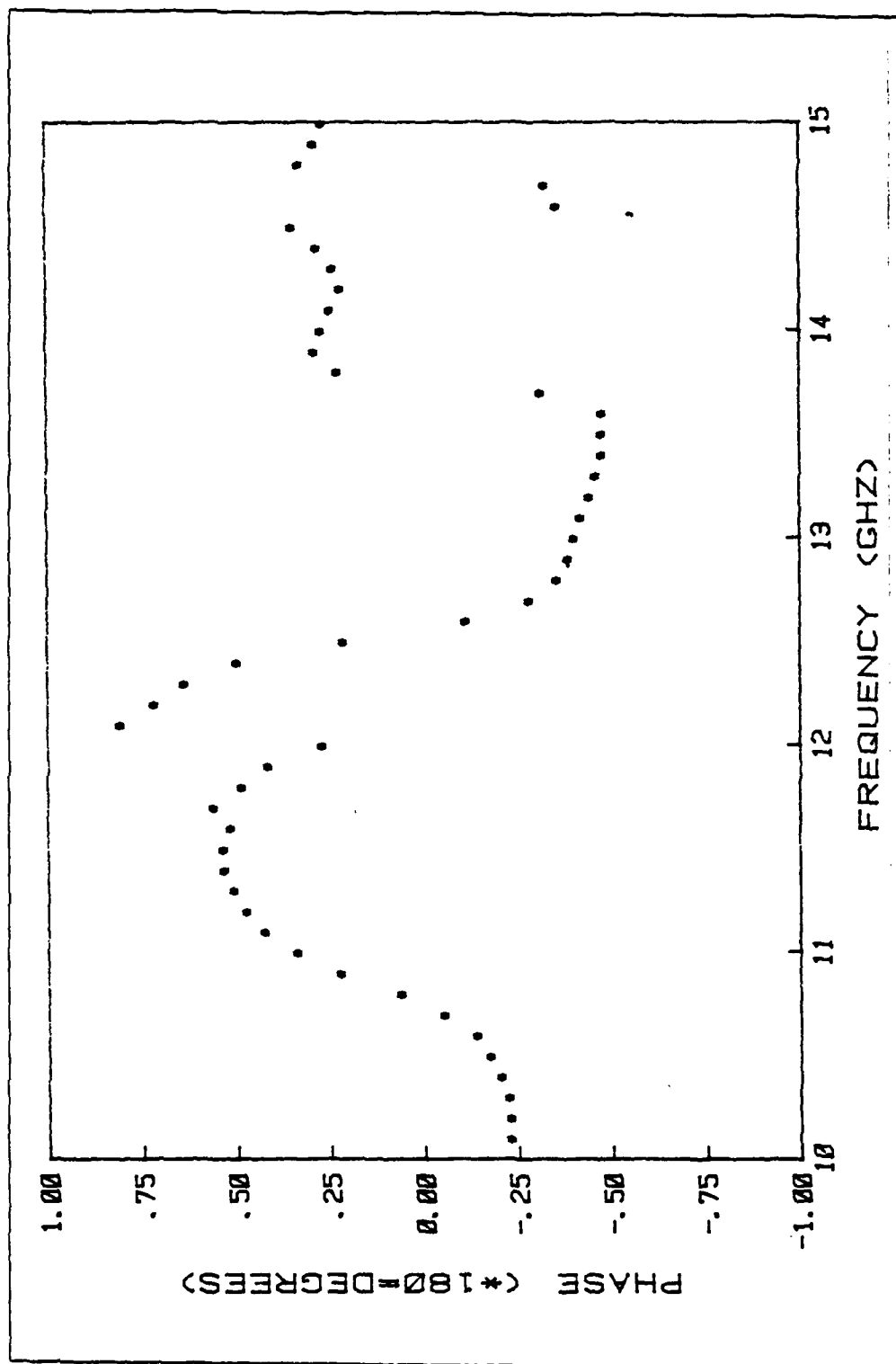


Figure 3.41 Cylinder 18 : Phase

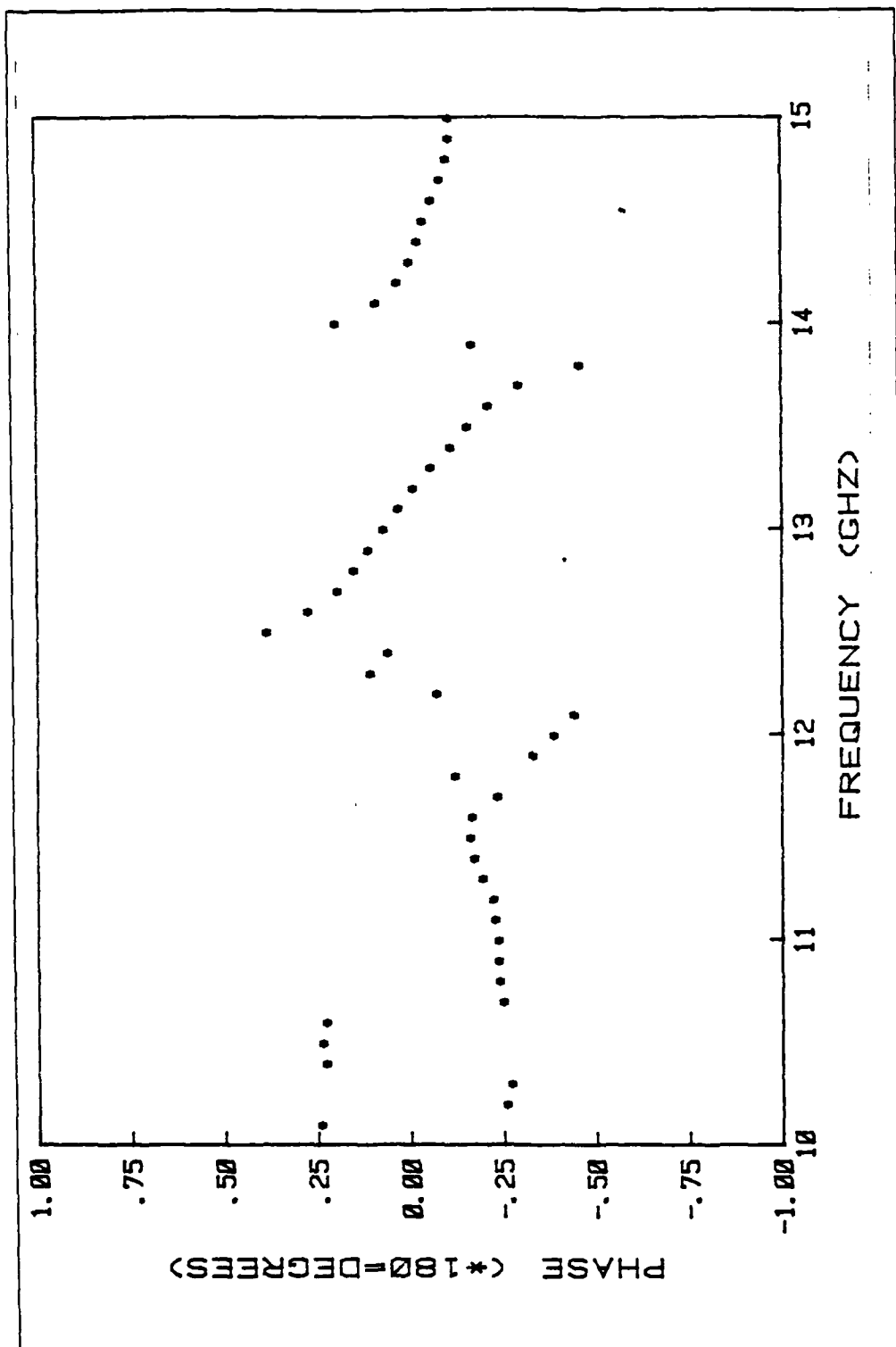


Figure 3.42 Cylinder 19 : Phase

TABLE IV
CYLINDER 1 : MEASUREMENT DATA

FREQ (GHZ)	CRSEC (SCR. METER)	PHASE (DEG /180)
10.10	00067	81100
10.20	00079	80115
10.30	00073	80277
10.40	00066	79728
10.50	00069	80771
10.60	00068	79765
10.70	00053	79672
10.80	00044	80615
10.90	00037	79443
11.00	00030	78492
11.10	00032	79346
11.20	00015	77824
11.30	00009	77119
11.40	00004	79891
11.50	00001	35530
11.60	00000	- 21900
11.70	00002	- 27320
11.80	00006	- 26422
11.90	00015	- 25851
12.00	00024	- 26311
12.10	00032	- 26265
12.20	00044	- 26705
12.30	00056	- 25354
12.40	00066	- 27605
12.50	00079	- 26872
12.60	00095	- 29899
12.70	00106	- 29000
12.80	00123	- 28417
12.90	00127	- 28039
13.00	00127	- 29366
13.10	00127	- 29346
13.20	00119	- 30808
13.30	00117	- 32000
13.40	00115	- 32387
13.50	00107	- 32066
13.60	00097	- 30809
13.70	00079	- 30090
13.80	00059	- 30413
13.90	00047	- 30695
14.00	00034	- 30177
14.10	00025	- 29744
14.20	00014	- 26515
14.30	00007	- 23605
14.40	00003	- 03994
14.50	00002	25038
14.60	00005	41404
14.70	00013	46770
14.80	00024	49523
14.90	00036	51192
15.00	00052	52885

TABLE V
CYLINDER 2 : MEASUREMENT DATA

FREQ (GHZ)	CRSEC (SQ. METER)	PHASE (DEG./180)
10.10	00243	75042
10.20	00253	74758
10.30	00229	73692
10.40	00211	73600
10.50	00201	74873
10.60	00180	74620
10.70	00137	75941
10.80	00112	77473
10.90	00092	77653
11.00	00067	78308
11.10	00045	80012
11.20	00029	83111
11.30	00017	90352
11.40	00010	- 92217
11.50	00009	- 72678
11.60	00015	- 58633
11.70	00030	- 53223
11.80	00054	- 50119
11.90	00077	- 48089
12.00	00117	- 48458
12.10	00150	- 45457
12.20	00168	- 43847
12.30	00185	- 43560
12.40	00214	- 44482
12.50	00242	- 43857
12.60	00265	- 43844
12.70	00300	- 43706
12.80	00344	- 42522
12.90	00329	- 41176
13.00	00313	- 41793
13.10	00308	- 42205
13.20	00289	- 42141
13.30	00278	- 42609
13.40	00273	- 42103
13.50	00260	- 41851
13.60	00245	- 39668
13.70	00209	- 37251
13.80	00156	- 35734
13.90	00133	- 36180
14.00	00124	- 35231
14.10	00113	- 32577
14.20	00088	- 29377
14.30	00077	- 28123
14.40	00071	- 22931
14.50	00050	- 20034
14.60	00039	- 18170
14.70	00030	- 17233
14.80	00014	- 12712
14.90	00020	30304
15.00	00073	18100

TABLE VI
CYLINDER 3 : MEASUREMENT DATA

FREQ (GHZ)	CRSEC (SQR. METER)	PHASE (DEG./180)
10.10	00248	21671
10.20	00226	13965
10.30	00180	16965
10.40	00134	15911
10.50	00096	15977
10.60	00055	14575
10.70	00016	19677
10.80	00008	42554
10.90	00010	58653
11.00	00018	71527
11.10	00036	75428
11.20	00057	74765
11.30	00069	73491
11.40	00075	73467
11.50	00073	71169
11.60	00062	68985
11.70	00053	66575
11.80	00042	63823
11.90	00030	58250
12.00	00020	56590
12.10	00009	55353
12.20	00003	23130
12.30	00004	- 13730
12.40	00009	- 19358
12.50	00020	- 30593
12.60	00041	- 35545
12.70	00058	- 37592
12.80	00086	- 39823
12.90	00102	- 40210
13.00	00118	- 42857
13.10	00132	- 44989
13.20	00139	- 47454
13.30	00151	- 49879
13.40	00165	- 51511
13.50	00160	- 52388
13.60	00155	- 53717
13.70	00141	- 54123
13.80	00115	- 54749
13.90	00094	- 58524
14.00	00086	- 62113
14.10	00075	- 64749
14.20	00053	- 67578
14.30	00044	- 23328
14.40	00031	- 28767
14.50	00018	- 36955
14.60	00016	- 31350
14.70	00017	- 34736
14.80	00021	- 72350
14.90	00032	- 65684
15.00	00042	- 61797

TABLE VII
CYLINDER 4 : MEASUREMENT DATA

FREQ (GHZ)	CRSEC (SQ. METER)	PHASE (DEG /180)
10.10	.00015	.53061
10.20	.00002	.58500
10.30	.00001	.20200
10.40	.00001	.01606
10.50	.00005	- .11191
10.60	.00011	- .11427
10.70	.00016	- .11172
10.80	.00024	- .08653
10.90	.00034	- .09819
11.00	.00051	- .12872
11.10	.00062	- .12305
11.20	.00073	- .12099
11.30	.00086	- .13990
11.40	.00100	- .12528
11.50	.00097	- .12105
11.60	.00094	- .14149
11.70	.00101	- .14609
11.80	.00093	- .15085
11.90	.00087	- .16902
12.00	.00095	- .17255
12.10	.00079	- .13638
12.20	.00051	- .13333
12.30	.00041	- .16057
12.40	.00036	- .14970
12.50	.00022	- .12691
12.60	.00012	- .16895
12.70	.00006	- .14507
12.80	.00002	.02394
12.90	.00002	.51034
13.00	.00005	.36005
13.10	.00010	.75957
13.20	.00021	.74512
13.30	.00037	.74675
13.40	.00055	.76702
13.50	.00071	.75434
13.60	.00094	.76560
13.70	.00110	.76920
13.80	.00115	.78251
13.90	.00122	.77252
14.00	.00136	.75553
14.10	.00150	.75551
14.20	.00162	.76438
14.30	.00160	.76063
14.40	.00156	.76987
14.50	.00130	.77432
14.60	.00106	.76907
14.70	.00095	.75172
14.80	.00082	.76255
14.90	.00061	.77362
15.00	.00046	.78120

TABLE VIII
CYLINDER 5 : MEASUREMENT DATA

FREQ (GHZ)	CRSEC (SQR. METER)	PHASE (DEG./100)
10.10	.00000	.85126
10.20	.00003	- .38443
10.30	.00005	- .56296
10.40	.00016	- .46025
10.50	.00033	- .41097
10.60	.00062	- .40914
10.70	.00083	- .40267
10.80	.00116	- .37869
10.90	.00151	- .37820
11.00	.00187	- .39541
11.10	.00221	- .40625
11.20	.00269	- .39817
11.30	.00292	- .39523
11.40	.00302	- .39026
11.50	.00307	- .38968
11.60	.00287	- .39398
11.70	.00271	- .40377
11.80	.00274	- .41224
11.90	.00254	- .40500
12.00	.00234	- .39843
12.10	.00191	- .38645
12.20	.00157	- .36604
12.30	.00113	- .33416
12.40	.00078	- .32596
12.50	.00059	- .30133
12.60	.00045	- .24710
12.70	.00030	- .14248
12.80	.00025	- .02427
12.90	.00031	.08398
13.00	.00043	.18538
13.10	.00057	.25209
13.20	.00074	.27611
13.30	.00107	.28727
13.40	.00146	.30843
13.50	.00184	.32772
13.60	.00210	.35150
13.70	.00224	.36153
13.80	.00240	.35898
13.90	.00259	.36655
14.00	.00274	.36405
14.10	.00293	.35618
14.20	.00322	.36683
14.30	.00319	.37422
14.40	.00300	.37210
14.50	.00276	.36845
14.60	.00239	.36789
14.70	.00224	.32210
14.80	.00225	.26797
14.90	.00089	.23036
15.00	.00056	.33964

TABLE IX
CYLINDER 6 : MEASUREMENT DATA

FREQ (GHZ)	CRSEC (COR. METER)	PHASE (DEG./180)
10.10	.00009	23014
10.20	.00005	35187
10.30	.00000	21920
10.40	.00008	- 73178
10.50	.00024	- 71112
10.60	.00047	- 71325
10.70	.00067	- 72644
10.80	.00086	- 74323
10.90	.00104	- 75908
11.00	.00107	- 77276
11.10	.00104	- 80413
11.20	.00102	- 81426
11.30	.00085	- 79568
11.40	.00056	- 79528
11.50	.00038	- 78158
11.60	.00025	- 72080
11.70	.00014	- 63394
11.80	.00012	- 54424
11.90	.00020	- 42345
12.00	.00035	- 30731
12.10	.00037	- 22721
12.20	.00044	- 25444
12.30	.00053	- 29340
12.40	.00069	- 23313
12.50	.00060	- 24378
12.60	.00065	- 27371
12.70	.00072	- 26562
12.80	.00060	- 25291
12.90	.00043	- 20682
13.00	.00033	- 32114
13.10	.00021	- 32798
13.20	.00008	- 38499
13.30	.00003	- 56888
13.40	.00003	- 83977
13.50	.00004	37386
13.60	.00014	37482
13.70	.00031	77329
13.80	.00043	76508
13.90	.00052	70698
14.00	.00077	67531
14.10	.00104	67964
14.20	.00113	67575
14.30	.00134	64963
14.40	.00150	63582
14.50	.00126	64893
14.60	.00119	61635
14.70	.00124	59310
14.80	.00106	59481
14.90	.00087	55937
15.00	.00085	55141

TABLE X
CYLINDER 7 : MEASUREMENT DATA

FREQ (GHZ)	CRSEC (SQR. METER)	PHASE (DEG /180)
10.10	00051	- 27641
10.20	00062	- 26206
10.30	00063	- 26263
10.40	00069	- 28534
10.50	00080	- 27050
10.60	00085	- 28241
10.70	00069	- 28484
10.80	00062	- 26957
10.90	00058	- 27013
11.00	00054	- 28944
11.10	00041	- 28903
11.20	00031	- 29767
11.30	00023	- 29871
11.40	00013	- 27982
11.50	00004	- 25442
11.60	00001	- 24695
11.70	00000	37470
11.80	00004	61601
11.90	00009	63519
12.00	00020	60815
12.10	00036	62896
12.20	00055	64955
12.30	00060	65435
12.40	00070	61442
12.50	00090	61292
12.60	00105	62563
12.70	00118	62120
12.80	00137	62072
12.90	00137	62265
13.00	00123	61241
13.10	00109	60690
13.20	00096	60066
13.30	00086	59325
13.40	00070	59960
13.50	00055	59522
13.60	00040	61393
13.70	00023	63828
13.80	00009	69122
13.90	00003	32204
14.00	00001	08397
14.10	00005	- 67478
14.20	00017	- 57053
14.30	00031	- 53141
14.40	00049	- 52406
14.50	00070	- 52495
14.60	00087	- 51447
14.70	00102	- 53291
14.80	00128	- 54296
14.90	00149	- 53833
15.00	00160	- 52256

TABLE XI
CYLINDER 8 : MEASUREMENT DATA

FREQ (GHZ)	CRSEC (SOR. METER)	PHASE (DEG./180)
10.10	.00217	- 42571
10.20	.00238	- 42100
10.30	.00239	- 42658
10.40	.00253	- 44138
10.50	.00271	- 42710
10.60	.00276	- 43605
10.70	.00216	- 43201
10.80	.00189	- 40807
10.90	.00169	- 40692
11.00	.00143	- 41974
11.10	.00107	- 41129
11.20	.00079	- 39877
11.30	.00052	- 36620
11.40	.00028	- 30251
11.50	.00013	- 17437
11.60	.00009	02111
11.70	.00018	18680
11.80	.00037	28663
11.90	.00060	31495
12.00	.00095	33594
12.10	.00141	36171
12.20	.00180	37883
12.30	.00209	38931
12.40	.00227	37589
12.50	.00261	37830
12.60	.00296	38692
12.70	.00326	39135
12.80	.00365	39895
12.90	.00350	40389
13.00	.00317	40112
13.10	.00279	40725
13.20	.00241	40463
13.30	.00220	40417
13.40	.00192	42026
13.50	.00157	43605
13.60	.00128	46981
13.70	.00089	51680
13.80	.00062	57019
13.90	.00048	63586
14.00	.00043	70315
14.10	.00049	20500
14.20	.00057	36932
14.30	.00072	- 00154
14.40	.00087	- 04605
14.50	.00099	- 02379
14.60	.00098	- 03421
14.70	.00089	- 09758
14.80	.00016	- 67256
14.90	.00172	- 67504
15.00	.00205	- 31483

TABLE XII
CYLINDER 9 : MEASUREMENT DATA

FREQ (GHZ)	CRSEC (SQ. METER)	PHASE (DEG./180)
10.10	.00312	- 67000
10.20	.00295	- 69214
10.30	.00269	- 71842
10.40	.00260	- 73067
10.50	.00234	- 72272
10.60	.00219	- 72874
10.70	.00159	- 73603
10.80	.00118	- 73457
10.90	.00082	- 74466
11.00	.00049	- 75237
11.10	.00027	- 77819
11.20	.00010	- 80600
11.30	.00001	- 79215
11.40	.00002	21511
11.50	.00012	20002
11.60	.00023	15530
11.70	.00038	12920
11.80	.00048	12031
11.90	.00056	10150
12.00	.00059	10029
12.10	.00056	11626
12.20	.00043	13474
12.30	.00033	14961
12.40	.00025	16934
12.50	.00016	21630
12.60	.00011	31566
12.70	.00013	44114
12.80	.00017	55943
12.90	.00023	63467
13.00	.00031	67024
13.10	.00039	69595
13.20	.00048	69870
13.30	.00057	69811
13.40	.00064	70764
13.50	.00064	69445
13.60	.00063	70219
13.70	.00052	70606
13.80	.00038	69799
13.90	.00028	68566
14.00	.00019	65787
14.10	.00012	63506
14.20	.00003	56354
14.30	.00001	28867
14.40	.00002	- 11082
14.50	.00009	- 25611
14.60	.00018	- 26804
14.70	.00029	- 29835
14.80	.00045	- 33356
14.90	.00064	- 33665
15.00	.00080	- 32927

TABLE XIII
CYLINDER 10 : MEASUREMENT DATA

FREQ (GHZ)	CRSEC (SQRT. METER)	PHASE (DEG./180)
10.10	.00033	- .08945
10.20	.00021	- .05847
10.30	.00013	- .06532
10.40	.00005	- .08114
10.50	.00001	- .04930
10.60	.00000	.54352
10.70	.00002	.91051
10.80	.00007	.91995
10.90	.00016	.42149
11.00	.00027	.40637
11.10	.00040	.90210
11.20	.00057	.89773
11.30	.00071	.90214
11.40	.00086	.90664
11.50	.00092	.90614
11.60	.00092	.89911
11.70	.00092	.88692
11.80	.00091	.87492
11.90	.00090	.88772
12.00	.00083	.87336
12.10	.00065	.88740
12.20	.00044	.89081
12.30	.00029	.90225
12.40	.00017	.40420
12.50	.00000	- .07662
12.60	.00002	- .04707
12.70	.00001	- .56788
12.80	.00004	- .21964
12.90	.00013	- .18575
13.00	.00027	- .17052
13.10	.00041	- .17423
13.20	.00059	- .18424
13.30	.00081	- .19233
13.40	.00108	- .18083
13.50	.00120	- .18171
13.60	.00142	- .17782
13.70	.00136	- .17355
13.80	.00129	- .16735
13.90	.00122	- .17164
14.00	.00121	- .18043
14.10	.00113	- .18213
14.20	.00098	- .16864
14.30	.00076	- .16544
14.40	.00055	- .14821
14.50	.00032	- .13133
14.60	.00015	- .11071
14.70	.00006	- .01850
14.80	.00003	.22248
14.90	.00006	.52809
15.00	.00016	.63416

TABLE XIV
CYLINDER 11 : MEASUREMENT DATA

FREQ (GHZ)	CRSEC (SQ. METER)	PHASE (DEG./180)
10.10	.00102	- 20023
10.20	.00053	- 16601
10.30	.00028	- 16183
10.40	.00011	- 11379
10.50	.00003	18171
10.60	.00000	50651
10.70	.00021	61264
10.80	.00045	66713
10.90	.00083	68402
11.00	.00126	67177
11.10	.00171	67479
11.20	.00221	67867
11.30	.00261	67842
11.40	.00297	68982
11.50	.00306	69116
11.60	.00296	68763
11.70	.00283	68033
11.80	.00273	68017
11.90	.00247	68775
12.00	.00231	68792
12.10	.00192	21020
12.20	.00127	- 26132
12.30	.00083	- 23651
12.40	.00054	- 20496
12.50	.00036	- 12492
12.60	.00023	- 00377
12.70	.00020	- 32244
12.80	.00035	- 18446
12.90	.00065	- 09585
13.00	.00094	- 55299
13.10	.00122	- 53217
13.20	.00162	- 52973
13.30	.00212	- 52452
13.40	.00268	- 50577
13.50	.00294	- 49673
13.60	.00332	- 48385
13.70	.00317	- 47309
13.80	.00299	- 46699
13.90	.00289	- 46091
14.00	.00288	- 46160
14.10	.00282	- 46181
14.20	.00263	- 44668
14.30	.00231	- 43539
14.40	.00194	- 42012
14.50	.00147	- 41210
14.60	.00106	- 41389
14.70	.00069	- 45892
14.80	.00004	03977
14.90	.00082	- 18786
15.00	.00069	- 26882

TABLE XV
CYLINDER 12 : MEASUREMENT DATA

FREQ (GHZ)	CRSEC (SQRT. METER)	PHASE (DEG./180)
10.10	00470	- 79066
10.20	00346	- 36286
10.30	00227	- 44819
10.40	00119	- 05353
10.50	00059	00230
10.60	00033	56942
10.70	00030	36625
10.80	00046	27550
10.90	00080	21551
11.00	00109	15340
11.10	00130	12496
11.20	00150	11367
11.30	00167	10058
11.40	00162	09802
11.50	00154	08360
11.60	00130	06705
11.70	00101	04567
11.80	00077	02637
11.90	00054	03203
12.00	00031	06122
12.10	00013	06728
12.20	00005	09690
12.30	00002	43261
12.40	00005	73577
12.50	00011	81860
12.60	00019	82103
12.70	00029	82379
12.80	00036	84429
12.90	00034	85823
13.00	00032	84593
13.10	00029	37029
13.20	00022	39815
13.30	00016	- 06318
13.40	00013	- 00532
13.50	00011	- 40856
13.60	00013	- 76419
13.70	00016	- 65515
13.80	00018	- 58639
13.90	00025	- 56707
14.00	00038	- 55445
14.10	00050	- 53767
14.20	00055	- 52082
14.30	00060	- 52587
14.40	00063	- 51611
14.50	00050	- 51275
14.60	00041	- 53179
14.70	00031	- 54892
14.80	00024	- 53522
14.90	00013	- 55992
15.00	00006	- 56080

TABLE XVI
CYLINDER 13 : MEASUREMENT DATA

FREQ (GHZ)	CRSEC (SOR. METER)	PHASE (DEG./180)
10.10	.00026	.52011
10.20	.00028	. - .03685
10.30	.00046	.44106
10.40	.00060	.45625
10.50	.00070	. - .03695
10.60	.00077	. - .04266
10.70	.00069	. - .03491
10.80	.00071	. - .02670
10.90	.00073	. - .02308
11.00	.00059	.45700
11.10	.00051	.43799
11.20	.00045	.44603
11.30	.00028	. - .02343
11.40	.00013	. - .03048
11.50	.00006	. - .02486
11.60	.00001	. - .42811
11.70	.00001	. - .14594
11.80	.00005	. - .10856
11.90	.00017	. - .13184
12.00	.00039	. - .10895
12.10	.00053	. - .06273
12.20	.00055	. - .07983
12.30	.00077	. - .09254
12.40	.00095	. - .08040
12.50	.00105	. - .07835
12.60	.00115	. - .09568
12.70	.00131	. - .10050
12.80	.00126	. - .07784
12.90	.00100	. - .07662
13.00	.00084	. - .08504
13.10	.00068	. - .07916
13.20	.00044	. - .07499
13.30	.00026	. - .07608
13.40	.00013	. - .05863
13.50	.00005	.03834
13.60	.00002	.48856
13.70	.00007	.73730
13.80	.00016	.81574
13.90	.00030	.32548
14.00	.00055	.31314
14.10	.00089	.33014
14.20	.00114	.34130
14.30	.00144	.33673
14.40	.00163	.34956
14.50	.00155	.35459
14.60	.00144	.34276
14.70	.00150	.33157
14.80	.00141	.34664
14.90	.00116	.34683
15.00	.00102	.36290

TABLE XVII
CYLINDER 14 : MEASUREMENT DATA

FREQ (GHZ)	CRSEC (SQR. METER)	PHASE (DEG./180)
10.10	00089	51727
10.20	00158	53735
10.30	00176	54824
10.40	00200	52699
10.50	00254	53597
10.60	00287	53157
10.70	00247	54380
10.80	00237	55893
10.90	00233	55279
11.00	00218	53846
11.10	00175	54958
11.20	00129	54893
11.30	00094	55853
11.40	00061	60952
11.50	00026	69062
11.60	00009	31730
11.70	00012	- 43788
11.80	00034	- 26180
11.90	00060	- 67512
12.00	00091	- 67754
12.10	00155	- 66627
12.20	00203	- 63532
12.30	00220	- 61205
12.40	00234	- 63144
12.50	00294	- 63683
12.60	00333	- 61493
12.70	00324	- 61862
12.80	00346	- 61582
12.90	00312	- 59500
13.00	00247	- 58453
13.10	00191	- 58971
13.20	00161	- 57920
13.30	00124	- 54774
13.40	00086	- 49150
13.50	00051	- 43266
13.60	00038	- 33938
13.70	00041	- 21310
13.80	00055	- 08015
13.90	00070	01611
14.00	00085	04495
14.10	00133	05135
14.20	00187	09017
14.30	00210	11085
14.40	00235	10322
14.50	00261	11329
14.60	00227	12027
14.70	00200	06079
14.80	00149	08331
14.90	00173	08574
15.00	00083	02996

TABLE XVIII
CYLINDER 15 : MEASUREMENT DATA

FREQ (GHZ)	CRSEC (SQR. METER)	PHASE (DEG./180)
10.10	.00040	- 74258
10.20	.00065	- 78944
10.30	.00149	- 51923
10.40	.00278	- 35060
10.50	.00381	- 28960
10.60	.00430	- 23403
10.70	.00354	- 19871
10.80	.00317	- 17604
10.90	.00312	- 14635
11.00	.00249	- 09790
11.10	.00180	- 05134
11.20	.00123	- 00386
11.30	.00070	- 03237
11.40	.00030	- 11976
11.50	.00014	- 31060
11.60	.00011	- 55435
11.70	.00025	- 74912
11.80	.00044	- 32298
11.90	.00062	- 37720
12.00	.00089	- 41743
12.10	.00110	- 41520
12.20	.00095	- 41645
12.30	.00090	- 44500
12.40	.00089	- 45759
12.50	.00083	- 43894
12.60	.00063	- 44822
12.70	.00052	- 46941
12.80	.00037	- 43758
12.90	.00017	- 38006
13.00	.00007	- 30369
13.10	.00004	- 69648
13.20	.00006	- 45200
13.30	.00011	- 31795
13.40	.00017	- 24721
13.50	.00020	- 21772
13.60	.00026	- 21796
13.70	.00033	- 18354
13.80	.00030	- 14738
13.90	.00021	- 11238
14.00	.00018	- 12645
14.10	.00019	- 07661
14.20	.00016	- 03626
14.30	.00011	- 15154
14.40	.00012	- 19947
14.50	.00019	- 30946
14.60	.00022	- 39573
14.70	.00023	- 41532
14.80	.00035	- 40835
14.90	.00046	- 44520
15.00	.00043	- 48910

TABLE XIX
CYLINDER 16 : MEASUREMENT DATA

FREQ (GHZ)	CRSEC (SQR. METER)	PHASE (DEG. / 180)
10.10	00057	- 11223
10.20	00046	- 11179
10.30	00045	- 15322
10.40	00041	- 14631
10.50	00037	- 12283
10.60	00034	- 13382
10.70	00023	- 14540
10.80	00017	- 13547
10.90	00014	- 10811
11.00	00010	- 13266
11.10	00006	- 19219
11.20	00004	- 15893
11.30	00001	- 08275
11.40	00000	38979
11.50	00000	35570
11.60	00002	79752
11.70	00005	81097
11.80	00009	81313
11.90	00014	76511
12.00	00030	78311
12.10	00036	82692
12.20	00034	81252
12.30	00047	79649
12.40	00063	79238
12.50	00066	80190
12.60	00081	77463
12.70	00101	77038
12.80	00117	78923
12.90	00112	78486
13.00	00120	76813
13.10	00125	76579
13.20	00121	76606
13.30	00121	74598
13.40	00135	74424
13.50	00142	74286
13.60	00141	76727
13.70	00111	76916
13.80	00101	74986
13.90	00103	74893
14.00	00096	76071
14.10	00083	75374
14.20	00091	74718
14.30	00076	76204
14.40	00055	78468
14.50	00043	76290
14.60	00037	77893
14.70	00024	81136
14.80	00014	79670
14.90	00013	80841
15.00	00008	- 85789

TABLE XX
CYLINDER 17 : MEASUREMENT DATA

FREQ (GHZ)	CRSEC (SQ. METER)	PHASE (DEG /180)
10.10	.00504	.25110
10.20	.00321	.15671
10.30	.00108	- .02183
10.40	.00022	- .31498
10.50	.00030	- .68948
10.60	.00074	- .29194
10.70	.00111	- .32604
10.80	.00146	- .33530
10.90	.00167	- .35996
11.00	.00147	- .40171
11.10	.00107	- .41981
11.20	.00048	- .40863
11.30	.00013	- .27796
11.40	.00014	- .42467
11.50	.00042	- .32856
11.60	.00064	- .33939
11.70	.00067	- .37965
11.80	.00053	- .42759
11.90	.00024	- .48389
12.00	.00004	- .25408
12.10	.00014	.72544
12.20	.00054	.59362
12.30	.00119	.52669
12.40	.00181	.46450
12.50	.00216	.41056
12.60	.00235	.35705
12.70	.00218	.31255
12.80	.00172	.25532
12.90	.00105	.16532
13.00	.00063	.01586
13.10	.00048	- .20033
13.20	.00071	- .40937
13.30	.00118	- .53682
13.40	.00179	- .61609
13.50	.00224	- .18096
13.60	.00254	- .21192
13.70	.00222	- .23782
13.80	.00168	- .28110
13.90	.00130	- .34269
14.00	.00089	- .42276
14.10	.00046	- .53679
14.20	.00027	.75889
14.30	.00036	.53903
14.40	.00060	.39172
14.50	.00096	.30939
14.60	.00119	.36255
14.70	.00127	.20245
14.80	.00143	.16931
14.90	.00130	.16087
15.00	.00093	.14278

TABLE XXI
CYLINDER 18 : MEASUREMENT DATA

FREQ (GHZ)	CRSEC (SQR. METER)	PHASE (DEG./180)
10.10	00470	22575
10.20	00501	- 27196
10.30	00499	- 28574
10.40	00493	21227
10.50	00528	22087
10.60	00487	21147
10.70	00388	- 26518
10.80	00375	- 25323
10.90	00340	- 25317
11.00	00275	- 25227
11.10	00235	- 24334
11.20	00215	- 23759
11.30	00178	- 20958
11.40	00138	- 18723
11.50	00103	- 17765
11.60	00069	- 18288
11.70	00017	- 25039
11.80	00041	- 13677
11.90	00110	- 34410
12.00	00110	- 40106
12.10	00066	- 45644
12.20	00028	- 08708
12.30	00008	09267
12.40	00027	04465
12.50	00106	37145
12.60	00202	25773
12.70	00279	17979
12.80	00321	13480
12.90	00317	09632
13.00	00288	05552
13.10	00261	01576
13.20	00219	- 02563
13.30	00172	- 07248
13.40	00133	- 12612
13.50	00096	- 17081
13.60	00060	- 22551
13.70	00031	- 30990
13.80	00016	- 47410
13.90	00014	- 18319
14.00	00020	18254
14.10	00031	07385
14.20	00046	01688
14.30	00062	- 01735
14.40	00075	- 03815
14.50	00079	- 05268
14.60	00080	- 07433
14.70	00083	- 09813
14.80	00087	- 11604
14.90	00078	- 12410
15.00	00074	- 12392

TABLE XXII
CYLINDER 19 : MEASUREMENT DATA

FREQ (GHZ)	CRSEC (SQ. METER)	PHASE (DEG./180)
10.10	.00509	- 24433
10.20	.00506	- 24298
10.30	.00453	- 23896
10.40	.00353	- 21686
10.50	.00278	- 18905
10.60	.00191	- 15276
10.70	.00103	- 06687
10.80	.00068	.04822
10.90	.00067	.20810
11.00	.00079	.32301
11.10	.00122	.41018
11.20	.00197	.45956
11.30	.00270	.49431
11.40	.00325	.52002
11.50	.00351	.52180
11.60	.00338	.50214
11.70	.00251	.54718
11.80	.00221	.47188
11.90	.00052	.40411
12.00	.00136	.25737
12.10	.00292	.79508
12.20	.00262	.70424
12.30	.00213	.62484
12.40	.00127	.48510
12.50	.00056	.19957
12.60	.00057	- 12609
12.70	.00081	- 29497
12.80	.00112	- 36835
12.90	.00133	- 39932
13.00	.00144	- 41401
13.10	.00137	- 43310
13.20	.00127	- 45660
13.30	.00104	- 47292
13.40	.00075	- 48801
13.50	.00039	- 48832
13.60	.00012	- 48928
13.70	.00002	- 32755
13.80	.00007	.21391
13.90	.00021	.27338
14.00	.00029	.25859
14.10	.00035	.23339
14.20	.00033	.20721
14.30	.00020	.22620
14.40	.00005	.26747
14.50	.00001	.33486
14.60	.00008	- 37157
14.70	.00033	- 33874
14.80	.00061	.31416
14.90	.00091	.27497
15.00	.00132	.25345

IV. SUMMARY AND CONCLUSIONS

A. ANALYSIS OF MEASURED DATA

The back scattering cross section of a tubular cylinder depends upon several parameters. To simplify the problem, many of them were kept constant: The polarization of the receiving and transmitting antennas were kept constant during all measurements, all the cylinders were from the same material and the aspect angle and tilt of the different cylinders relative to the antennas plane were unchanged.

The parameters that were changed and their effects on the cross section were the subjects of this study were:

1. The cylinder length. (2h)
2. The cylinder diameter. (2a)
3. The transmitting frequency.

The cross section of a tubular cylinder can be written as a function of three parameters as shown in equation 4.1

$$\sigma = F_1(a,h,f) = F_2(a,h,k) \quad (\text{eqn 4.1})$$

where:

$$k = 2\pi/\lambda = 2\pi f/c$$

$$c = 3 \times 10^8 \text{ m/sec}$$

From the theory described in Chapter the following relations can be obtained:

(eqn 4.2)

$$\frac{\sigma}{\pi a^2} = F_3(l_1, l_2) = F_4(l_1, \frac{l_2}{l_1}) = F_s(ka, \frac{h}{a})$$

where:

$$l_1 = ka$$

$$l_2 = kh$$

The measurements taken can be divided into two steps. In the first step, 19 cylinders with different lengths and diameters were placed in the anechoic chamber, and plots of cross section and phase versus frequency were obtained on each of the cylinders. (figures 3.5 through 3.42) Except for gathering data and viewing the resonance frequencies, there is nothing much to say on the results because too many parameters were changed and the resulting analysis became too difficult and complicated.

The second step of measurements was based on the conclusion from the theory (equation 4.2).

Only eight scaled cylinders were put into the anechoic chamber, four of the cylinders had a constant ratio of length to diameter equals 4, ($h/a=4$), and four cylinders had a constant ratio of length to diameter equals 6, ($h/a=6$).

An overall plot with expanded frequency range was achieved by using those scaled cylinders.

The overall plots can be compared to the theoretical plots obtained by Prof.H.M.Lee at the Naval Postgraduate School.

Both the theoretical and experimental plots of cross section/area and phase versus ka are shown in Figures 4.1 through 4.8 and the overlapping ranges of the scaled cylinders in ka can be noticed from Tables XXIII through XXX. The theoretical and experimental curves can be seen on the same graph for the two sets of scaled cylinders in Figures 4.9 and 4.10.

Comparison of the experimental results to the theoretical plots show agreement away from the cutoff frequencies of the H_{11} circular waveguide mode at $ka=1.8415$.

In the theoretical calculations an infinitesimal wall thickness is assumed for the tubular cylinder, but practically the cylinders used in the measurements had some thickness (Table III). The outer diameter of the cylinder is used for $2a$ in the computations while the H_{11} mode cutoff frequency depends on the inner diameter of the cylinder. This fact caused the deviation in the cross section plots between the theoretical curve and the experimental curve near the cutoff frequency.

Problems occur in the phase plot because the averaging procedure did not properly take care of the phase shifts with values near ± 180 degrees. Because of the complicated behavior of the phase shift near the H_{11} cutoff at $ka=1.8415$ and near $ka=2.4046$, no conclusion can be made related to the actual behavior of the phase shift curve.

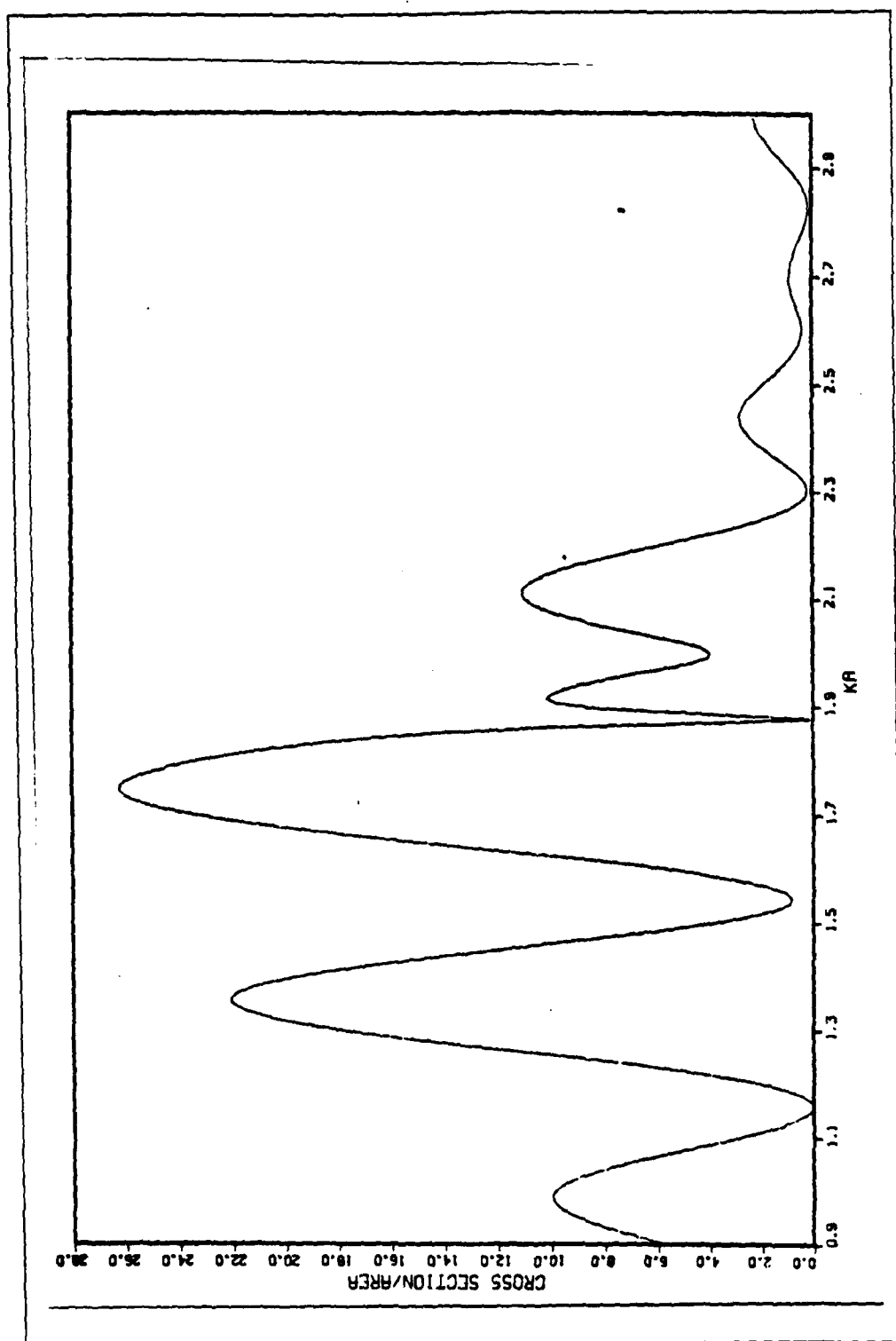


Figure 4.1 Theory Cross section Curve, $(h/a)=4$

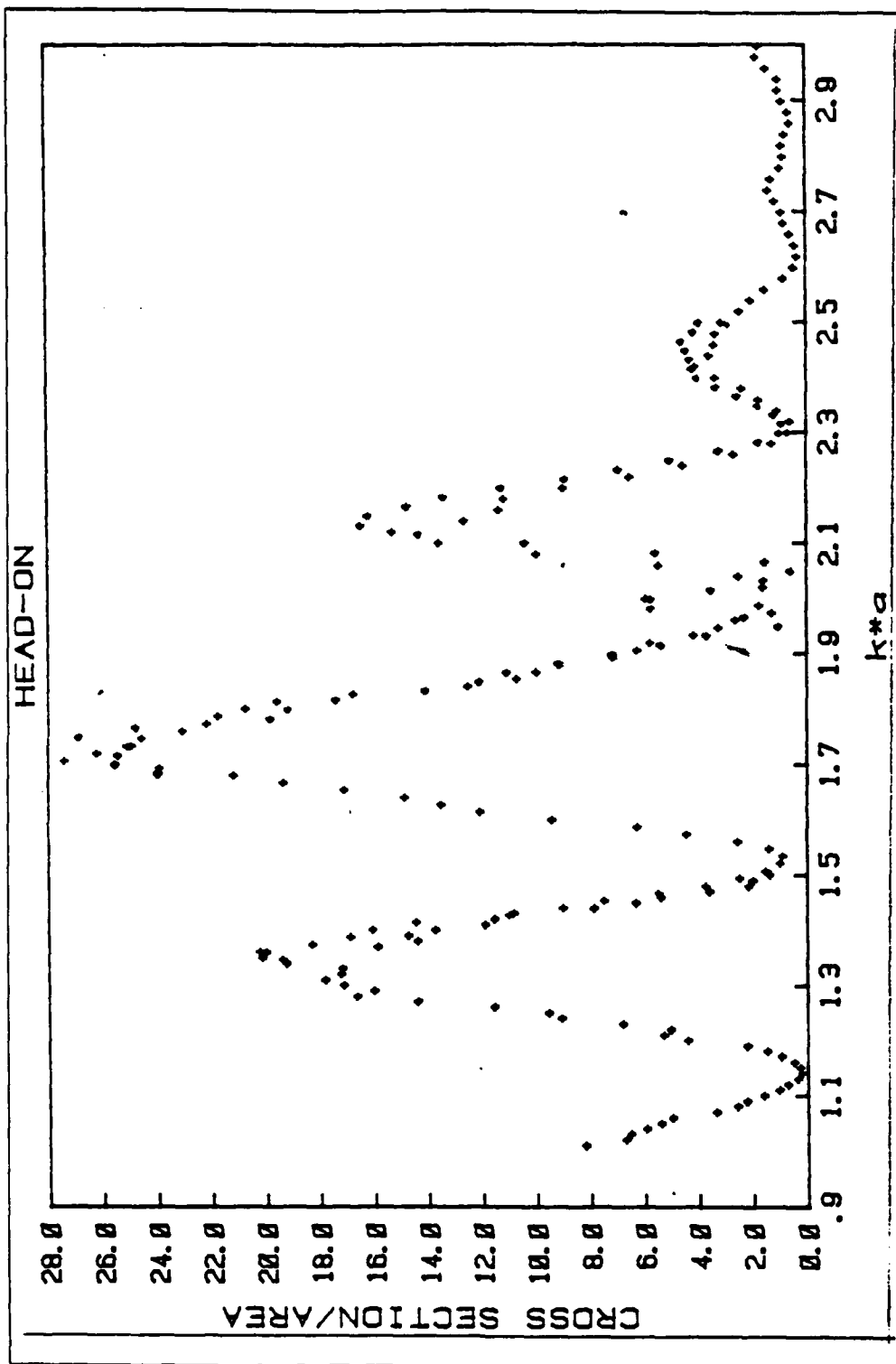


Figure 4.2 Experimental Cross section Curve, $(h/a)=4$

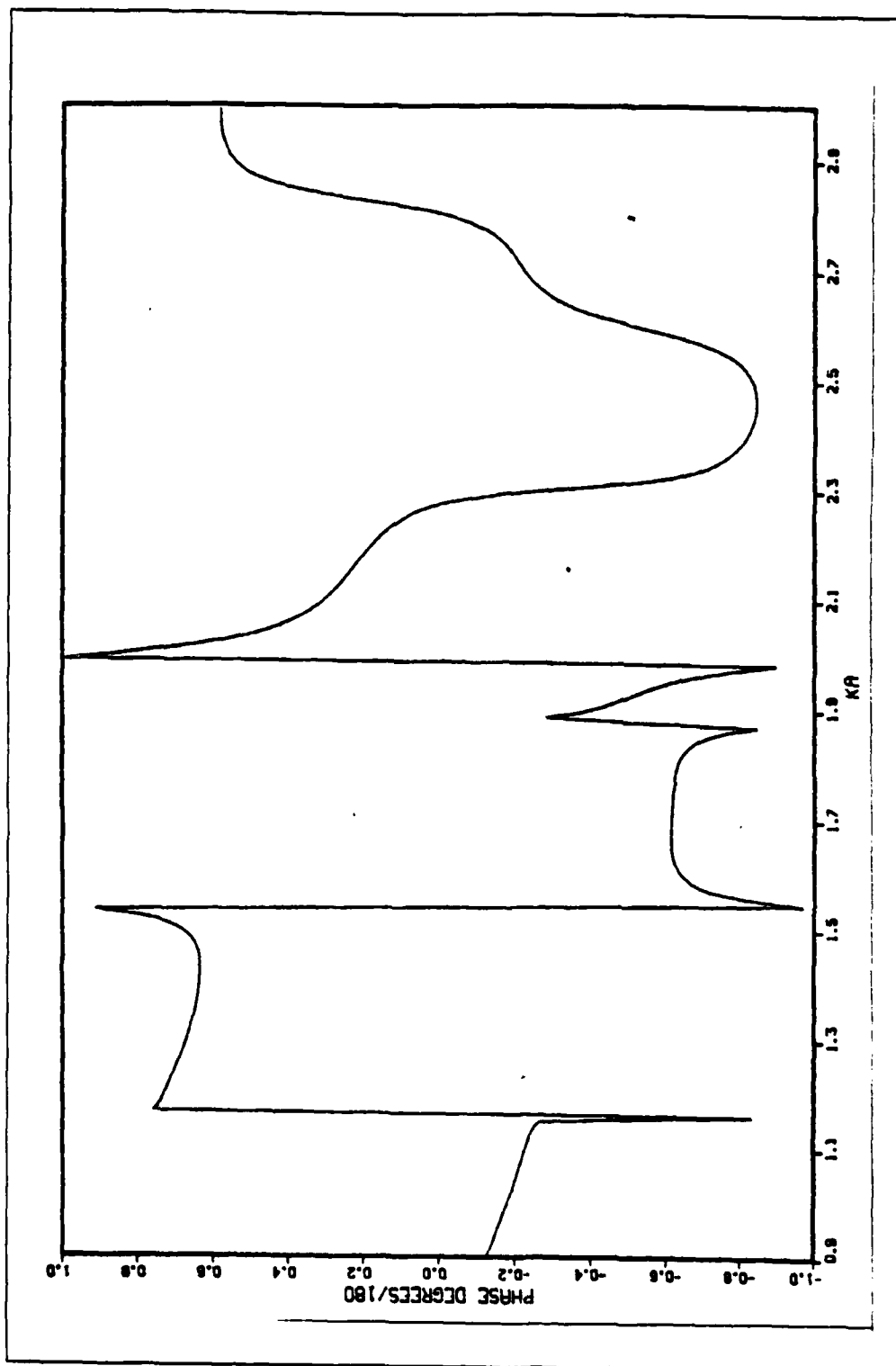


Figure 4.3 Theory Phase Curve, $(h/a)=4$

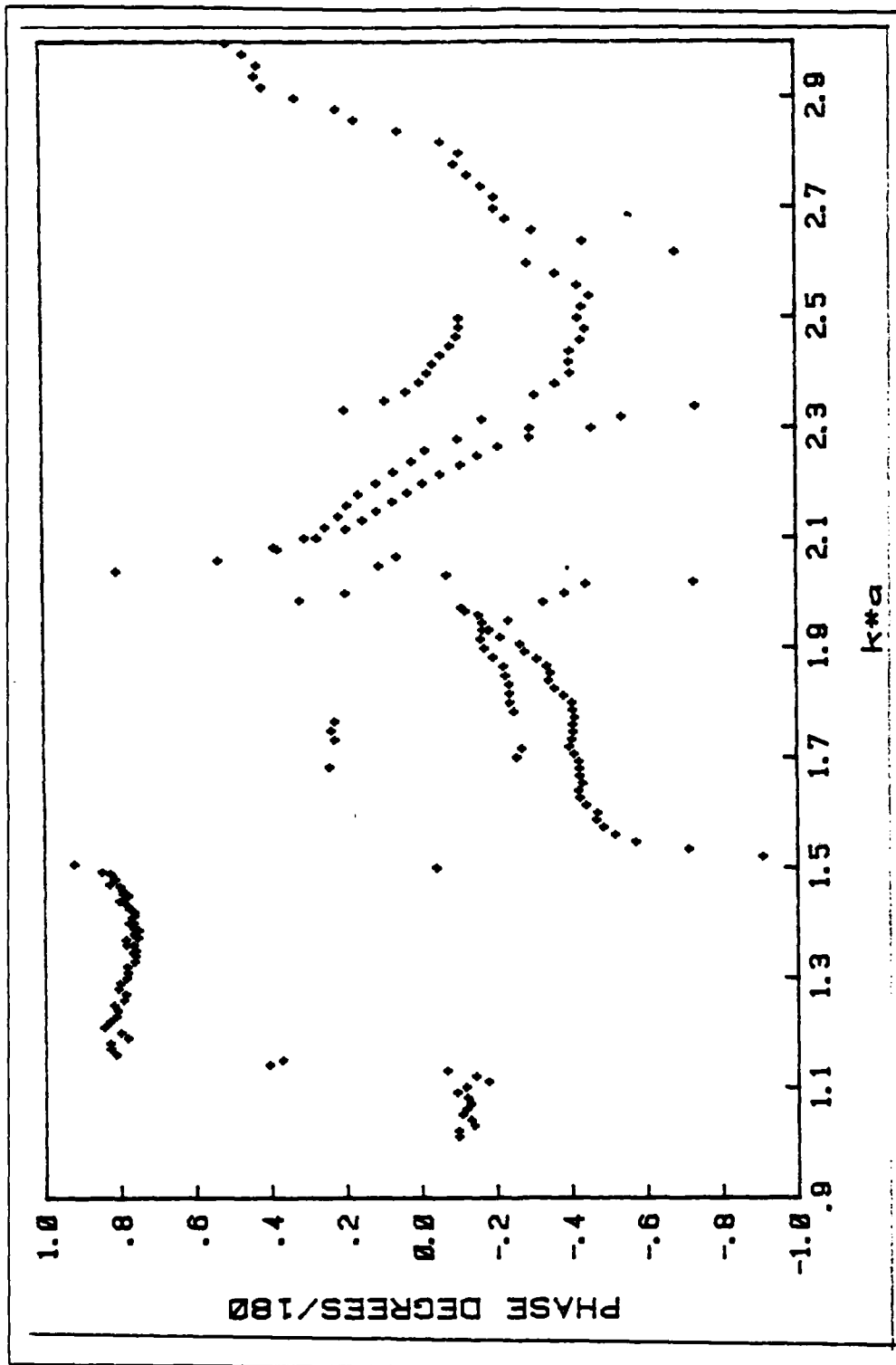


Figure 4.4 Experimental Phase Curve, $(h/a)=4$

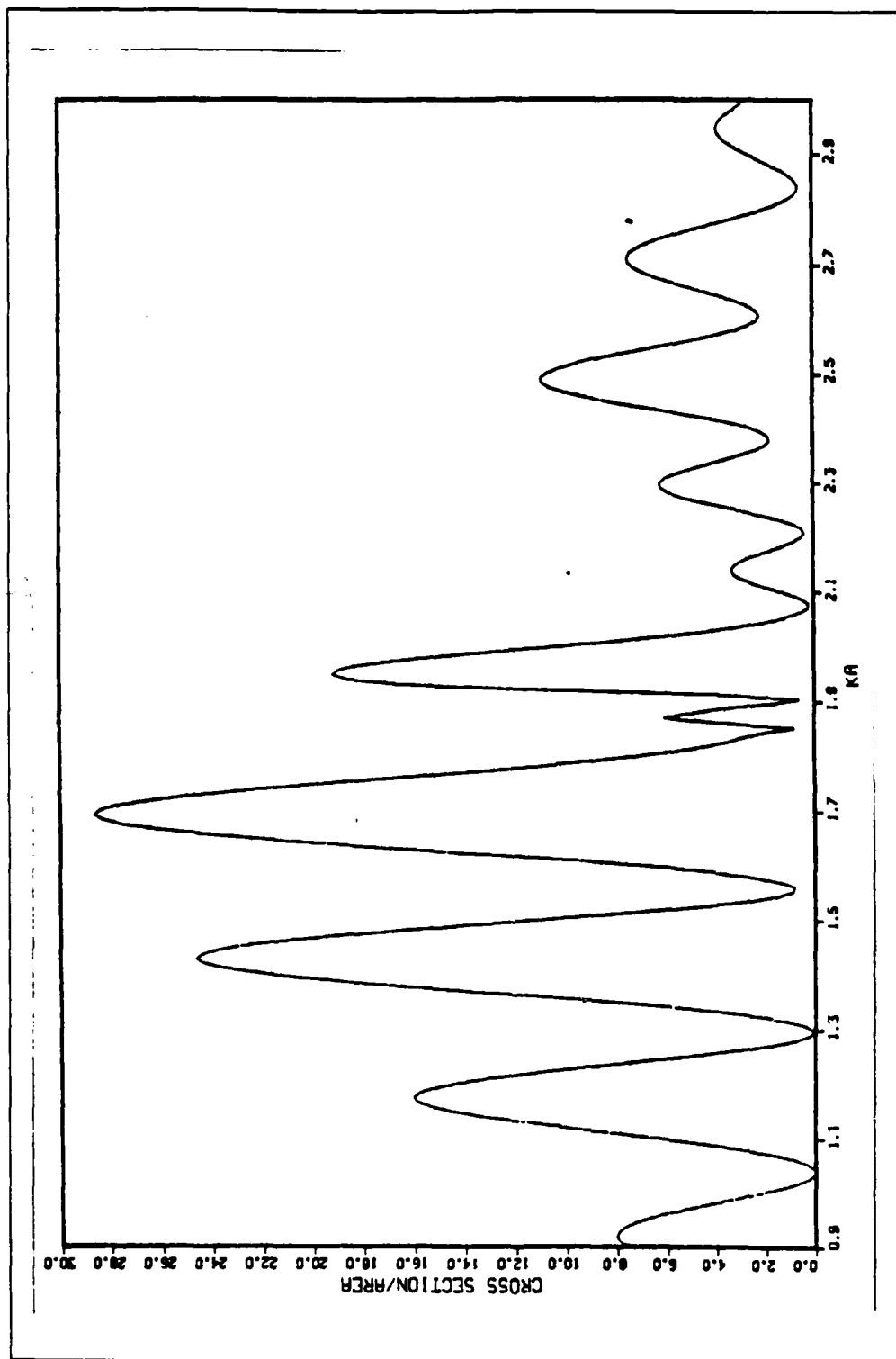


Figure 4.5 Theory Cross section Curve, $(h/a)=6$

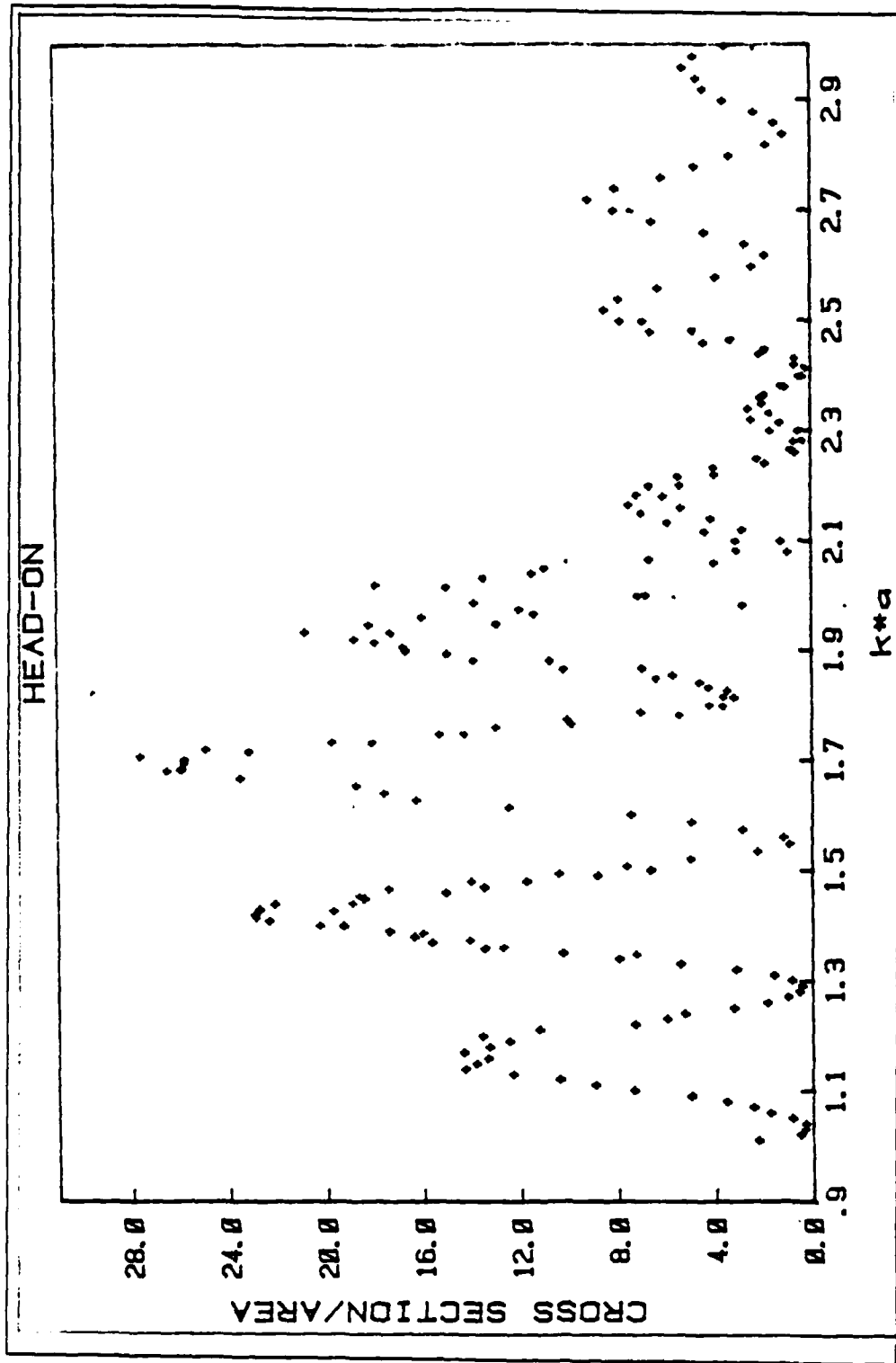


Figure 4.6 Experimental Cross section Curve, $(h/a)=6$

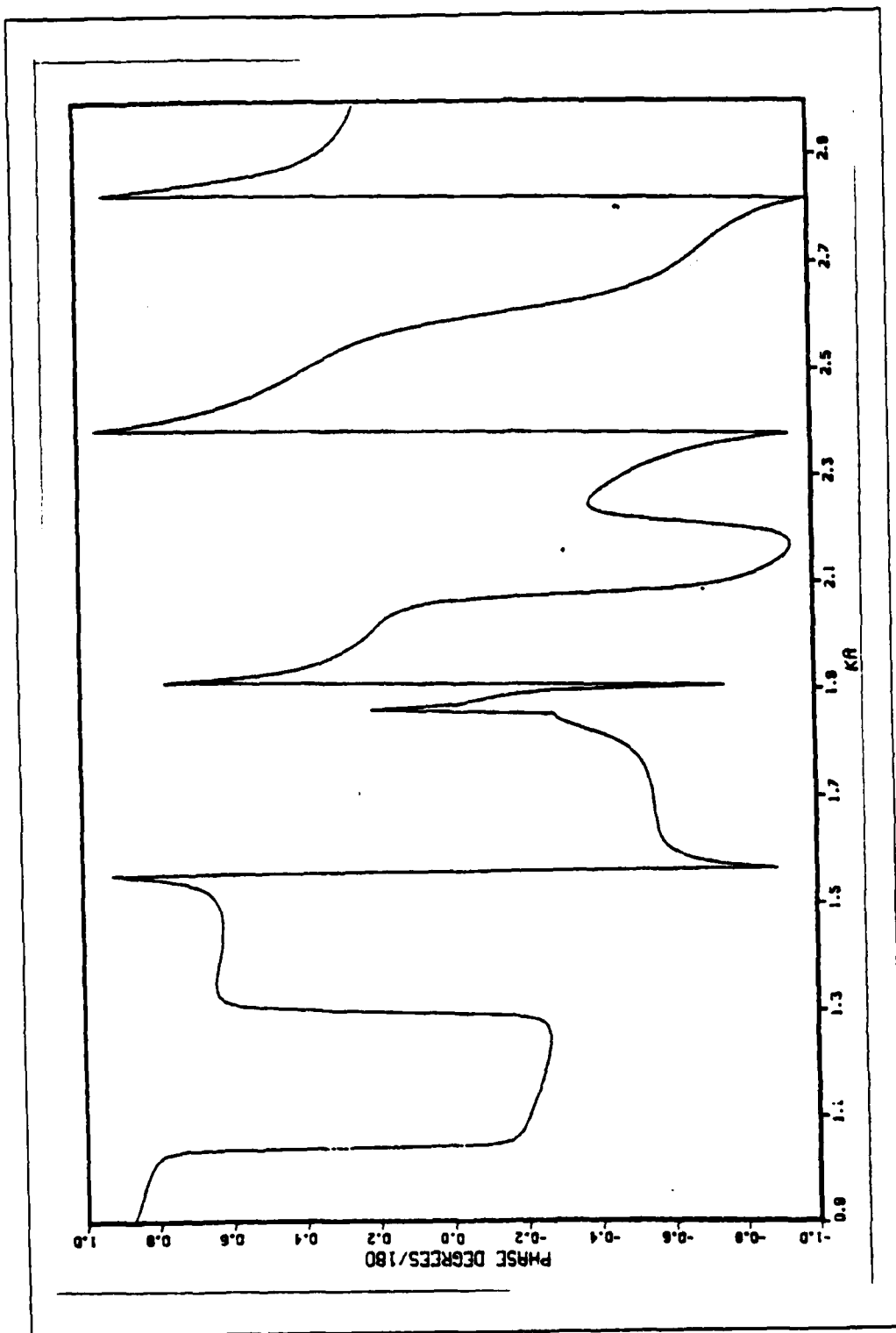


Figure 4.7 Theory Phase Curve, $(h/a)=6$

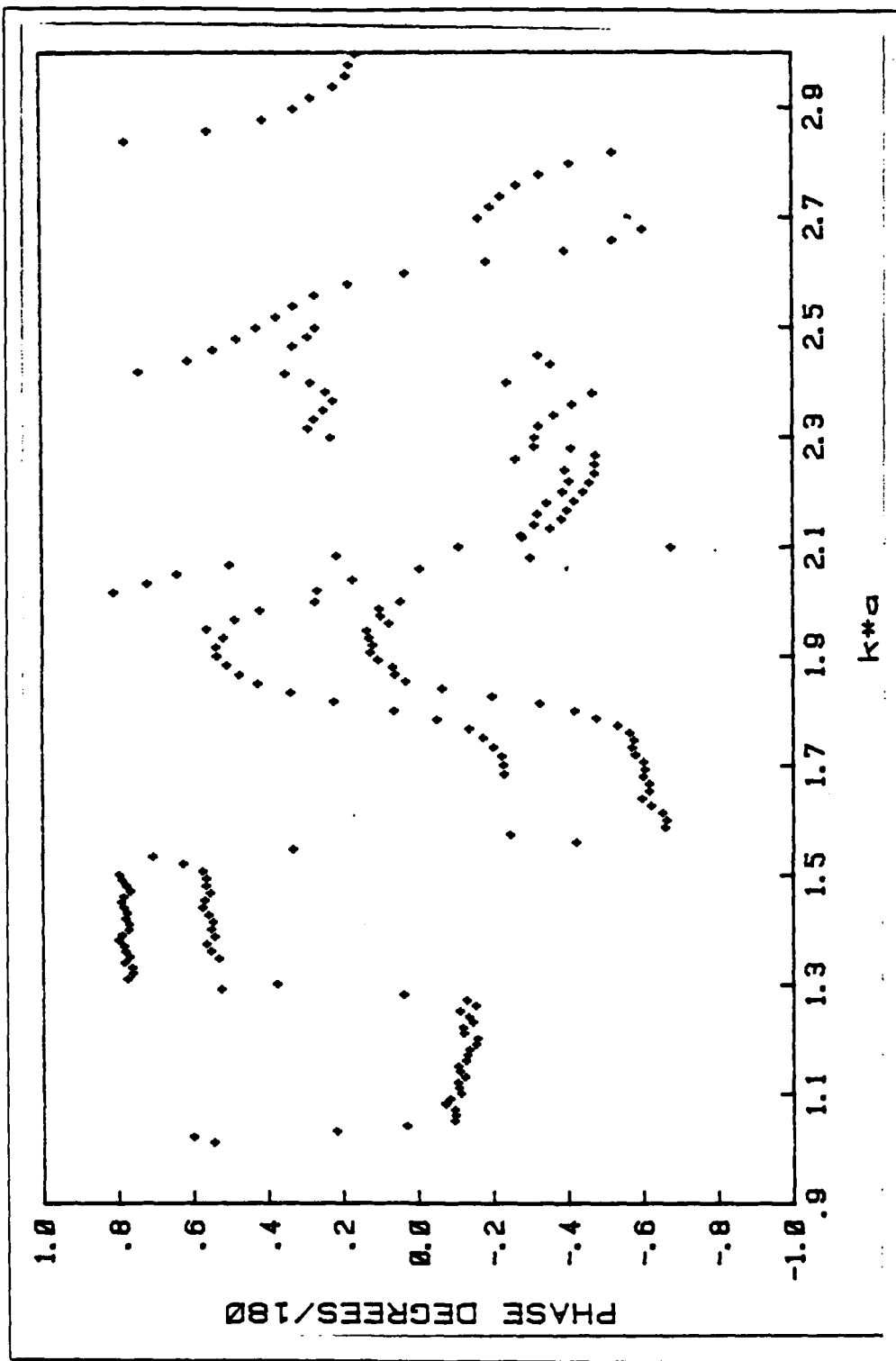


Figure 4.8 Experimental Phase Curve, $(h/a)=6$

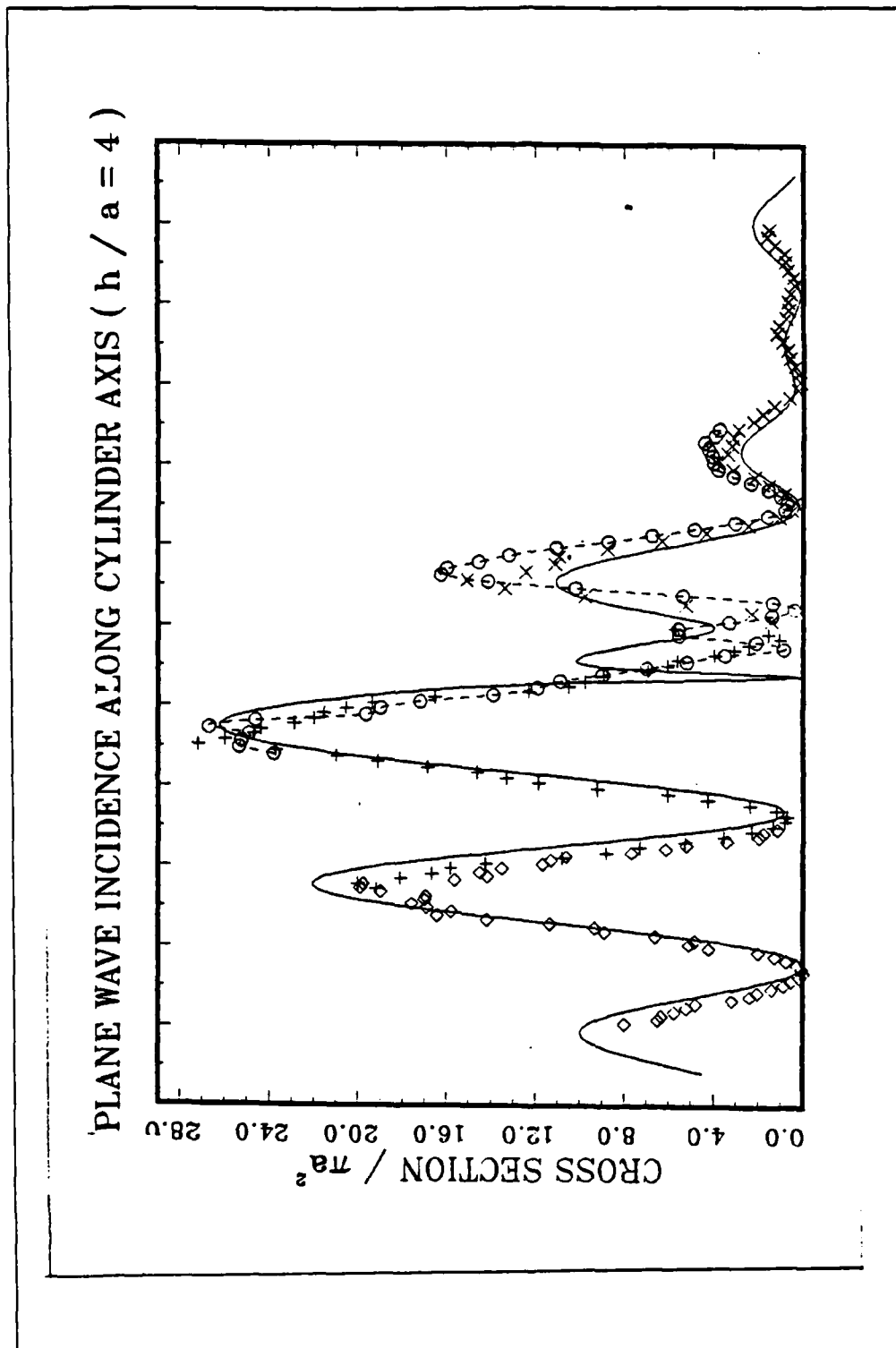


Figure 4.9 Summary Cross section Curve, $(h/a)=4$

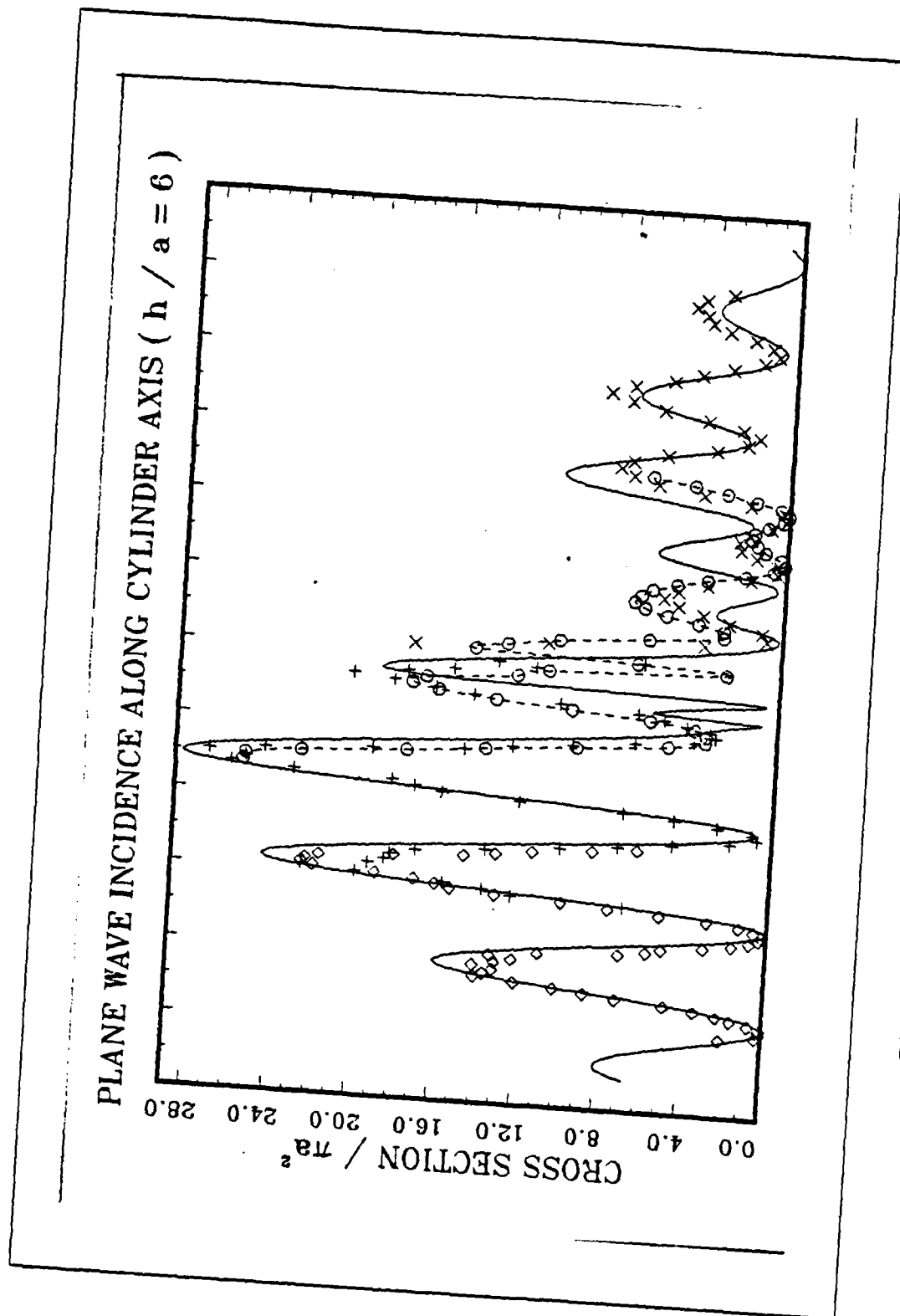


Figure 4.10 Summary Cross section Curve, $(h/a)=6$

TABLE XXIII
CYL16.4:1 RATIO

(K* λ)	CRS/AREA	PHASE
1.01	7.98048	- 11223
1.02	6.47129	- 11179
1.03	6.31745	- 15322
1.04	5.74212	- 14631
1.05	5.20176	- 12283
1.06	4.77216	- 13382
1.07	3.15763	- 14540
1.08	2.36279	- 13547
1.09	2.02704	- 10811
1.10	1.39104	- 13266
1.11	.84484	- 19219
1.12	.52367	- 15893
1.13	.15757	- 88275
1.14	.01278	.38979
1.15	.06595	.35570
1.16	.28497	.79752
1.17	.74825	.81097
1.18	1.26015	.81313
1.19	2.00129	.76511
1.20	4.21242	.78311
1.21	5.09609	.82692
1.22	4.83217	.81252
1.23	6.59277	.79649
1.24	8.85242	.79238
1.25	9.32048	.80190
1.26	11.32329	.77463
1.27	14.16269	.77038
1.28	16.40123	.78923
1.29	15.77985	.78406
1.30	16.89116	.76818
1.31	17.57577	.76579
1.32	16.98933	.76606
1.33	16.94235	.74598
1.34	18.99431	.74424
1.35	19.88837	.74296
1.36	19.76976	.76727
1.37	15.63468	.76916
1.38	14.16704	.74906
1.39	14.49831	.74893
1.40	13.51394	.76071
1.41	11.66735	.75374
1.42	11.30841	.74718
1.43	10.61584	.76204
1.44	7.65596	.78468
1.45	6.09910	.76290
1.46	5.18411	.77893
1.47	3.38999	.81136
1.48	1.94840	.79670
1.49	1.76829	.80841
1.50	1.15132	- .05789

TABLE XXIV
CYL.2,4:1 RATIO

(K* λ)	CRS/AREA	PHASE
1.34	19.15600	75042
1.36	20.00226	74758
1.37	19.00020	73692
1.38	16.65371	73600
1.40	15.83342	74873
1.41	14.23158	74620
1.42	10.78658	75941
1.44	8.80181	77473
1.45	7.28389	77653
1.46	5.26837	78308
1.48	3.52917	80012
1.49	2.27844	83111
1.50	1.34228	90352
1.52	0.80247	- 92217
1.53	0.71345	- 72678
1.54	1.19646	- 58633
1.56	2.35333	- 53223
1.57	4.23303	- 50119
1.58	6.05087	- 48089
1.60	9.20139	- 48458
1.61	11.85641	- 45457
1.62	13.29945	- 43847
1.64	14.62398	- 43560
1.65	16.85144	- 44482
1.66	19.10082	- 43857
1.68	20.94878	- 43844
1.69	23.69675	- 43706
1.70	27.16252	- 42522
1.72	35.97547	- 41176
1.73	24.69738	- 41793
1.74	24.33352	- 42205
1.76	22.84831	- 42141
1.77	21.94228	- 42609
1.78	21.52064	- 42103
1.80	20.52089	- 41851
1.81	19.34106	- 39668
1.82	16.52921	- 37351
1.84	12.29346	- 36734
1.85	10.49181	- 36180
1.86	9.76595	- 35331
1.88	8.90492	- 32577
1.89	6.93451	- 29377
1.90	6.05790	- 28123
1.92	5.58183	- 22931
1.93	3.94764	- 20034
1.94	3.04452	- 18170
1.96	2.40618	- 17233
1.97	1.07580	- 12712
1.98	1.54311	30304
2.00	5.72731	18100

TABLE XXV
CYL.18,4:1 RATIO

(K* λ)	CRS/AREA	PHASE
1.68	23.76109	225575
1.70	25.32330	27196
1.71	25.21696	28574
1.73	24.88478	21227
1.75	26.66999	22087
1.76	24.58522	21147
1.78	19.61015	26518
1.80	12.96222	25323
1.81	17.18261	25317
1.83	13.88797	25227
1.85	11.89179	24334
1.86	10.86691	23759
1.88	8.96653	20958
1.90	6.97575	18723
1.91	5.18603	17765
1.93	3.48556	19288
1.95	2.85780	25039
1.96	2.07882	13677
1.98	5.54562	34410
2.00	5.56593	40106
2.01	3.31155	45644
2.03	1.39360	88708
2.04	3.38438	89267
2.06	1.34761	84465
2.08	5.37220	37145
2.09	10.19076	25773
2.11	14.11280	17979
2.13	16.23851	13480
2.14	15.99765	89632
2.16	14.54523	85552
2.18	13.18422	81576
2.19	11.85801	82563
2.21	8.71222	87648
2.23	6.74130	12612
2.24	4.83704	17081
2.26	3.82207	22551
2.28	1.56277	38990
2.29	7.9976	47410
2.31	7.1833	18319
2.33	1.88433	18254
2.34	1.57723	87385
2.36	2.33872	81688
2.38	3.12035	81735
2.39	3.79240	83815
2.41	3.98212	85268
2.43	4.85947	87433
2.44	4.28697	89813
2.46	4.38268	11684
2.48	3.94173	12410
2.49	3.73704	12392

TABLE XXVI
CYL.15,4:1 RATIO

(K* λ)	CRS/AREA	PHASE
2.01	1.39855	- 74258
2.03	2.29128	. 78944
2.05	5.24254	. 51923
2.07	9.74204	. 36060
2.09	13.35799	. 28960
2.11	15.06872	. 23493
2.13	12.41624	. 19871
2.15	11.12595	. 17604
2.17	10.24182	. 14635
2.19	9.74727	. 09780
2.21	6.30424	. 05134
2.23	4.31722	. 00386
2.25	2.44645	- .03237
2.27	1.04940	- .11976
2.29	.48325	- .31069
2.31	.39121	- .55435
2.33	.06108	- .74912
2.35	1.54024	- .32268
2.37	2.17072	- .37729
2.39	3.13193	- .41743
2.41	3.06058	- .41520
2.43	3.34463	- .41645
2.45	3.17247	- .44500
2.47	3.11824	- .45759
2.49	2.89608	- .43894
2.51	2.21701	- .44822
2.53	1.82208	- .46341
2.55	1.30832	- .43758
2.57	.60718	- .38006
2.59	.24243	- .30369
2.61	.12789	- .69548
2.63	.20603	- .45290
2.65	.30354	- .31795
2.67	.60146	- .24721
2.69	.70282	- .21772
2.71	.92764	- .21796
2.73	1.16504	- .19354
2.75	1.05605	- .14708
2.77	.74843	- .11238
2.79	.63639	- .12645
2.81	.67702	- .07661
2.83	.55476	.03626
2.85	.30160	.15154
2.87	.40693	.19947
2.89	.65564	.38946
2.91	.70697	.39573
2.93	.00097	.41532
2.95	1.24401	.40835
2.97	1.60738	.44520
2.99	1.51583	.48910

TABLE XXVII
CYL.4,6:1 RATIO

(K*A)	CRS/AREA	PHASE
1.01	2.04153	.53061
1.02	.31989	.58500
1.03	.13499	.20200
1.04	.11681	.01606
1.05	.66338	- .11191
1.06	1.53998	- .11427
1.07	2.23471	- .11172
1.08	3.32647	- .08653
1.09	4.77929	- .09819
1.10	7.13720	- .12872
1.11	8.71983	- .12305
1.12	10.18899	- .12099
1.13	12.09665	- .13990
1.14	14.05688	- .12528
1.15	13.62556	- .12105
1.16	13.15790	- .14149
1.17	14.13970	- .14609
1.18	13.07867	- .15085
1.19	12.25699	- .16902
1.20	13.34913	- .17255
1.21	11.02020	- .13638
1.22	7.10885	- .13333
1.23	5.77909	- .16057
1.24	5.04011	- .14970
1.25	3.02973	- .12691
1.26	1.64849	- .16895
1.27	.82758	- .14507
1.28	.34862	.02394
1.29	.23634	.51034
1.30	.65147	.36005
1.31	1.37317	.75957
1.32	2.93036	.74512
1.33	5.22181	.74675
1.34	7.73788	.76702
1.35	10.02615	.75434
1.36	13.24143	.76560
1.37	15.43289	.76920
1.38	16.14492	.78251
1.39	17.18208	.77252
1.40	19.07168	.75553
1.41	22.11272	.75551
1.42	22.69478	.76438
1.43	22.49472	.76063
1.44	21.06116	.76887
1.45	18.19212	.77432
1.46	14.83870	.76907
1.47	13.27210	.75172
1.48	11.51208	.76255
1.49	8.61260	.77362
1.50	6.43010	.78120

TABLE XXVIII
CYL. 14, 6:1 RATIO

(K*A)	CRS/AREA	PHASE
1.34	7.02071	51727
1.36	12.48490	53735
1.37	13.86212	54824
1.38	15.79053	52699
1.40	20.04838	53597
1.41	22.64391	53157
1.42	19.46970	54300
1.44	18.66974	55893
1.45	18.40048	55279
1.46	17.19148	53846
1.48	13.78473	54958
1.49	10.19180	54893
1.50	7.40630	55853
1.52	4.77792	60952
1.53	2.03223	69062
1.54	72849	31730
1.56	96713	- 43700
1.57	2.65575	- 26180
1.58	4.74772	- 67512
1.60	7.21936	- 67754
1.61	12.24048	- 66627
1.62	16.05264	- 63532
1.64	17.36613	- 61205
1.65	18.48037	- 63144
1.66	23.23715	- 63093
1.68	26.26219	- 61493
1.69	25.57187	- 61862
1.70	27.34014	- 61582
1.72	24.65080	- 59500
1.73	19.47188	- 58453
1.74	15.06061	- 58971
1.76	12.73489	- 57920
1.77	9.82364	- 54774
1.78	6.80038	- 49150
1.80	3.99227	- 43266
1.81	2.96407	- 33938
1.82	3.23305	- 21310
1.84	4.37421	- 08015
1.85	5.49957	01611
1.86	6.72582	04496
1.88	10.51165	05135
1.89	14.72184	09017
1.90	16.56665	11085
1.92	18.56020	10322
1.93	20.57776	11329
1.94	17.93638	12027
1.96	15.75472	06079
1.97	11.76505	08331
1.98	13.62429	08574
2.00	6.57103	02986

TABLE XXIX
CYL.19,6:1 RATIO

(K* λ)	CRS/AREA	PHASE
1.68	25.70153	- 24433
1.70	25.57289	- 24388
1.71	22.89440	- 23896
1.73	17.82078	- 21686
1.75	14.03504	- 18905
1.76	9.64284	- 15276
1.78	5.22148	- 96687
1.80	3.43279	.04822
1.81	3.40385	.20810
1.83	3.99704	.32301
1.85	6.16449	.41018
1.86	9.96011	.45956
1.88	13.62728	.49431
1.90	16.42378	.52002
1.91	17.70543	.52180
1.93	17.05691	.50214
1.95	12.68742	.54718
1.96	11.16303	.47188
1.98	2.61156	.40411
2.00	6.88857	.25737
2.01	14.76554	.79508
2.03	13.24172	.70424
2.04	10.74471	.62484
2.06	6.42516	.48510
2.08	2.85055	.19957
2.09	2.86949	- 12609
2.11	4.10476	- 29497
2.13	5.66190	- 36835
2.14	6.72861	- 39932
2.16	7.25138	- 41401
2.18	6.92239	- 43310
2.19	6.40136	- 45660
2.21	5.23189	- 47292
2.23	3.77498	- 48801
2.24	1.98992	- 48832
2.26	62948	- 48928
2.28	11326	- 32755
2.29	32986	- 21391
2.31	1.07370	- 27338
2.33	1.47316	- 25859
2.34	1.75891	- 23339
2.36	1.65185	- 20721
2.38	1.00417	- 22620
2.39	27726	- 26747
2.41	03262	- 33486
2.43	42159	- 37157
2.44	1.65714	- 33874
2.46	3.06600	- 31416
2.48	4.62044	- 27497
2.49	6.65582	- 25345

TABLE XXX
CYL.17,6:1 RATIO

(K* λ)	CRS/AREA	PHASE
2.01	17.68300	25110
2.03	11.25900	15571
2.05	3.77202	- 02193
2.07	78277	- 31498
2.09	1.04333	- 68948
2.11	2.68843	- 29194
2.13	3.89893	- 32604
2.15	5.12081	- 33530
2.17	5.84094	- 35996
2.19	5.15915	- 40171
2.21	3.74639	- 41981
2.23	1.68442	- 40863
2.25	45121	- 27796
2.27	50104	- 42467
2.29	1.47997	- 32856
2.31	2.23265	- 33939
2.33	2.34436	- 37965
2.35	1.86574	- 42759
2.37	84300	- 48309
2.39	14335	- 25408
2.41	48523	72544
2.43	1.90451	59362
2.45	4.17311	52569
2.47	6.36317	46450
2.49	7.58925	41056
2.51	8.23789	35705
2.53	7.65558	31255
2.55	6.04383	25532
2.57	3.67849	16532
2.59	2.21335	01586
2.61	1.66792	- 20033
2.63	2.48493	- 40937
2.65	4.14738	- 53682
2.67	6.29309	- 61609
2.69	7.85760	- 18096
2.71	8.89772	- 21192
2.73	7.78321	- 23782
2.75	5.88572	- 28110
2.77	4.55990	- 34269
2.79	3.11087	- 42276
2.81	1.62694	- 53679
2.83	93475	75809
2.85	1.26845	53903
2.87	2.10465	39172
2.89	3.36370	30939
2.91	4.18119	26255
2.93	4.45483	20245
2.95	5.00443	16531
2.97	4.57189	16087
2.99	3.27827	14278

B. CONCLUSIONS AND RECOMENDATIONS

The results showed agreement between the theory and the experimental data obtained. Some deviations between the theoretical and experimental plots could be explained.

The problem caused by averaging as observed in the phase plot can be overcome by refining the program in the following way: If the two values to be averaged deviate more than a pre-determined value, say, 200 degrees, both will be converted to a positive value before the average is taken. The averaged value is then adjusted so that it lies between -180 and +180 degrees. A new set of measurements with targets having length to inner diameter ratios of 4 and 6 is planned. This refinement of averaging procedure will be adopted.

For the next step in the comparative study of target back scattering characteristics based on the canonical model of the tubular cylinder of finite length, more complicated models varying from a tubular cylinder to a missile by adding fins and wings will be constructed and studied. Figures 4.11 and 4.12 show the experimental patterns of a finite tubular cylinder with four fins in two aspect angles, the first, with the fins parallel to the antennas, and the second twisted in 45 degrees. Both Figures can be compared to Figure 3.19 showing the same cylinder without the fins.

This work is the first step to gain the capability of radar target identification. Its contribution lies in the justification that the canonical model is a useful one: the theory is correct so that the theoretical results can provide information about surface current distribution on the cylinder.

Another application of this work could be in the study of the back scattering characteristics of aircraft engines.

Since the signals are modulated, target detection will be easier. And because of the smaller size of the air-intake, the results will be directly applicable to radars now in existence.

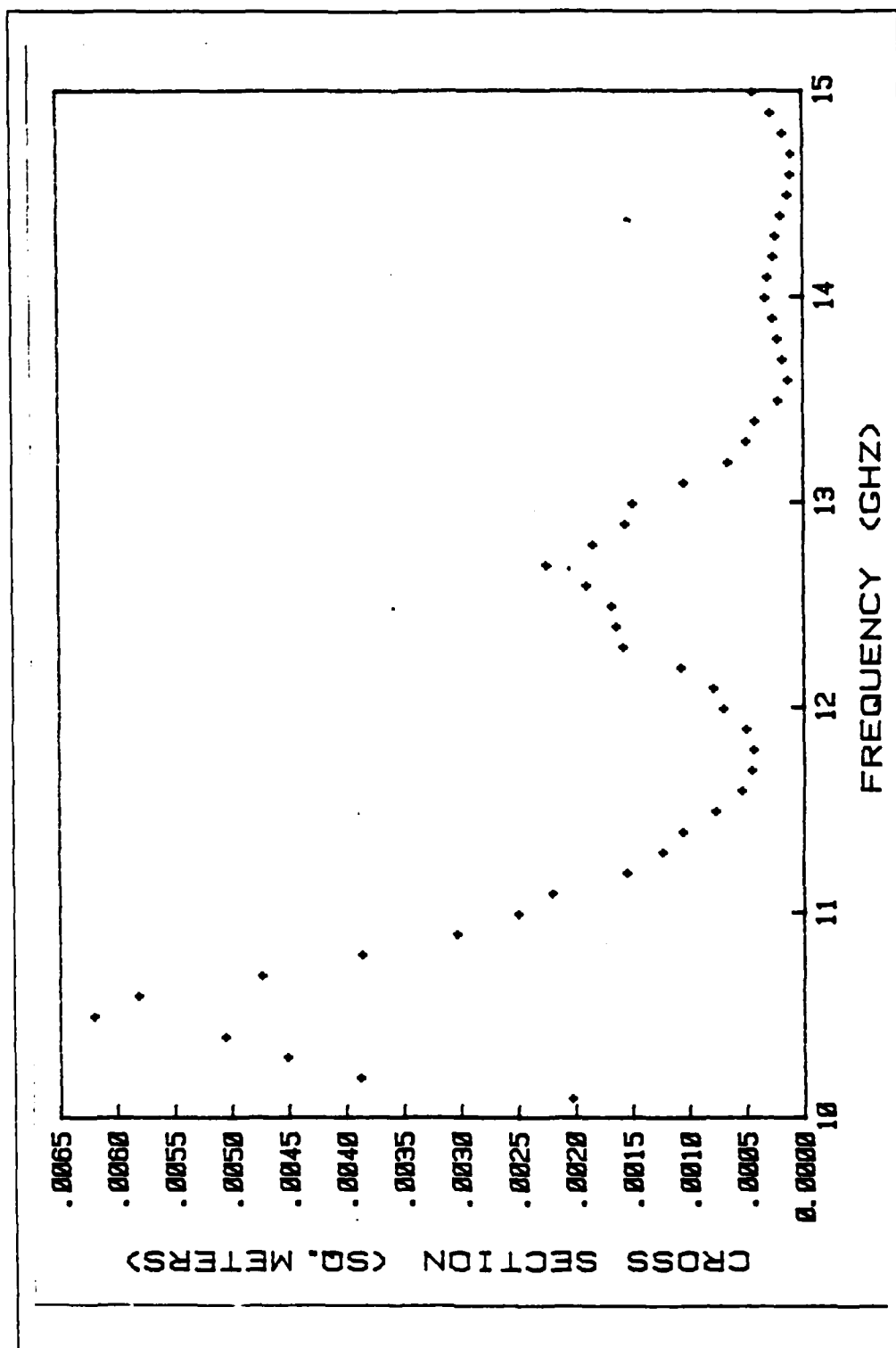


Figure 4.11 Cylinder 15 with Fins, 90 Deg

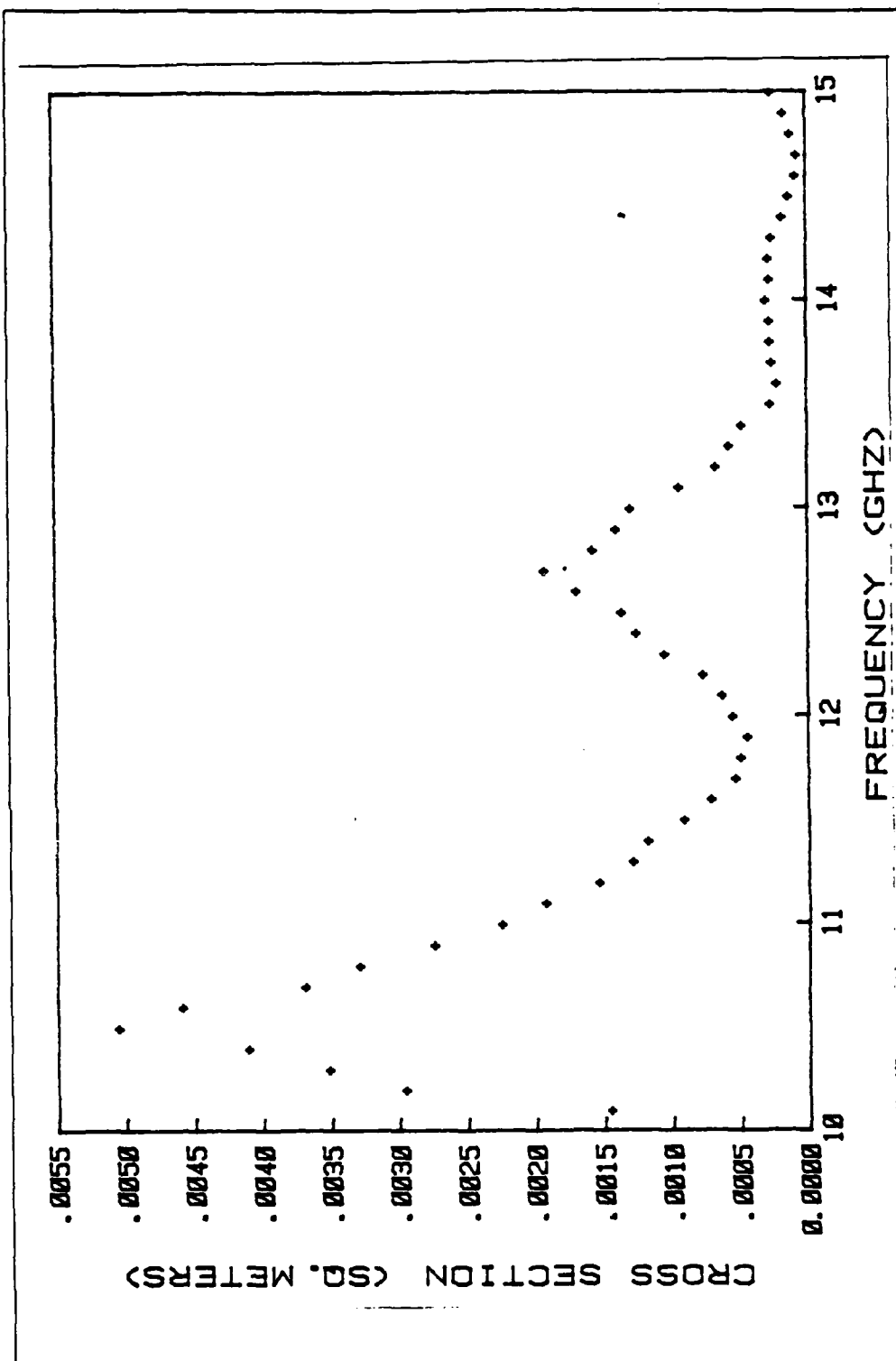


Figure 4.12 Cylinder 15 with Fins, 45 Deg

APPENDIX A
COMPUTER PROGRAMS

```

10  ! "SPHERE.DRIVE0" .
20  !
30  ! COMPUTE BACK SCATTERED
40  ! FAR-FIELD FROM A PERFECTLY
    ! CONDUCTING SPHERE.
50  !
60  ! THE INCIDENT FIELD IS A
70  ! LINEARLY POLARIZED PLANE W
    ! AVE WITH ZERO PHASE AT THE C
    ! ENTER OF THE SPHERE.
80  ! THE THEORETICAL VALUES TO
    ! BE COMPUTED ARE THE BACK-SC
    ! ATTERING CROSS-SECTION AND
90  ! THE PHASE OF THE FAR FIELD
    ! INTERPOLATED TO THE CENTER
    ! OF THE SPHERE. .
100 !
110 ! THEORETICAL VALUES ARE
120 ! STORED IN FILES OF 800
130 ! RECORDS, ONE FOR EACH FREQ
    ! UENCY FROM 2.02 GHZ TO 18 GH
    ! Z AT 0.02 GHZ STEPS.
140 !
150 ! "THEOR1.DRIVE1" FOR THE
160 ! 1" DIAMETER SPHERE
170 ! "THEOR3.DRIVE1" FOR THE
180 ! 3.187" DIAMETER SPHERE
190 ! "THEOR4.DRIVE1" FOR THE
200 ! 4.75" DIAMETER SPHERE
210 ! "THEOR6.DRIVE1" FOR THE
220 ! 6" DIAMETER SPHERE
230 !
240 !
250 ! FILE H$ STORES THE
    ! COMPUTED RESULT
260 H$="THEOR6.DRIVE1"
270 !
280 R0=6*.0254/2 ! SPHERE
    ! RADIUS IN METERS
290 !
300 !
310 X9=2*PI ! PARAMETER
320 !
330 !
340 Q1=2 ! STARTING FREQ IN GHZ
350 Q2=18 ! FINAL FREQ IN GHZ
360 Q4=.02 ! FREQ STEP IN GHZ
370 ON ERROR GOTO 390
380 PURGE H$
390 OFF ERROR

```

```

400 CREATE H$,800,16 ! OPEN A NE
    W FILE WITH 800 RECORDS
410 ! OF 16 BYTES EACH. EVERY
420 ! RECORD STORES ONE MAGNITU
    DE AND ONE PHASE DATA.
430 !
440 ASSIGN# 1 TO H$
450 DIM B8(144),B9(144),D8(144),
    D9(144) ! 144>L0=INT(2*K0*A0
    +3)
460 F0=Q1
470 FOR I=1 TO 800
480 DISP "FREQ LOOP=",I
490 F0=F0+Q4
500 DISP "FREQ (GHZ)=",F0
510 K1=.3/F0 ! WAVELENGTH
520 K0=X9/K1 ! WAVE NUMBER
530 GOSUB 650
540 DISP "E =",E0
550 DISP "P =",P0
560 PRINT# 1,I ; E0,P0
570 NEXT I
580 ASSIGN# 1 TO *
590 CLEAR
600 DISP "END OF COMPUTATION"
610 END
620 !
630 !
640 L0=INT(2*K0*A0+3)
650 IF L0<145 THEN 670
660 DISP "K0*A0 TOO LARGE FOR
    CURRENT ARRAY DIM"
670 Z=K0*A0
680 GOSUB 910
690 E8=0
700 E9=0
710 FOR N=1 TO L0
720 L=L0-N+1
730 M8=D8(L)^2+D9(L)^2
740 M9=B8(L)^2+B9(L)^2
750 A7=(L+.5)/M8/M9
760 A8=A7*(B9(L)*D9(L)-B8(L)*D8(
    L))
770 A9=A7*(B8(L)*D9(L)+B9(L)*D8(
    L))
780 E8=A8-E8
790 E9=A9-E9
800 NEXT N
810 E8=-E8
820 E9=-E9
830 E0=E8^2+E9^2
840 P0=ATN2(E9,E8)
850 E0=E0/K0^2+K1 ! CROSS-SECTIO
    N
860 P0=P0-X9*INT(P0/X9)
870 IF P0<PI THEN 890
880 P0=P0-X9

```

```

890 P0=-P0
900 RETURN
910 !
920 IF Z>L0-1 THEN 1230
930 Z2=Z^2/2
940 N2=2*Z2+L0+1
950 D1=2*N2+3
960 D2=D1*(2*N2+5)
970 D3=D2*(2*N2+7)
980 D4=D3*(2*N2+9)
990 F1=1-Z2/D1+Z2^2/(2*D2)-Z2^3/
    (6*D3)
1000 F2=Z*(1/D1-Z2/D2+Z2^2/(2*D3
    )-Z2^3/(6*D4))
1010 M=2*Z2
1020 S1=F1
1030 F1=(2*M+1)*F1/Z-F2
1040 F2=S1
1050 IF ABS(F1)<1.E100 THEN 1090
1060 F1=F1*1.E-100
1070 F2=F2*1.E-100
1080 S1=S1*1.E-100
1090 M=M-1
1100 IF M+1>L0 THEN 1020
1110 B8(L0)=F2
1120 B8(L0-1)=F1
1130 N0=L0-2
1140 FOR K=1 TO N0
1150 N=L0-K-1
1160 B8(N)=(2*N+3)*B8(N+1)/Z-B8(
    N+2)
1170 NEXT K
1180 A1=(SIN(Z)/Z-COS(Z))/B8(1)
1190 FOR K=1 TO L0
1200 B8(K)=A1*B8(K)
1210 NEXT K
1220 GOTO 1280
1230 B8(1)=SIN(Z)/Z-COS(Z)
1240 B8(2)=(3/Z^2-1)*SIN(Z)-3*CO
    S(Z)/Z
1250 FOR N=3 TO L0
1260 B8(N)=(2*N-1)*B8(N-1)/Z-B8(
    N-2)
1270 NEXT N
1280 B9(1)=-SIN(Z)-COS(Z)/Z
1290 B9(2)=(1-3/Z^2)*COS(Z)-3*SI
    N(Z)/Z
1300 FOR N=3 TO L0
1310 B9(N)=(2*N-1)*B9(N-1)/Z-B9(
    N-2)
1320 NEXT N
1330 D8(1)=(1-1/Z^2)*SIN(Z)+COS(
    Z)/Z
1340 D9(1)=(1/Z^2-1)*COS(Z)+SIN(
    Z)/Z
1350 FOR N=2 TO L0
1360 D8(N)=B8(N-1)-N*B8(N)/Z

```

1370 D9(N)=B9(N-1)-N*B9(N)/Z
1380 NEXT N
1390 RETURN

```

10  | "CALIB DRIVE0"
20  |
30  | CALIBRATION USING A SPHERE
40  | OVER L9-U9 GHZ AT F9 GHZ
50  | STEPS BASED ON THEORETICAL
    | VALUES COMPUTED USING THE P
    | ROGRAM "SPHERE.DRIVE0"
60  | THE RESULTED SYSTEM TRANS-
    | FER FUNCTION IS STORED AS:
70  |
80  | "CALIB3.DRIVE1" (3.187")
90  |
100 | A$ IS THE FILE STORING THE
110 | BACKGROUND DATA.
120 |
130 | C$ IS THE FILE STORING THE
    | SYSTEM TRANSFER FUNCTION
140 |
150 | H$ IS THE FILE STORING
    | THEORETICAL DATA OF THE SPHE
    | RE
160 |
170 | S$ DESCRIBES THE SPHERE
180 |
190 |
200 | C$="CALIB3.DRIVE1"
210 | H$="THEOR3.DRIVE1"
220 | S$="3.187 INCH SPHERE"
230 | A$="BKGRND.DRIVE1"
240 |
250 | X9=2*PI ! A PARAMETER
260 |
270 | OPTION BASE 1
280 | N0=3 ! NUMBER OF READINGS
290 | TAKEN AND AVERAGED FOR ONE
300 | FREQ.
310 |
320 | F9=.1 ! FREQ. STEP IN GHZ
330 |
340 | M1=51 ! M1=(U9-L9)/F9+2
350 | NUMBER OF FREQ. CHECKED.
360 |
370 | L9=10.1 ! LOWER FREQ IN GHZ
380 | U9=15 ! UPPER FREQ IN GHZ
390 |
400 | DIM A(51,2) ! BACKGROUND
    | DATA
410 | DIM B(51,2) ! TARGET DATA
420 | DIM G3(51,2) ! THEORY
430 | ! CREATE C$.M1,16
440 | ! CREATE A$.M1,16
450 | ! STORE CALIBRATION AND BACK
    | GROUND DATA IN A FILE OF M1
    | RECORDS
460 | ! EACH RECORD CONTAINS ONE
    | MAGNITUDE AND ONE PHASE
470 | ! DATA AT A FREQUENCY

```

```

480 !
490 ! READING THE THEORETICAL DA
    TA
500 !
510 ASSIGN# 1 TO H$
520 K0=(L9-2-F9*2)*50
530 FOR I=1 TO M1
540 K0=K0+50*F9
550 READ# 1,K0 : G3(I,1),G3(I,2)
560 NEXT I
570 ASSIGN# 1 TO *
580 GOSUB 2230 ! HEADER.
590 DISP "DO YOU WANT TO USE THE
    MOST RECENT BACKGROUND DATA
    ?      Y/N "

600 INPUT P$
610 IF P$="N" THEN 620
620 !
630 ! READING BACKGROUND DATA.
640 !
650 ASSIGN# 4 TO A$
660 READ# 4 : A(),
670 ASSIGN# 4 TO *
680 GOTO 340
690 CLEAR
700 REMOTE 7 ! REMOTE ALL
    DEVICES
710 CLEAR 7 ! CLEAR ALL DEVICES
720 ! INITIALIZE SIG.GEN TO FREQ
    T FREQ.
730 OUTPUT 719 : "P",L9,"Z1K0L3M0
    N601"
740 CLEAR
750 DISP "REMOVE TARGET FROM CHA
    MBER,PUSH 'CONT' WHEN READY"
760 LOCAL 7
770 BEEP @ BEEP
780 PAUSE
790 REMOTE 7
800 CLEAR
810 DISP "TAKING BACKGROUND DATA
    "
820 PRINT
830 ! PRINT "BACKGROUND DATA"
840 PRINT
850 OUTPUT 719 : "P",L9,"Z1K0L3M0
    N601"
860 WAIT 200 ! WAIT FOR FREQ TO
    STABILIZE
870 GOSUB 1330
880 !
890 ! STORING BACKGROUND DATA
900 !
910 ASSIGN# 3 TO A$
920 PRINT# 3 : A(),
930 ASSIGN# 3 TO *
940 CLEAR

```



```

950 LOCAL 7
960 DISP "PUT TARGET INTO CHAMBE
      R. PUSH 'CONT' WHEN READY"
970 DISP "TARGET IS ",S$
980 BEEP @ BEEP
990 PAUSE
1000 REMOTE 7
1010 CLEAR
1020 DISP "COMPUTING TARGET DATA
      "
1030 PRINT
1040 ! PRINT "TARGET DATA"
1050 PRINT
1060 OUTPUT 719 ; "P",L9,"ZIK0L3M
      0N501"
1070 WAIT 200
1080 GOSUB 1970
1090 PRINT " "
1100 PRINT "TRANS. FUNCTION",S$
1110 PRINT " "
1120 !
1130 ! CALCULATE AND STORE TRANS
      FER FUNCTION.
1140 !
1150 ASSIGN# 2 TO C$
1160 FOR M=1 TO M1
1170 N1=B(M,1)-A(M,1)
1180 N2=B(M,2)-A(M,2)
1190 X6=G3(M,1)/(N1^2+N2^2)
1200 X7=G3(M,2)-ATN2(N2,N1)
1210 X7=X7-X9*INT(X7/X9)
1220 IF X7>PI THEN X7=X7-X9
1230 PRINT# 2,M ; X6,X7
1240 ! PRINT USING 970 ; M,X6,X7
1250 IMAGE DD,1X,"X6=",S0.D00E,1
      X,"X7=",S0.D00E
1260 NEXT M
1270 ASSIGN# 2 TO *
1280 CLEAR
1290 DISP "CALIBRATION COMPLETED
      ,DATA STORED IN",C$
1300 BEEP @ BEEP @ BEEP
1310 LOCAL 7
1320 END
1330 !
1340 !
1350 !
1360 !
1370 !
1380 ! BACKGROUND DATA COLLECTIO
      N SUBROUTINE
1390 !
1400 ! OUTPUT(L9-F9)TO U9 GHZ AT
      F9 GHZ STEPS
1410 J=10*(L9-2*F9) ! FREQUENCY
      STARS AT L9-F9 GHZ

```

```

1420 FOR K=1 TO N1 ! NUMBER OF
    FREQUENCY STEPS
1430 J=J+10*F2
1440 IMAGE 1A.3Z.14A
1450 OUTPUT 719 USING 1440 ; "P"
    ;J,"00Z1K0L3M0N601"
1460 ! TAKE DATA IN FROM 722&720

1470 GOSUB 1640
1480 !
1490 ! CALCULATE REAL&IMAGINARY
    FROM AMP.&PHASE
1500 !
1510 R1=A1*CDOS(P1)
1520 I1=A1*SIN(P1)
1530 A(K,1)=R1
1540 A(K,2)=I1
1550 ! PRINT USING 2040 ; A(K,1)
    ;A(K,2)
1560 NEXT K
1570 OUTPUT 719 ; "P",L9,"Z1K0L3M
    0N601"
1580 RETURN
1590 !
1600 !
1610 !
1620 !
1630 !
1640 ! SUBROUTINE TO ENTER AMPLI
    TUDE AND PHASE DATA FROM DI
    GITAL VOLTMETERS
1650 !
1660 ! PREPARE DIGITAL VOLTMETER
    TO SEND AMPLITUDE DATA
1670 ! NO READINGS TAKEN AND AVE
    RAGED FOR ONE FREQ.
1680 !
1690 !
1700 V1=0 ! PARAMETERS FOR THE
1710 F1=0 ! AVERAGING PROCESS.
1720 FOR L=1 TO N0
1730 OUTPUT 720 ; "P0F1R1T1Z1FL0M
    0"
1740 WAIT 10
1750 ENTER 720 ; V
1760 WAIT 10
1770 OUTPUT 722 ; "F1R7T1M3A0H1"
1780 WAIT 10
1790 ENTER 722 ; F
1800 V1=V1+V
1810 F1=F1+F
1820 WAIT 10
1830 NEXT L
1840 V=V1/N0
1850 F=F1/N0
1860 A1=10^F ! TRANSFER TO MAG.
    FROM VOLTS.

```

```

1870 P1=10010 ! TRANSFER TO DEG.
      FROM VOLTS.
1880 P1=DTR(P1)
1890 ! PRINT USING 1810 ; K,A1,P
      1
1900 IMAGE DD,2X,"A=",MD.000E,2X
      ,"P=",SD.000E
1910 RETURN
1920 !
1930 !
1940 !
1950 !
1960 !
1970 ! TARGET DATA COLLECTION
      SUBROUTINE
1980 !
1990 ! OUTPUT(L9-F9) TO U9 GHZ AT
      F9 GHZ STEPS
2000 J=10*(L9-2*F9) ! FREQUENCY
      STARS AT L9-F9 GHZ

2010 FOR K=1 TO M1 ! NUMBER OF
      FREQUENCY STEPS.
2020 J=J+10*F9
2030 IMAGE 1A,3Z,14A
2040 OUTPUT 719 USING 2030 ; "P"
      ,J,"00Z1K0L3M0N601"
2050 ! TAKE DATA IN FROM 722&720
      1820 GOSUB 1410
2060 GOSUB 1540
2070 ! CALCULATE REAL&IMAG FROM
      AMP&PHASE
2080 R1=A1*COS(P1)
2090 I1=A1*SIN(P1)
2100 B(K,1)=R1
2110 B(K,2)=I1
2120 ! PRINT USING 2040 ; B(K,1)
      ,B(K,2)
2130 IMAGE 4X,"R=",SD.000E,2X,"I
      =" ,SD.000E
2140 NEXT K
2150 OUTPUT 719 ; "P",L9,"Z1K0L3M
      0N601"
2160 RETURN
2170 !
2180 !
2190 !
2200 !
2210 ! HEADER SUBROUTINE
2220 !
2230 PRINT " "
2240 PRINT " "
2250 CLEAR
2260 DISP "CALIBRATION STANDARD"
      ,S#
2270 PRINT "CALIBRATION STANDARD
      ",S#

```

```
2280 PRINT "*****"  
2290 PRINT "*****"  
2300 PRINT " "  
2310 CLEAR  
2320 RETURN
```

```

10  ! "TARGET.DRIVE0"
20  !
30  ! TARGET BACK-SCATTERING
40  ! USING C# DATA & STORE
   ! RESULTS IN G#
50  ! FREQUENCIES L9-U9 GHZ AT
   ! F9 GHZ STEPS
60  !
70  ! FILE C# STORES THE SYSTEM
   ! TRANSFER FUNCTION
80  !
90  ! FILE G# STORES TARGET DATA
   ! OBTAINED FROM THIS PROGRAM
100 !
110 ! FILE H# STORES THEORETICAL
   ! VALUES FOR PLOTTING OVERLAY
120 !
130 ! FILE A# STORES BACKGROUND
   ! DATA
140 !
150 C#="CALIB3.DRIVE1"
160 G#="SCR3.DRIVE1"
170 H#="THEOP3.DRIVE1"
180 A#="BKGRND.DRIVE1"
190 !
200 ! CREATE G#,52,24
210 ! STORE TARGET DATA IN FILE
220 ! OF M1+1 RECORDS FIRST ONE
230 ! FOR THE AVERAGE PROCEDURE
240 ! AND THE REST CONTAINS THE
250 ! FREQUENCY MAGNETUDE AND
260 ! PHASE SHIFT.
270 !
280 ! CREATE A#,51,16
290 ! STORE CALIB. AND BACKGROUN
   ! DATA IN A FILE OF M1 RECORDS
300 ! EACH RECORD CONTAINS ONE M
   ! AG AND PHASE AT A FREQ.
310 !
320 OPTION BASE 1
330 N0=2 ! NUMBER OF READINGS
340 ! TAKEN AND AVERAGED FOR ONE
   ! FREQUENCY.
350 !
360 DIM A(51,2) ! BACKGROUND DAT
   ! A
370 DIM B(51,2) ! TARGET DATA
380 DIM G4(51,3) ! CALIBRATION
390 DIM N(51,3) ! RESULTANT
400 DIM M0(51,3)
410 !
420 N1=51 !
430 ! N1=(U9-L9)/F9+2 NUMBER OF
440 ! FREQ. CHECKED
450 F9=.1 ! FREQ.STEPS IN GHZ.

```

```

460 U9=15 ! UPPER FREQ. IN GHz
470 L9=10 ! LOWER FREQ. IN GHz
480 DIM T(800,2) ! STORES THEORETICAL DATA
490 X9=2*PI
500 !
510 ! READING TRANSFER FUNCTION
520 !
530 ASSIGN# 1 TO C$
540 READ# 1 : G4( )
550 ASSIGN# 1 TO *
560 ! MAT PRINT USING 330 : G4
570 IMAGE 2X,3D,4D
580 !
590 REMOTE 7 ! REMOTE ALL DEVICES
600 CLEAR 7 ! CLEAR ALL DEVICES
610 OUTPUT 719 : "P1Z1K0L3M0N601"
! INITIAL SETUP OF 719
620 CLEAR
630 DISP "DO YOU WANT TO USE THE MOST RECENT BACKGROUND DATA ? Y/N"
640 INPUT P$
650 !
660 IF P$="N" THEN 740
670 !
680 ! READING BACKGROUND DATA
690 !
700 ASSIGN# 4 TO A$
710 READ# 4 : A( )
720 ASSIGN# 4 TO *
730 GOTO 800
740 DISP "REMOVE TARGET FROM CHAMBER, PUSH 'CONT' WHEN READY"
750 LOCAL 7
760 BEEP @ BEEP
770 PAUSE
780 DISP "TAKING BACKGROUND DATA"
790 REMOTE 7
800 OUTPUT 719 : "P"/L9,"Z1K0L3M0N601" ! INITIAL SETUP OF 719
810 WAIT 100
820 GOSUB 2560
830 !
840 ! STORING BACKGROUND DATA
850 !
860 ASSIGN# 5 TO A$
870 PRINT# 5 : A( )
880 ASSIGN# 5 TO *
890 CLEAR
900 DISP "PUT TARGET INTO CHAMBER, PUSH 'CONT' WHEN READY"
910 LOCAL 7
920 BEEP @ BEEP
930 PAUSE

```

```

940 REMOTE 7
950 OUTPUT 719 ; "P",L9,"ZIKOL3M0
    NS01" ; INITIAL SETUP OF 719
960 WAIT 500
970 GOSUB 3410
980 CLEAR
990 DISP "COMPUTING TARGET DATA"
1000 GOSUB 3130
1010 !
1020 ! COMPUTING TARGET DATA
1030 ! WITHOUT BACKGROUND AND TH
    E
1040 ! FREQ. FOR EACH RECORD.
1050 F0=L9-2*F9
1060 FOR M=1 TO N1
1070 F0=F0+F9
1080 N(M,1)=F0
1090 X7=B(M,1)-A(M,1)
1100 X8=B(M,2)-A(M,2)
1110 X6=(X7^2+X8^2)*G4(M,1)
1120 N(M,2)=X6
1130 X9=ATN2(X8,X7)+G4(M,2)
1140 X8=X8-X9*INT(X8/X9)
1150 IF X8>PI THEN X8=X8-X9
1160 N(M,3)=X8
1170 NEXT M
1180 DISP "PRINT DATA? Y/N"
1190 BEEP @ BEEP
1200 INPUT P#
1210 IF P#="N" THEN 1250
1220 PRINT "      FREQ      CRSEC
        PHASE"
1230 MAT PRINT USING 1240 ; N
1240 IMAGE 2X/3D.4D
1250 CLEAR
1260 LOCAL 7
1270 DISP "PLOT MAGNITUDE FOR
        THIS MEASUREMENT? Y/N"
1280 INPUT P#
1290 IF P#="N" THEN 1330
1300 DISP "SELECT PEN. PUSH
        'CONT' WHEN READY"
1310 PAUSE
1320 GOSUB 3570
1330 CLEAR
1340 DISP "PLOT PHASE FOR THIS
        MEASUREMENT ? Y/N"
1350 BEEP @ BEEP
1360 INPUT P#
1370 IF P#="N" THEN 1410
1380 DISP "SELECT PEN. PUSH
        'CONT' WHEN READY"
1390 PAUSE
1400 GOSUB 4610
1410 CLEAR

```

```

1420 DISP "DO YOU WANT TO MAKE
      AVERAGE WITH PREVIOUS
      DATA?"
1430 DISP "? Y/N"
1440 BEEP @ BEEP
1450 INPUT P$
1460 IF P$="Y" THEN 1750
1470 DISP "DO YOU WANT TO STORE
      DATA ? Y/N "
1480 INPUT P$
1490 IF P$="N" THEN 2280
1500 M0=1
1510 DISP "DO YOU WANT TO STORE
      DATA IN FILE"
1520 DISP G$
1530 DISP "? Y/N"
1540 INPUT P$
1550 IF P$="Y" THEN 1620
1560 DISP "ENTER NAME OF THE DAT
      A FILE TO BE USED FOR STORE
      GE"
1570 INPUT G$
1580 DISP "IS THIS AN OLD FILE
      TO BE UPDATED ? Y/N "
1590 INPUT P$
1600 IF P$="Y" THEN 1620
1610 CREATE G$,53,24
1620 DISP "ENTER LENGTH OF TARGE
      T"
1630 BEEP @ BEEP
1640 INPUT M1
1650 DISP "ENTER DIAMETER OF TAR
      GET"
1660 BEEP @ BEEP
1670 INPUT M2
1680 !
1690 ! STORE MEASURED DATA.
1700 !
1710 ASSIGN# 2 TO G$
1720 PRINT# 2 , M0,M1,M2,N(),)
1730 ASSIGN# 2 TO *
1740 GOTO 2280
1750 DISP "DOES THE DATA STORED
      IN FILE"
1760 DISP G$
1770 DISP "? Y/N"
1780 INPUT P$
1790 IF P$="Y" THEN 1870
1800 DISP "ENTER NAME OF DATA
      FILE TO BE USED FOR THE
      AVERAGE"
1810 !
1820 INPUT G$
1830 !
1840 ! READ OLD DATA
1850 ! AND MAKES WIGHTED AVERAGE
1860 ! WITH NEW DATA.
1870 !

```



```

1870 ASSIGN# 5 TO G#
1880 READ# 5 : M0,M1,M2,M9(,)
1890 ASSIGN# 6 TO #
1900 FOR K=1 TO N1
1910 M9(K,2)=M9(K,2)*M0+N(K,2)
1920 M9(K,2)=M9(K,2)/(M0+1)
1930 M9(K,3)=M9(K,3)*M0+N(K,3)
1940 M9(K,3)=M9(K,3)/(M0+1)
1950 N(K,2)=M9(K,2)
1960 N(K,3)=M9(K,3)
1970 NEXT K
1980 M0=M0+1
1990 !
2000 ! STORE NEW AVERAGE
2010 ASSIGN# 7 TO G#
2020 PRINT# 7 : M0,M1,M2,N(,)
2030 ASSIGN# 7 TO #
2040 PRINT "DATA IS AVERAGE OF",
M0,"MEASUREMENTS"
2050 DISP "PRINT DATA? Y/N"
2060 BEEP @ BEEP
2070 INPUT P#
2080 IF P#="N" THEN 2120
2090 PRINT "      FREQ      CRSEC
      PHASE"
2100 MAT PRINT USING 1240 : N
2110 IMAGE 2X,30,40
2120 DISP "PLOT MAGNITUDE? Y/N"
2130 BEEP @ BEEP
2140 INPUT P#
2150 IF P#="N" THEN 2190
2160 DISP "SELECT PEN FOR MAGNIT
UDE PLOT PUSH 'CONT' WHEN
READY."
2170 PAUSE
2180 GOSUB 3570
2190 CLEAR
2200 DISP "PLOT PHASE? Y/N"
2210 BEEP @ BEEP
2220 INPUT P#
2230 IF P#="N" THEN 2270
2240 DISP "SELECT PEN AND CHANGE
PAPER FOR PHASE PLOT. PUS
H 'CONT' WHEN READY."
2250 PAUSE
2260 GOSUB 4610
2270 CLEAR
2280 DISP "DO YOU WANT TO"
2290 DISP "OBTAIN DATA"
2300 DISP "FOR A NEW TARGET?"
2310 DISP " "
2320 DISP "ENTER Y/N"
2330 INPUT P#
2340 IF P#="N" THEN 2470
2350 DISP "DO YOU WANT TO USE
THE SAME FILE"
2360 DISP G#

```

```

2370 DISP "TO STORE NEW DATA? Y/
N"
2380 INPUT P$
2390 IF P$="Y" THEN 2460
2400 DISP "ENTER NEW FILE NAME T
O STORE TARGET DATA"
2410 INPUT G$
2420 DISP "IS THIS AN OLD FILE
TO BE UPDATED? Y/N"
2430 INPUT P$
2440 IF P$="Y" THEN 2460
2450 CREATE G$,52,24
2460 GOTO 590
2470 CLEAR
2480 DISP "END OF PROGRAM"
2490 BEEP @ BEEP @ BEEP
2500 END
2510 !
2520 !
2530 !
2540 !
2550 !
2560 ! BACKGROUND DATA COLLECTIO
N SUBROUTINE
2570 ! OUTPUT(L9-F9) TO U9 GHZ
2580 J=10*(L9-2*F9) ! FREQUENCY
STARTS AT L9-F9 GHZ TO BE
INCREASED AT F9 GHZ STEPS

2590 FOR K=1 TO N1 ! NUMBER OF F
FREQUENCY STEPS

2600 J=J+10*F9
2610 IMAGE 1A,3Z,14A
2620 OUTPUT 719 USING 2610 ; "P"
,J,"00ZIK0L3M0N601"
2630 ! 50 MSEC WAIT FOR FREQUENC
Y TO STABILIZE
2640 WAIT 50
2650 ! TAKE DATA IN FROM 722 AND
720
2660 GOSUB 3820
2670 ! REAL AND IMAGINARY PARTS
2680 ! FROM AMP. AND PHASE
2690 R1=A1*COS(P1)
2700 I1=A1*SIN(P1)
2710 A(K,1)=R1
2720 A(K,2)=I1
2730 ! PRINT "I1=",A(K,2)
2740 ! PRINT "R1=",A(K,1)
2750 NEXT K
2760 OUTPUT 719 ; "P",L9,"ZIK0L3M
0N601" ! INITIAL SETUP OF 7
19
2770 RETURN
2780 !
2790 !

```

```

2800 !
2810 !
2820 ! SUBROUTINE TO ENTER AMPLI
      TUDE AND PHASE DATA FROM DI
      GITAL VOLTMETER.
2830 !
2840 ! PREPARE DIGITAL VOLTMETER
      TO SEND AMPLITUDE DATA
2850 ! NO READINGS TAKEN AND AVE
      RAGED FOR ONE FREQUENCY.
2860 V1=0 ! PARAMETERS FOR AVERA
      GING PROCESS.
2870 W1=0
2880 FOR L=1 TO N0
2890 OUTPUT 720 ; "F1R1T1Z1FL0M0"
2900 WAIT 10
2910 ENTER 720 ; V0
2920 WAIT 10
2930 OUTPUT 722 ; "F1R7T1M3A0H1"
2940 WAIT 10
2950 ENTER 722 ; W0
2960 V1=V1+V0
2970 W1=W1+W0
2980 WAIT 10
2990 NEXT L
3000 V0=V1/N0
3010 W0=W1/N0
3020 ! TRANSFERS FROM VOLTS TO
      AMPL.
3030 A1=10^W0
3040 ! TRANSFERS TO DEG. FROM VO
      LTS.
3050 P1=100*V0
3060 ! PRINT "A1=" ; A1
3070 P1=DTR(P1)
3080 ! PRINT "P1=" ; P1
3090 RETURN
3100 !
3110 !
3120 !
3130 ! DATA COLLECTION SUBROUTIN
      E
3140 ! OUTPUT(L9-F9) TO U9 GHZ AT
      F9 GHZ STEPS
3150 J=10*(L9-2*F9) ! INITIAL FR
      EQUENCY AT L9-F9 GHZ
3160 FOR K=1 TO N1 ! FREQUENCY S
      TEPs
3170 J=J+10*F9 ! F9 GHZ INCREME
      NTS
3180 IMAGE 1A,3Z,14A
3190 OUTPUT 719 USING 3180 ; "P"
      ;J;"00Z1K0L3M0N601"
3200 ! 50 MSEC WAIT FOR FREQUENC
      Y TO STABILIZE
3210 WAIT 50

```

```

3220 ! TAKE DATA IN FROM 722:730
3230 GOSUB 2320
3240 !
3250 ! REAL&IMAG FROM AMP.&PHASE
3260 R1=A1*COS(P1)
3270 I1=A1*SIN(P1)
3280 B(K,1)=R1
3290 B(K,2)=I1
3300 ! PRINT "R1=",B(K,1)
3310 ! PRINT "I1=",B(K,2)
3320 NEXT K
3330 OUTPUT 719,"P",L9,"Z1K0L3M
0N601" ! INITIAL SETUP OF 7
19
3340 RETURN
3350 !
3360 !
3370 !
3380 ! HEADER SUBROUTINE
3390 !
3400 D$="MONTH/DATE/YEAR"
3410 PRINT " "
3420 PRINT " "
3430 CLEAR
3440 DISP "ENTER TODAY'S DATE -
MONTH,DATE,YEAR"
3450 INPUT D$
3460 DISP "ENTER TGT DESCRIPTION
"
3470 INPUT T$
3480 PRINT D$
3490 PRINT "TARGET IS ",T$
3500 PRINT "*****"
3510 PRINT "*****"
3520 PRINT " "
3530 CLEAR
3540 RETURN
3550 !
3560 !
3570 ! MAGNITUDE PLOTTING
3580 ! SUBROUTINE
3590 !
3600 PLOTTER IS 705
3610 LOCATE 32,122,20,65
3620 FRAME
3630 ! SEARCH FOR MAX & MIN.
3640 ! S0=N(2,2)
3650 ! S1=S0
3660 ! FOR M=3 TO N1
3670 ! IF S0>N(M,2) THEN S0=N(M,
2)
3680 ! IF S1<N(M,2) THEN S1=N(M,
2)
3690 ! NEXT M
3700 DISP "ENTER LOWER VALUE FOR
MAGNITUDE PLOTTING"

```

```

3710 BEEP @ BEEP
3720 INPUT S0
3730 DISP "ENTER UPPER VALUE FOR
      MAGNITUDE PLOTTING"
3740 INPUT S1
3750 L1=INT(L9)
3760 U1=CEIL(U9)
3770 !
3780 ! CALCULATE SCALE STEPS
3790 ! FOR MAGNETUDE.
3800 S3=LGT(S1)
3810 S4=INT(S3)-1
3820 S5=S3-S4
3830 S5=INT(10^S5)+1
3840 S4=10^S4
3850 L0=INT(S0/S4)
3860 IF S5-L0<=14 THEN 3940
3870 IF S5-L0>=50 THEN 3910
3880 S5=.5*S5
3890 S4=S4*2
3900 GOTO 3850
3910 S5=.2*S5
3920 S4=S4*5
3930 GOTO 3850
3940 L0=S4*L0
3950 U0=S5*S4
3960 D0=U0-L0
3970 SCALE L1,U1,L0,U0
3980 FXD 0,4
3990 LAXES -1,S4,L1,L0
4000 MOVE L1,0
4010 FOR K=2 TO N1
4020 M9=N(K,1)
4030 R9=N(K,2)
4040 GOSUB 4510
4050 NEXT K
4060 M5=(U1+L1)/2
4070 MOVE M5,L0+.09*D0
4080 LDRC 5 @ CSIZE 3,1,0
4090 ! LABEL "FREQUENCY (GHZ)"
4100 MOVE L1-1,.5*(L0+U0)
4110 LDIR PI/2
4120 ! LABEL "CROSS SECTION (SQ.
      METERS)"
4130 MOVE M5,U0+.09*D0
4140 LDIR 0
4150 CSIZE 3,1,0
4160 LABEL T#
4170 MOVE M5,U0+.03*D0
4180 LABEL D#
4190 PENUP
4200 DISP "OVERLAY THEORETICAL C
      URVE? Y/N"
4210 !
4220 INPUT P#
4230 IF P#="N" THEN 4490

```

```

4240 DISP "IS THE THEORETICAL
DATA STORED IN THE FILE",H$
4250 DISP "? Y/N"
4260 INPUT P$
4270 IF P$="Y" THEN 4300
4280 DISP "ENTER NAME OF THE
DATA FILE TO BE PLOTTED."
4290 INPUT H$
4300 BEEP @ BEEP
4310 DISP "CHANGE PEN IF DESIRED
PUSH 'CONT' WHEN READY."
4320 PAUSE
4330 ASSIGN# 3 TO H$
4340 J1=(L9-2)*50
4350 J2=(U9-2)*50
4360 FOR J=J1 TO J2
4370 READ# 3,J ; T(J,1),T(J,2)
4380 NEXT J
4390 ASSIGN# 3 TO *
4400 F0=L9
4410 R9=T(J1,1)
4420 MOVE F0,R9
4430 FOR I=J1+1 TO J2
4440 F0=F0+.02
4450 R9=T(I,1)
4460 DRAW F0,R9
4470 NEXT I
4480 PENUP
4490 RETURN
4500 !
4510 ! PLOT CROSS
4520 MOVE M9,R9
4530 CSIZE 2,.5,0
4540 LABEL "+"
4550 ! IMOVE .00025,.00025
4560 ! IDRAW -.0005,0
4570 RETURN
4580 !
4590 !
4600 !
4610 ! PHASE PLOTTING SUBROUTINE
4620 !
4630 PLOTTER IS 705
4640 LOCATE 32,123,20.85
4650 FRAME
4660 S4=.25
4670 U0=1
4680 L0=-1
4690 D0=U0-L0
4700 SCALE L1,U1,L0,U0
4710 FXD 0.3
4720 LAXES -1,S4,L1,L0
4730 MOVE L1,0
4740 FOR K=2 TO N1
4750 M9=NCK,1)
4760 R9=NCK,3)-PI
4770 GOSUB 5110

```

```

4780 NEXT K
4790 MOVE M5,L0-.09*00
4800 LONG 5 @ CSIZE 3,1,0
4810 ! LABEL "FREQUENCY (GHZ)"
4820 MOVE L1-1,.5*(L0+U0)
4830 LDIR PI/2
4840 LABEL "PHASE (PI)"
4850 MOVE M5,U0+.09*00
4860 LDIR 0
4870 CSIZE 3,1,0
4880 LABEL T#
4890 MOVE M5,U0+.03*00
4900 LABEL 0#
4910 PENUP
4920 DISP "OVERLAY THEORETICAL C
      URVE? Y/N"
4930 INPUT P#
4940 IF P#="N" THEN 5070
4950 BEEP @ BEEP
4960 DISP "CHANGE PEN IF DESIRED
      . PUSH 'CONT' WHEN READY."
4970 PAUSE
4980 F0=L9
4990 R9=T(J1,2)/PI
5000 MOVE F0,R9
5010 FOR I=J1+1 TO J2
5020 F0=F0+.02
5030 R9=T(I,2)/PI
5040 DRAW F0,R9
5050 NEXT I
5060 PENUP
5070 RETURN
5080 !
5090 !
5100 !
5110 ! PLOT DOT
5120 MOVE M9,R9
5130 CSIZE 2,.5,0
5140 LABEL "*"
5150 ! IMOVE .00025,.00025
5160 ! IDRAW -.0005,0
5170 RETURN

```

APPENDIX B

CHARACTERISTIC OF THE ABSORBER OF THE ANECHOIC CHAMBER

MECHANICAL SPECIFICATIONS:

Absorber Size (In.)	Absorber Height (In.)			Pyramid Base Size (In.)	Pyramids Per Absorber
	Overall	Base	Pyramid		
24 x 24	8-1/2	1-1/2	7	3 x 3	64

MAXIMUM REFLECTION AT NORMAL INCIDENCE:

Ku Band	X Band	C Band	S Band	L Band	500 MHz	300 MHz	200 MHz	120 MHz
50 db	50 db	45 db	40 db	30 db				

Specifications of the Absorber Material of the Floor

MECHANICAL SPECIFICATIONS:

Absorber Size (In.)	Absorber Height (In.)			Pyramid Base Size (In.)	Pyramids Per Absorber
	Overall	Base	Pyramid		
24 x 24	18-1/4	2-1/4	16	6 x 6	16

MAXIMUM REFLECTION AT NORMAL INCIDENCE:

Ku Band	X Band	C Band	S Band	L Band	500 MHz	200 MHz	120 MHz
50 db	50 db	50 db	45 db	40 db	30 db		

Specifications of the Absorber Material of the Walls

LIST OF REFERENCES

1. Sincler, G. "The Transmission and Reception of Elliptically Polarized Waves", Proc IRE, vol 38, pp.148-151, february 1950.
2. Berkowitz, R.S (ed): Modern Radar pp.560-565, John Wiley and Sons inc, 1965.
3. Mentzer J.R, Scattering and Diffraction of Radio Waves, p.10, Program Press, New york 1955.
4. Stratton J.A, Electromagnetic Theory p.464, McGraw Hill Book Company, New York 1941.
5. Richmand J.H, "Digital Computer Solutions of the Rigorous Equations for Scattering Problems," Proc IEEE, vol 53 pp.796-804 , August 1965.
6. Air Force Cambridge Res.Lab Rep E5070 Back Scattering from Conducting Surfaces , by Spencer R.C, April 1951.
7. Crispin J.W.Jr, and K.M Siegel Methods of Radar Cross-section Analysis p.62 Academic Press Inc, New York 1968.
8. Ibid, p.61.
9. Keller, J.B "Geometrical Theory of Diffraction J.opt Soc.Am, vol 52, pp.116-130, February 1962.
10. Buckley, E.F, Design and Evaluation of Microwave Anechoic Chambers Presented at the 1960 IRE Joint Meeting, Chicago, Ill and available in the international Memorandum, Emerson and Cuming Inc., Canton, Mass.
11. Robinson, L.A, Design of Anechoic Chambers for antenna and Radar Cross-section Measurements SRI International, 1982.
12. Frenny , C.C, "Target Support Measurement Associated with Radar Reflection Measurements", Proc IEEE , p.929.
13. Rome Air Develop Center Tech.AOC Report RADC-TDR-64-25 vol 1 AD 601364 vol 2 AD 6013365, Radar Reflection Measurements Symposium April 1964.

14. Stratton J.A, Electromagnetic Theory p.488, Mcgraw-Hill Book Company, New York, 1941.
15. Mario Lolic, Radar Target Identification Through Electromagnetic Studies Master Thesis Naval Postgraduate School, Dec 1984.
16. Double Series Expansion of the Green's Function for a Perfectly Conducting Cylinder of Finite Length Hung-Mou Lee, Gordon McKay Lab. Harvard University, Cambridge, Mass 02138, 1982.

BIBLIOGRAPHY

Bowman, J.J., T.B.A senior, P.L.E. Uslenghi Electromagnetic and Acoustic Scattering by Simple Shapes North Holland publishing company Amsterdam 1969.

King Ronald W.P. and Tai Tsun-Wu The Scattering and Diffraction of Waves, Harvard University Camb. Massachusetts.

Proceeding of the IEEE special issue on Radar Reflectivity, August 1965.

Skolnik, I. Merill, Introduction to Radar Systems, McGraw-Hill Book Company, N.Y., S.F., London, 1980.

Skolnik I Merril, Radar Handbook, MacGraw Hill Company, New York, 1970.

Uslenghi Piergiorgio L.E. Electromagnetic Scattering, University of Illinois Chicago, 1978.

INITIAL DISTRIBUTION LIST

		No.	Copies
1.	Library, Code 0142 Naval Postgraduate School Monterey, California 93943		2
2.	Defense Technical Information Center Cameron Station Alexandria, Virginia 22314		2
3.	Department Chairman, Code 62 Department of Electrical and Computer Engineering Naval Postgraduate School Monterey, California 93943		2
4.	Prof. Hung-Mou Lee, Code 62 Lh Department of Electrical and Computer Engineering Naval Postgraduate School Monterey, California 93943		2
5.	Prof. Jin. Fu Chang, Code 62 cn Department of Electrical and Computer Engineering Naval Postgraduate School Monterey, California 93943		1
6.	Lt. David Geller 33/A Hashkedim st. Qiryat-Tivon 36000 ISRAEL		7